Design, Synthesis and Characterization of I-BET567, a pan-Bromodomain and Extra Terminal (BET) Bromodomain Oral Candidate

Philip G. Humphreys,[†] Stephen J. Atkinson,[†] Paul Bamborough,[†] Rino A. Bit,[†] Chun-wa Chung,[†] Peter D. Craggs,[†] Leanne Cutler,[†] Rob Davis,[†] Alan Ferrie,[†] GangLi Gong,[⊥] Laurie J. Gordon,[†] Matthew Gray,[†] Lee A. Harrison,[†] Thomas G. Hayhow,[†] Andrea Haynes,[†] Nick Henley,[†] David J. Hirst,[†] Ian D. Holyer,[†] Matthew J. Lindon,[†] Cerys Lovatt,[†] David Lugo,[†] Scott McCleary,[†] Judit Molnar,[†] Qendresa Osmani,[†] Chris Patten,[†] Alex Preston,[†] Inmaculada Rioja,[†] Jonathan T. Seal,[†] Nicholas Smithers,[†] Fenglai Sun,[⊥] Dalin Tang,[⊥] Simon Taylor,[†] Natalie H. Theodoulou,[†,‡] Clare Thomas,[†] Robert J. Watson,[†] Christopher R. Wellaway,[†] Linrong Zhu,[⊥] Nicholas C. O. Tomkinson,[‡] Rab K. Prinjha[†]*

[†]GlaxoSmithKline R&D, Stevenage, Hertfordshire SG1 2NY, United Kingdom

[⊥]WuXi Shanghai STA Pharmaceutical R&D Co., Ltd., No 90 Delin Road, WaiGaoQiao Free Trade Zone, Shanghai, 200131, China

[‡]WestCHEM, Department of Pure and Applied Chemistry, Thomas Graham Building, University of Strathclyde, 295 Cathedral Street, Glasgow, G1 1XL, United Kingdom

ABSTRACT: Through regulation of the epigenome, the bromodomain and extra terminal (BET) family of proteins represent important therapeutic targets for the treatment of human disease. Through mimicking the endogenous N-acetyl-lysine group and disrupting the protein-protein interaction between histone tails and the bromodomain, several small molecule pan-BET inhibitors have progressed to oncology clinical trials. This work describes the medicinal chemistry strategy and execution to deliver an orally bioavailable tetrahydroquinoline (THQ) pan-BET candidate. Critical to the success of this endeavor was a potency agnostic analysis of a data set of 1999 THQ BET inhibitors within the GSK collection which enabled identification of appropriate lipophilicity space to deliver compounds with a higher probability of desired oral candidate quality properties. SAR knowledge was leveraged via Free-Wilson analysis within this design space to identify a small group of targets which ultimately delivered I-BET567 (**27**), a pan-BET candidate inhibitor that demonstrated efficacy in mouse models of oncology and inflammation.

KEYWORDS: Bromodomain, BET, Epigenetics, Bromodomain and Extra Terminal, Povarov Reaction, Free-Wilson, Lipophilic Efficiency

INTRODUCTION

The bromodomain and extra terminal (BET) family of bromodomain containing proteins are comprised of BRD2, BRD3, BRD4 and BRDT. These proteins contain tandem N-terminal epigenetic reader modules, BD1 (N-terminal to BD2) and BD2 (C-terminal to BD1), which recognize acetylated lysines on histone tails and regulate gene transcription.[1-3] The profound biology associated with the BET proteins and interacting transcription factors has driven research across academia and industry to target this tractable protein-protein interaction with small molecules for potential disease modification across a variety of therapeutic areas.[4-7] The majority of molecules described to date bind all eight bromodomains of the BET family, known as pan-

BET inhibitors, although there are increasing reports of compounds selective for BD1 or BD2. [8-13] As a direct result of this sustained and focused research effort, several pan-BET inhibitors have entered oncology clinical trials as a mixture of standalone and combination therapies (Figure 1).[14]

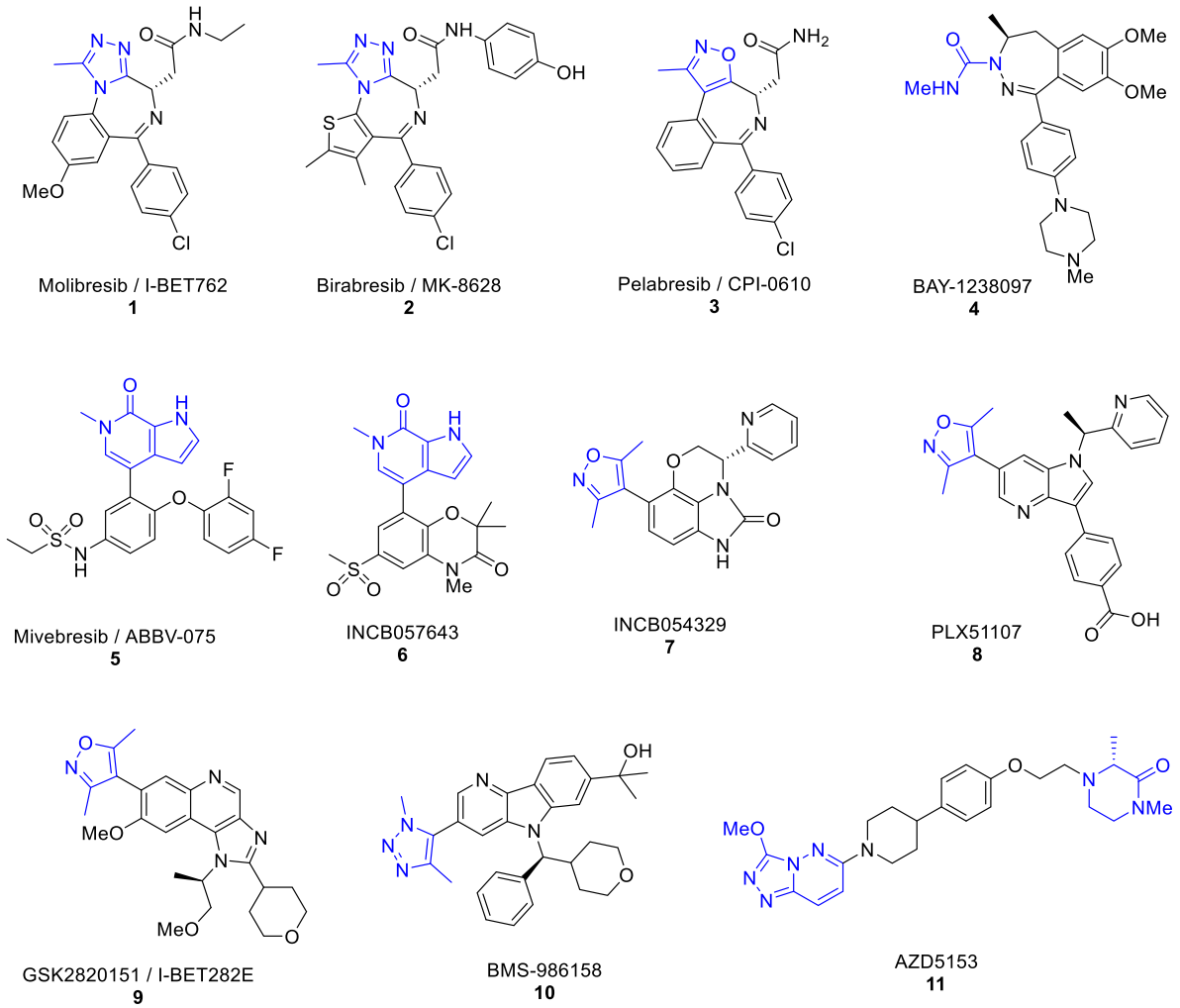

Figure 1. Clinical pan-BET molecules of known structure. The acetyl lysine mimetic is highlighted in blue.

The majority of clinical candidates whose structures have been disclosed fall broadly into three structural classes: benzodiazepines, pyrrolopyridinones and oxazoles. Molibresib (**1**),[15] birabresib (**2**),[16] pelabresib (**3**)[17] and BAY-1238097 (**4**)[18] all bear a similar core bicyclic benzo(di)azepine ring, with either a methyl substituted 5-membered heteroaromatic or urea acetyl lysine mimetic.

Mivebresib (**5**)[19] and INCB057643 (**6**)[20] both bear a pyrrolopyridinone acetyl lysine mimetic which makes a bidendate interaction with a conserved Asn residue (Asn140, BRD4 BD1 numbering, vide infra) via the pyridinone carbonyl and pyrrole NH group. The third structural class of molecules, INCB054329 (**7**),[21] PLX51107 (**8**),[22] GSK2820151 (**9**)[23] and BMS-986158 (**10**)[24] all share a bi- or tricyclic core with a dimethyl substituted 5-membered heteroaromatic warhead which makes a monodentate interaction to the conversed Asn residue. In a structural and mechanistic class of its own, AZD5153 (**11**) contains two acetyl lysine mimetics and binds both BD1 and BD2 of the BET bromodomains simultaneously in a bivalent fashion.[25,26]

The structure of the eight BET bromodomains are well characterized with numerous published apo and liganded crystal structures. The bromodomain consists of four antiparallel alpha helices (αZ, αA, αB, and αC) connected by two flexible loop regions (ZA and BC), which form the acetyl lysine binding pocket. Using 1,2,3,4-tetrahydroquinoline (THQ) I-BET726 (**12**) bound to BRD4 BD1 as an instructive example of the typical interactions between a small molecule and a pan-BET family bromodomain, the N-1 acetate mimics the endogenous acetyl lysine and makes a direct hydrogen bonding interaction with Asn140 and a through-water interaction with Tyr97 (Figure 2a and 2b). [27,28] This water molecule is part of a highly conserved network at the base of the binding pocket and the acetate methyl group protrudes into a small pocket adjacent to this network. The chiral C-2 methyl group has *S* absolute stereochemistry and occupies a small lipophilic area next to Leu94. The BRD4 BD1 gatekeeper residue is Ile146 which allows access to a lipophilic region known as the WPF shelf consisting of Trp 81, Pro82 and Phe83 (Figure 2c). The chiral *R*-amine positions the hydrophobic chloroaryl moiety onto the WPF shelf with the ring perpendicular to the protein surface and the chloro-group adjacent to Trp81. Occupation of the WPF shelf is a common strategy for both small molecule potency and selectivity at the BET bromodomains and removal

of this interaction is typically highly detrimental to activity.[29] The 6-position phenyl ring protrudes into the ZA channel making an edge-to-face interaction with Trp81 and the carboxylic acid group does not appear to make any interactions with the protein and sits surrounded by bulk solvent.

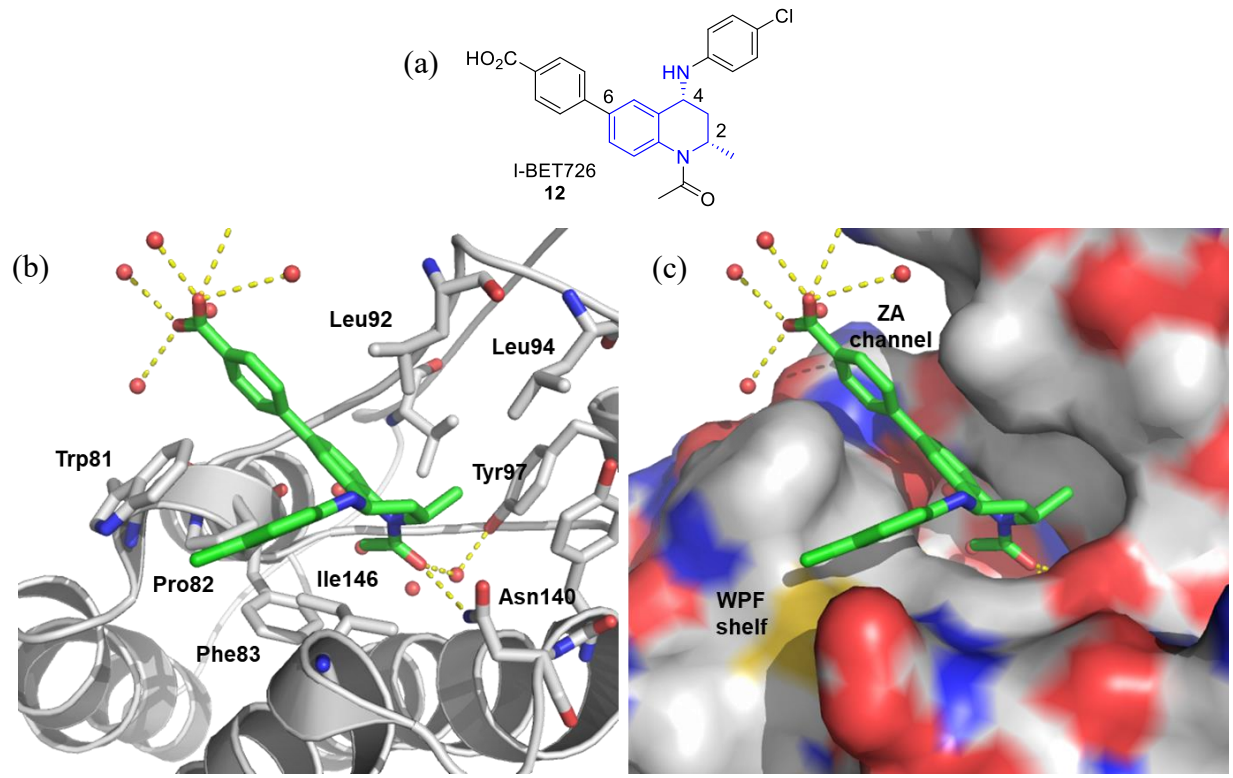

Figure 2. (a) Structure of I-BET726 (**12**). The 2*S*,4*R*-THQ core is highlighted in blue; (b) Crystal structure of **12** (green) bound to BRD4 BD1 (grey) (pdb: 4bjx). Water molecules are shown as red spheres and hydrogen bonds are marked in yellow; (c) As (b), but with the protein surface shown.

GSK has previously disclosed studies on the ligand efficient THQ template culminating with in vivo active pan-BET inhibitor I-BET726 (**12**),[28] and it is also of note that in 2016 Forma Therapeutics disclosed work on developing THQ BET inhibitors in the patent literature.[30] However, despite substantial internal work on this chemotype, challenges around unbound clearance, solubility, permeability and CYP3A4 inhibition still remained which precluded

identification of a candidate molecule and led to a shift of chemistry focus onto alternative templates.[15,23] In 2014, with molibresib (**1**) undergoing multiple clinical trials and GSK2820151 (**9**) progressing towards the clinic, there was a timebound portfolio need within GSK for additional pan-BET clinical candidates to improve the probability of success of delivering transformational medicines to patients. This portfolio approach aimed to mitigate lead molecule risks associated with potential off-target toxicities and developability challenges such as the discovery of a less soluble polymorph.[31] Herein, we describe how a wealth of THQ SAR and developability data generated over several years' worth of effort was leveraged to identify improved probability of success lipophilicity space (chromLog$D_{pH7.4}$ 2–4) for design. This led to the identification of orally bioavailable clinical candidate I-BET567 which addressed the limitations of previous molecules from this chemotype and demonstrated efficacy in mouse models of oncology and inflammation. Efforts to improve the synthetic route reduced the step count from 10 steps the first time the compound was made to a scalable four step route which ultimately delivered 4.18 kg of drug substance.

RESULTS AND DISCUSSION

Target Product Profile. For a pan-BET oral drug candidate, several key parameters were prioritised in accordance with GSK small molecule desired candidate criteria: BRD4 BD1 / BD2 $pIC_{50} > 6.5$ as representative members of the BET bromodomain family, passive permeability >30 nm/s as determined by in an artificial membrane permeability (AMP) assay, fasted state simulated intestinal fluid (FaSSIF) solubility >100 μg/mL, CYP3A4 $pIC_{50} < 4.5$ and property forecast index (PFI, defined as chromLog$D_{pH7.4}$ + number of aromatic rings) ≤6.[32] The solubility of a developable crystalline polymorph was a key parameter within this back-up effort due to the complexity brought about by the identification of a less soluble polymorph during the development of

GSK2820151 (**9**).[23] Molibresib (**1**) is predominantly eliminated by CYP3A4 metabolism and at the time it was hypothesized (and later confirmed) that coadministration of therapeutics that modulate CYP3A4 would alter molibresib exposure.[33] To mitigate this risk, a candidate that was not solely eliminated by a single metabolizing enzyme was a desirable profile. Finally, structural differentiation over existing GSK pan-BET candidates was required to mitigate the risk of potential idiosyncratic toxicities.[34] The THQ chemotype fit this requirement well with I-BET726 (**12**) demonstrating a Tanimoto similarity score of 0.301 and 0.254 when compared with molibresib (**1**) and GSK2820151 (**9**) respectively. At the outset of this effort, 1999 THQ molecules had already been generated and profiled against not just BRD4 BD1/BD2, but also a variety of developability assays within GSK. Despite challenges encountered previously with this template (vide supra), with a timebound opportunity to deliver a differentiated pan-BET candidate molecule, the chemistry team felt that leveraging the historical THQ dataset represented the highest probability of success.

Data visualization and compound design. The dataset of 1999 THQ molecules contained a wealth of SAR and developability knowledge and we set out to extensively mine this data in order to drive the medicinal chemistry design strategy. Initially, the molecules were classified as either acidic (121), basic (682) or neutral (1196) based on in silico predicted pK_a values. Comparison of these groups of compounds enabled a high-level understanding of design hypothesis parameters. While there was little dependence between ionization state and BRD4 BD1 potency (Figure 3a), there was a clear drop in passive permeability and solubility for acids compared with basic and neutral compounds, although this was based on an extremely limited number of acid solubility data points (Figure 3b and c). In contrast, acidic molecules showed less propensity for CYP3A4 inhibition, albeit with a reduced number of data points supporting this conclusion (Figure 3d).

Comparison of these findings to those reported by Gleeson in his analysis of a set of 30000 diverse molecules from the GSK collection showed the same trends between ionization for passive permeability and CYP3A4 inhibition.[35] However, in contrast to that observed for the set of THQ molecules, Gleeson found that for solubility acid > base > neutral highlighting the value of bespoke analyses where suitable data exists to enable them (Figure 3c). With an intracellular target and an oral route of administration required, focus turned to basic and neutral molecules as likely to offer the highest probability of success in delivering a soluble and permeable candidate molecule. However, the data also demonstrated that neutral and basic molecules represented the most lipophilic compounds made which due to similar potency levels concomitantly drove a dramatic and concerning drop in median lipophilic efficiency (LipE, calculated as BRD4 BD1 pIC_{50} – chrom$LogD_{pH7.4}$) values (Figure 3e and f).

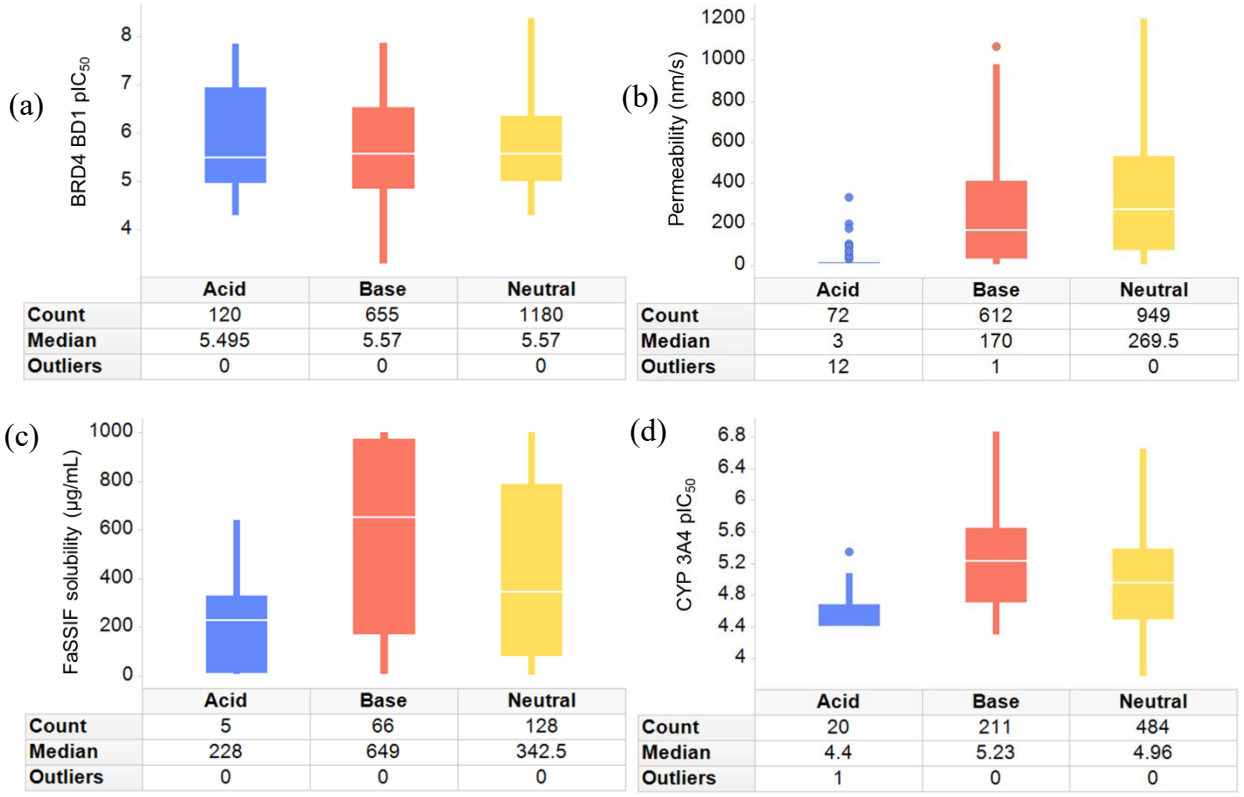

	Acid	Base	Neutral
Count	120	655	1180
Median	5.495	5.57	5.57
Outliers	0	0	0

	Acid	Base	Neutral
Count	72	612	949
Median	3	170	269.5
Outliers	12	1	0

	Acid	Base	Neutral
Count	5	66	128
Median	228	649	342.5
Outliers	0	0	0

	Acid	Base	Neutral
Count	20	211	484
Median	4.4	5.23	4.96
Outliers	1	0	0

8

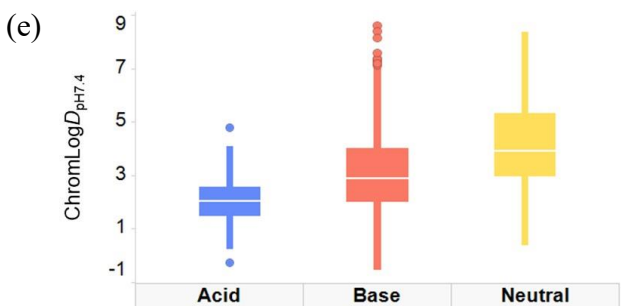

	Acid	Base	Neutral
Count	117	655	1080
Median	2.03	2.88	3.9
Outliers	2	9	0

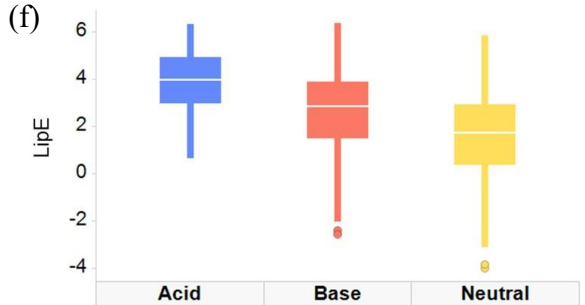

	Acid	Base	Neutral
Count	116	633	1072
Median	3.93	2.84	1.705
Outliers	0	2	2

Figure 3. Analysis comparing the impact that the ionization state of 1999 THQ molecules has against (a) BRD4 BD1 pIC_{50}; (b) Passive permeability as determined in the artificial membrane permeability assay (AMP); (c) FaSSIF solubility; (d) CYP3A4 pIC_{50}; (e) Chromlog$D_{pH7.4}$; (f) LipE as determined by BRD4 BD1 pIC_{50} – chromLog$D_{pH7.4}$.

Accordingly, attention turned to the lipophilicity space most likely to drive success to aid design hypothesis prioritization.[36] The chromLog$D_{pH7.4}$ values for all THQ molecules in this set were predicted using an internal GSK in silico model. The output was then correlated with measured values for the 1852 THQ compounds where data was available with an $R^2 = 0.919$ indicating excellent correlation between predicted and measured values (Supporting Information, Figure S1). To utilize as much data as possible across as wide a range of molecules, predicted lipophilicity values were used to identify desirable lipophilicity space for future molecules. Filtering the entire compound set to basic and neutral compounds with permeability, solubility and CYP3A4 data gave 140 THQ compounds which unfortunately represents only 7% of the total compounds and highlights the somewhat sporadic nature of historical data collection. Visualization of this data in a single chart demonstrated not only the strong dependence of these important developability measures on lipophilicity, but also enabled clear guidance of the desired lipophilicity space to target (Figure 4). Permeability (black line) showed a bell-shaped curve which required a

9

chromLog$D_{pH7.4}$ ≥1.5 to be measurable with a peak around 5. As expected, FaSSIF solubility (red line) dropped drastically with increasing lipophilicity and, in direct contrast, CYP3A4 inhibition increased steadily with lipophilicity. Of the compounds with a chromLog$D_{pH7.4}$ range 2–4, 32% (31 out of 97) demonstrated FaSSIF >100 µg/mL, permeability >30 nm/s and CYP3A4 pIC_{50} <4.5. In contrast, only 5% (2 out of 43) of the molecules outside of this lipophilicity range met these developability criteria. Thus, highlighting the complex and somewhat contradictory nature of lipophilicity on compound developability, a chromLog$D_{pH7.4}$ range of 2–4 appeared to give the highest probability of success for an oral drug candidate from the THQ chemotype.

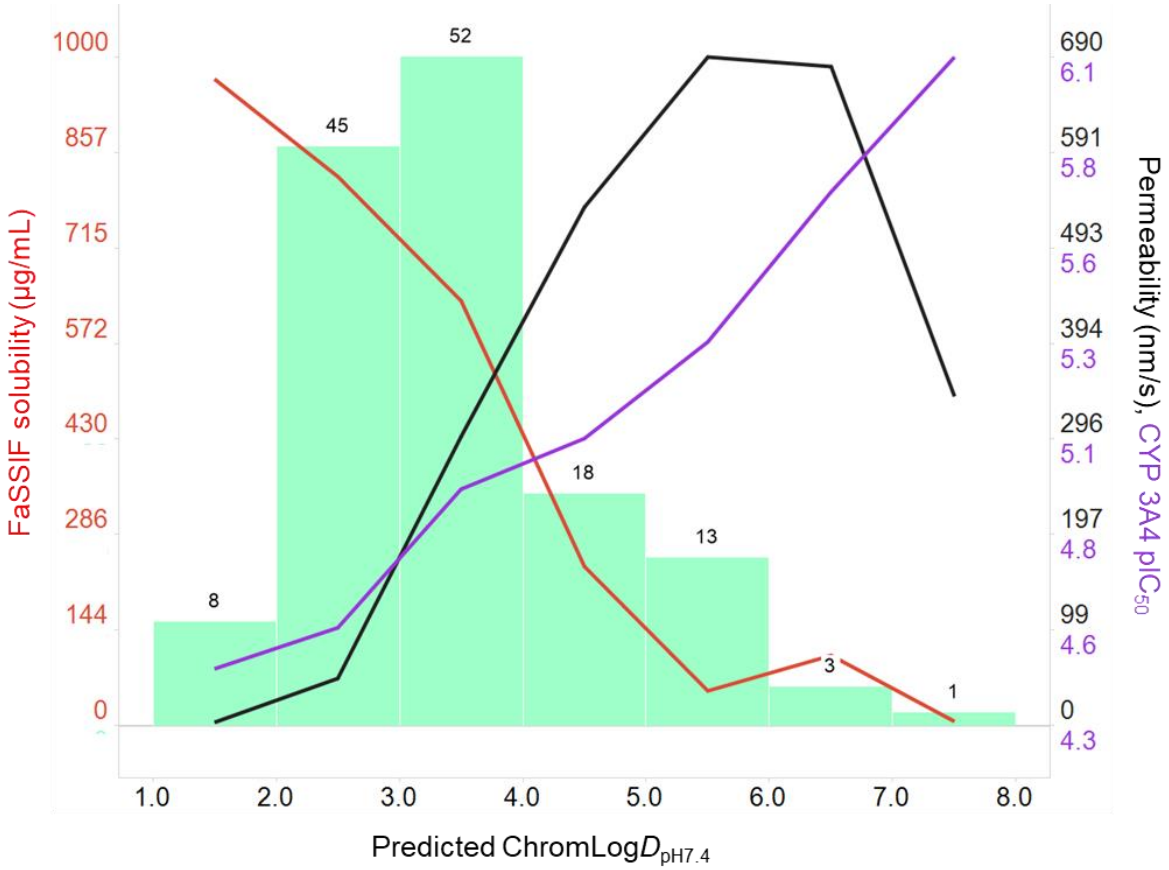

Figure 4. Visualization of binned predicted chromLog$D_{pH7.4}$ (green bar) compared to median artificial membrane passive permeability (nm/s) (black line) for each lipophilicity bin, median FaSSIF solubility (µg/mL) (red line) for each lipophilicity bin and median CYP3A4 pIC_{50} (purple

line) for each lipophilicity bin. The number of compounds in each lipophilicity bin is shown as a bar label.

With clear lipophilicity design parameters in hand, attention turned to activity against the BET bromodomains. BRD4 BD1 and BD2 TR-FRET assays have been used as representative members of the BET family throughout GSK's bromodomain drug discovery projects with data in both these assays for 1955 THQ molecules (pIC_{50} range <4 – 8.7). Most of the diversity in the compound set was in the groups occupying the WPF shelf, the 4-position, and the ZA channel protruding 6-position groups (Figure 2). To interrogate this data, a linear regression Free-Wilson analysis was undertaken across the 52 different 4-position and 74 different 6-position groups that appeared at least twice in the compound set (328 compounds in total).[37] This analysis demonstrated that not only was the structure-activity-relationship (SAR) across these two positions additive as judged by the R^2 correlation between the measured and predicted potency (Supporting Information, Figure S2), but also provided calculated coefficients for each unique group to predict the activity of novel compounds. This additive coefficient-based model predicted the BRD4 BD1 / BD2 potency with ±0.5 log unit accuracy of ≥95% compounds (BRD4 BD1: 319 / 328 (97%), BRD4 BD2: 313 / 328 (95%)) when utilized on molecules in the training set (Supporting Information, Figure S2).

The Free-Wilson analysis highlighted the importance of a substituted aryl ring in the 4-position in driving BRD4 activity via occupancy of the WPF shelf, however it had not escaped attention that these groups are embedded anilines (e.g. 4-chloroaniline in I-BET726 (**12**)), the potential release of which via elimination either in vivo or during manufacture was a carcinogenicity risk. The amino-aryl groups in the 4-position were assessed for known and predicted Ames[38] liability utilizing both an internal GSK database of Ames data and an internal in silico energy of the highest occupied molecular orbital (eHOMO) model.[39] Only those groups with a known Ames negative

result or if lacking experimental data, predicted to be low risk of Ames mutagenicity by the eHOMO model were carried forward (R^4, Table 1). Consideration of the target lipophilicity space (chromLog$D_{pH7.4}$ 2–4) against the GSK small molecule candidate criteria of PFI ≤6 (defined as chromLog$D_{pH7.4}$ + number of aromatic rings) strongly suggested that efforts should focus onto targets bearing only two aromatic rings.[32] With the baseline 6-position group as a benzene ring (Free-Wilson coefficient = 0), analysis of the coefficients of the 74 groups from the Free-Wilson analysis revealed that while substituted aromatic groups in the 6-position had a positive impact on BRD4 potency (Free-Wilson coefficients >0), all non-aromatic groups in this vector had a negative impact on potency (Free-Wilson coefficients <0) (Figure 5).

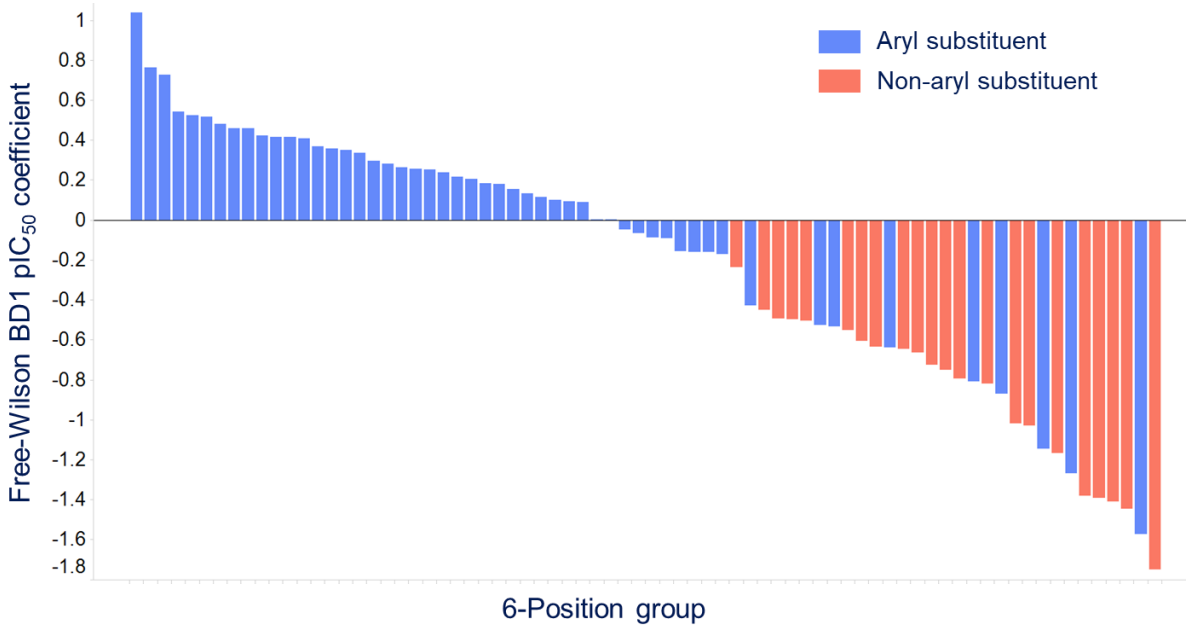

Figure 5. Bar chart showing the impact of the 6-position aryl (blue columns) and non-aryl (orange columns) groups on the Free-Wilson BRD4 BD1 pIC_{50} co-efficient for each group.

Nonetheless, in order to achieve the required PFI ≤6, the aromatic 6-position groups were removed and the non-aromatics with the least detrimental Free-Wilson coefficients identified (R^6, Table 1). Finally, virtual enumeration of the triaged 4- and 6-position groups gave 40 compounds

which following Free-Wilson potency and chromLog$D_{pH7.4}$ prediction were prioritised to give a target list of 22 THQ molecules (compounds **13-34**) in desirable lipophilicity space (Table 1). All the target molecules had a predicted BRD4 BD1 / BD2 pIC_{50} ≥6.1 which was considered acceptable bearing in mind the ±0.5 log unit accuracy of the prediction.

Table 1. Virtual enumeration of THQ molecules with predicted chromLog$D_{pH7.4}$ values

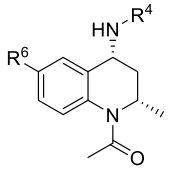

R^6 \ R^4	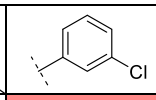	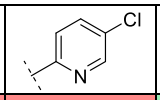	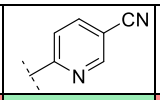	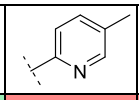	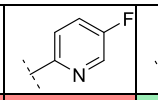	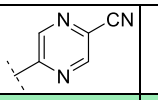	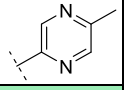	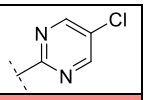
H	6.1	5.0	**13** 3.8	4.2	4.2	**14** 3.7	**15** 3.3	4.6
F	6.0	4.9	**16** 3.7	4.3	4.2	**17** 3.6	**18** 3.3	4.5
CN	5.6	4.5	**19** 3.3	**20** 3.9	**21** 3.8	**22** 3.2	**23** 3.0	4.1
$CONH_2$	**24** 3.7	**25** 2.6	1.7	**26** 2.0	1.9	1.5	1.3	**27** 2.2
CONHEt	4.7	**28** 3.5	**29** 2.5	**30** 2.9	**31** 2.8	**32** 2.4	**33** 2.1	**34** 3.1

Compound numbers are shown in bold. Predicted chromLog$D_{pH7.4}$ values <2 or >4 are colored red, values 2–4 are colored green.

Compound synthesis. A variety of different synthetic routes were utilized to access the target molecules taking advantage of bulk intermediates available within GSK from historical work on the THQ template. In particular, enantiopure isopropyl carbamate **35** proved especially versatile allowing rapid access to a number of targets.[28] Halogen-lithium exchange of bromide **35** with 2 equivalents of sec-BuLi was carried out with the aim of trapping with ethyl chloroformate to provide access to an intermediate to targets **24-34**.(Scheme 1). However, the major product of the reaction was the dehalogenated THQ which following carbamate deprotection gave amine **36**.

Subsequent palladium catalyzed Buchwald-Hartwig arylation provided the required targets **13-15** with R^6 = H.

Scheme 1. Synthesis of compounds **13-15**[a]

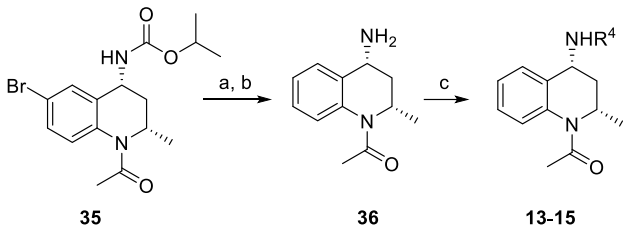

[a]Reagents and conditions: (a) s-BuLi (2 eq.), THF, –78 °C, 45 min then $ClCO_2Et$, –78 °C to –30 °C, 36%; (b) TBAF, THF, 65 °C, 60%; (c) ArBr, IPentPEPPSI, Cs_2CO_3, 1,4-dioxane, 100 °C.

Enantio- and diastereo-selective aza-Michael reaction with **37** afforded aniline **38** which was cyclized using sodium borohydride and magnesium chloride to give **39**, isolated as a single cis-diastereomer (Scheme 2).[40] Acetylation was followed by acid-mediated Boc cleavage to give amine **40**. Buchwald-Hartwig amination or thermal SNAr provided the target compounds which underwent chiral purification to increase the enantiomeric excess from ~87% to >95%.

Scheme 2. Synthesis of compounds **16-18**[a]

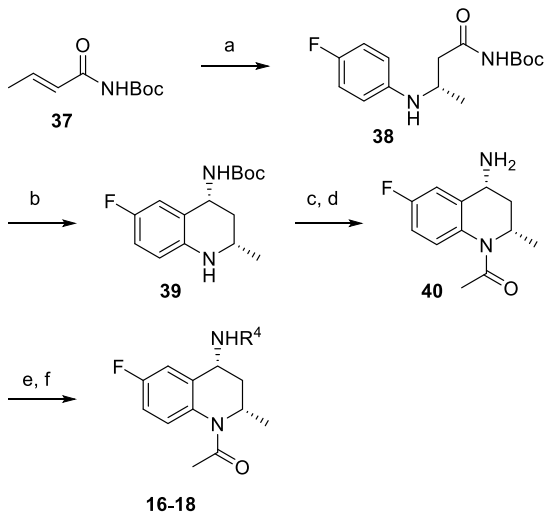

[a]Reagents and conditions: (a) 4-fluoroaniline, [(*R*)-(BINAP)Pd(MeCN)$_2$](OTf)$_2$, toluene, 35 °C, 14%; (b) $NaBH_4$, $MgCl_2$, EtOH / H_2O, –15 °C to rt, 34%; (c) Ac_2O, pyridine, CH_2Cl_2, rt, 99%; (d)

TFA, CH_2Cl_2, rt, 94%; (e) aryl halide, DIPEA, $PhCF_3$, 150 °C or ArBr, IPentPEPPSI, Cs_2CO_3, 1,4-dioxane, 100 °C; (f) chiral purification.

As disclosed previously, commercially available enantiopure amine **41** underwent Buchwald-Hartwig amination with bromobenzene, which was followed by regioselective electrophilic aromatic bromination to give **42** (Scheme 3).[41] Acid-mediated hydrolysis and then imide formation with Boc anhydride gave cyclisation precursor **43**. Cyclization with sodium borohydride and magnesium chloride formed the THQ ring system which underwent acetylation with acetyl chloride to give THQ **44** as a single *cis*-diastereomer. Palladium catalyzed Negishi cyanation with zinc cyanide was followed by acid-mediated deprotection to give amine **45**. This intermediate underwent thermal SNAr chemistry with the requisite aryl halides to give targets **19**, **22** and intermediate **46**. Base mediated nitrile hydrolysis of **46** with hydrogen peroxide provided primary carboxamide **27**.

Scheme 3. Synthesis of compounds **19**, **22** and **27**[a]

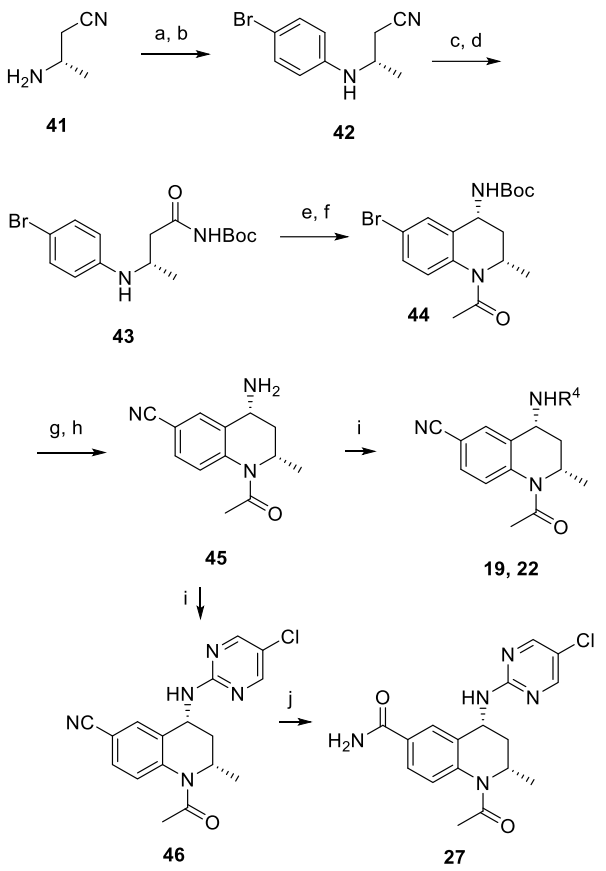

[a]Reagents and conditions: (a) Bromobenzene, $Pd(OAc)_2$, DavePhos, $PhB(OH)_2$, Cs_2CO_3, THF, toluene, 80 °C, 35%; (b) NBS, DMF, 0 °C, 82%; (c) H_2SO_4, toluene, 60 °C, 89%; (d) Boc_2O, *t*-BuOLi, THF, –10 °C to 0 °C, 77%; (e) $NaBH_4$, $MgCl_2 \cdot 6H_2O$, EtOH, H_2O, –5 °C, 86%; (f) AcCl, pyridine, CH_2Cl_2, rt, 82%; (g) $Zn(CN)_2$, $Pd(PPh_3)_4$, DMF, 115 °C, 79%; (h) HCl, 1,4-dioxane, rt, 90%; (i) aryl halide, DIPEA, NMP, 160–180 °C; (j) H_2O_2, K_2CO_3, DMSO, H_2O, rt, 59%.

Lewis acid mediated deprotection of known *n*-butyl ester **47** proceeded smoothly to give primary amine **48** (Scheme 4).[41] Palladium catalyzed Buchwald amination introduced the required 4-position aromatics to give **49a**, **c-g** and subsequent hydrolysis with lithium hydroxide provided carboxylic acid intermediates **50a-g**. In contrast, Buchwald amination between **48** and 2-bromo-5-chloropyridine resulted in concomitant ester hydrolysis to directly generate **50b**. Amide bond formation between the appropriate carboxylic acid **50a-g** with either an ammonium salt or with ethylamine provided target compounds **24-26**, **28-32** and **34**.

Scheme 4. Synthesis of compounds **24-26**, **28-32** and **34**[a]

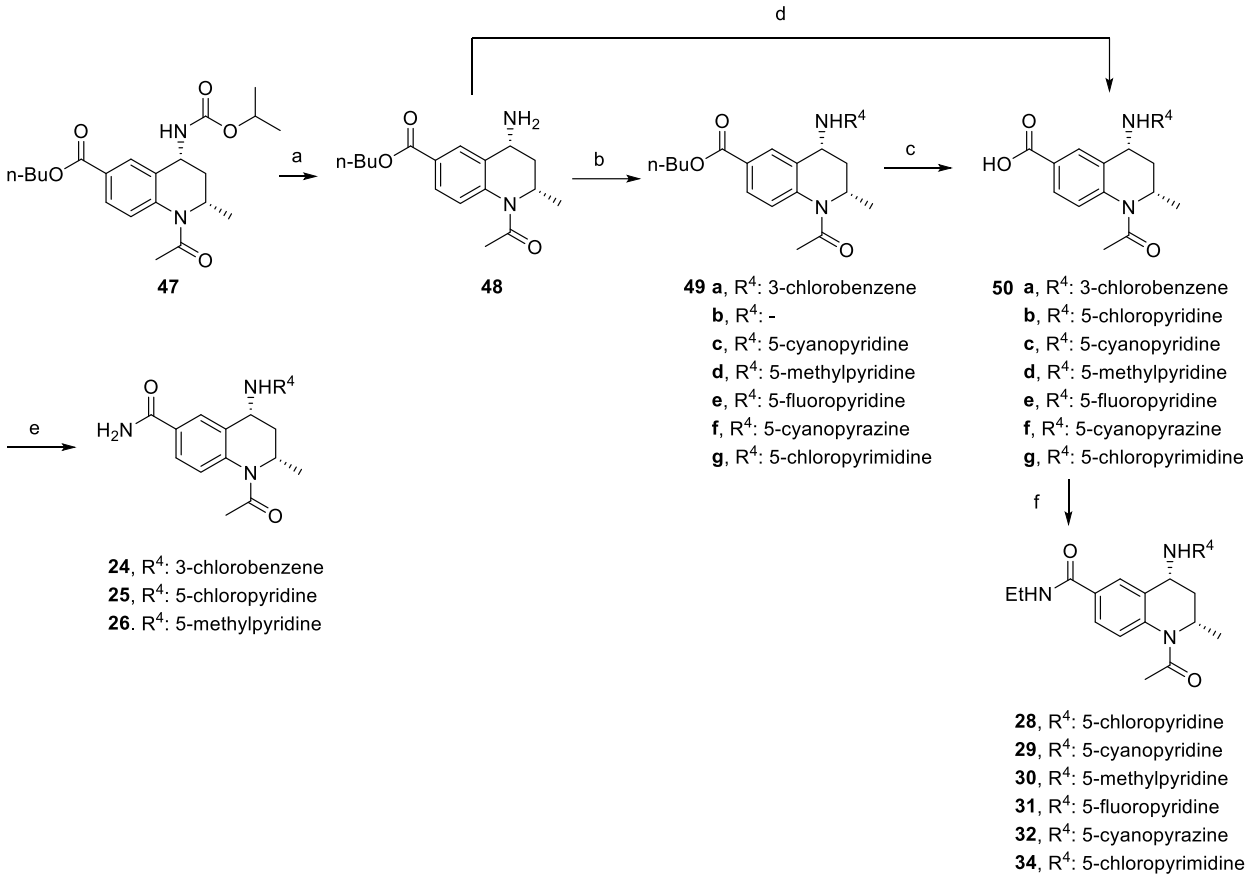

[a]Reagents and conditions: (a) $AlCl_3$, NEt_3, CH_2Cl_2, MeOH, 0 °C to rt, 86%; (b) aryl halide, Pd catalyst, phosphine ligand, base, solvent, heat; (c), LiOH, MeOH, THF, rt; (d) 2-bromo-5-chloropyridine, $Pd_2(dba)_3$, DavePhos, NaO*t*-Bu, 1,4-dixoane, 120 °C, 11%; (e) 1-hydroxy-1*H*-benzotriazole ammonium salt, EDC, N-ethylmorpholine, DMF, rt or NH_4Cl, HATU, DIPEA, DMF, rt; (f) $EtNH_2 \cdot HCl$, HOBt, EDC, N-ethylmorpholine, DMF, rt or $EtNH_2 \cdot HCl$, HATU, DIPEA, DMF, rt.

Initial biological and developability profiling. Ultimately 18 of the targeted 22 compounds were accessed and profiled with the syntheses of four molecules (**20, 21, 23** and **33**) unsuccessful in the time available to the chemistry team for compound synthesis. In accordance with the target product profile, initial screening focused on potency (desired BRD4 BD1/ BD2 pIC_{50} >6.5), lipophilicity (desired chrom$Log D_{pH7.4}$ = 2–4), solubility (desired FaSSIF >100 μg/mL) and permeability (desired AMP >30 nm/s) at the first stage of the cascade (Table 2). It was accepted that the initial FaSSIF solubility data would highly likely be generated using amorphous material

and thus represented a best-case scenario with the crystalline solubility expected to ultimately be lower.

Table 2. Profile of compounds **13-19**, **22**, **24-32** and **34**.

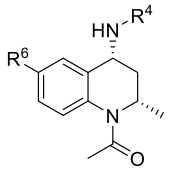

	R^6	R^4	BRD4 BD1/BD2 FRET pIC_{50}	chromLog $D_{pH7.4}$	BRD4 BD1/BD2 LipE[a]	FaSSIF (μg/mL)	AMP (nm/s)
13	H	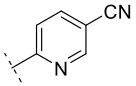	6.0 / 6.5	3.7	2.3 / 2.8	533	480
14	H	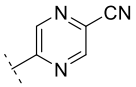	5.9 / 5.9	3.3	2.6 / 2.6	955	320
15	H	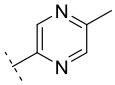	6.0 / 6.3	3.1	2.9 / 3.2	270	540
16	F	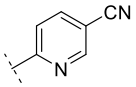	6.1 / 6.5	3.8	2.3 / 2.7	558	510
17	F	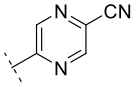	5.9 / 6.0	3.6	2.3 / 2.4	99[b]	300
18	F	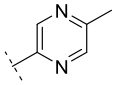	5.9 / 6.2	3.3	2.6 / 2.9	>1000	520
19	CN	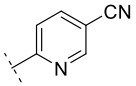	6.3 / 6.8	3.5	2.8 / 3.3	279	310
22	CN	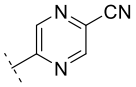	6.3 / 6.3	3.2	3.1 / 3.1	60	190
24	$CONH_2$	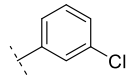	6.7 / 7.7	3.5	3.2 / 4.2	33	400
25	$CONH_2$	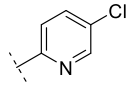	6.6 / 7.1	2.7	3.9 / 4.4	884	150
26	$CONH_2$	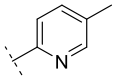	6.1 / 6.8	2.2	3.9 / 4.6	≥143[b]	82
27	$CONH_2$	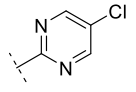	6.9 / 7.2	2.1	4.8 / 5.1	>1000	68
28	CONHEt	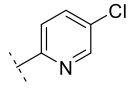	6.5 / 7.1	3.6	2.9 / 3.5	90	350

29	CONHEt	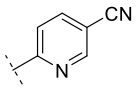	6.7 / 7.0	2.6	4.1 / 4.4	>1000	46
30	CONHEt	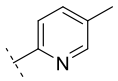	6.1 / 6.8	3.1	3.0 / 3.7	44	250
31	CONHEt	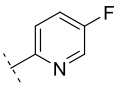	6.1 / 6.8	3.0	3.1 / 3.8	≥126[b]	230
32	CONHEt	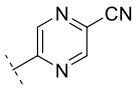	6.3 / 6.0	2.4	3.9 / 3.6	≥73[b]	<3
34	CONHEt	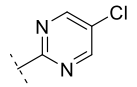	7.0 / 7.1	3.1	3.9 / 4.0	82	180

[a] LipE = BRD4 BD1 / BD2 pIC_{50} – chromLog$D_{pH7.4}$; [b] chemiluminescent nitrogen detection (CLND) solubility data

Pleasingly, across all the compounds prepared, the predicted chromLog$D_{pH7.4}$ matched the measured values with a R^2 correlation = 0.928 (Figure 6a). The result of this was that all the THQ compounds made had a measured PFI <6, a critical target of the medicinal chemistry effort.[32] A comparison of the Free-Wilson analysis predicted BRD4 BD1/BD2 pIC_{50} values highlighted that both models consistently overestimated the measured potency of this set of THQ molecules (Figure 6b). The overestimation was far more pronounced for the BRD4 BD2 predictions which unfortunately showed a larger than expected (>0.5 log unit) difference between measured and predicted values. The reasons behind the increased BRD4 BD2 overprediction relative to the BRD4 BD1 overprediction is not currently understood. However, all the BRD4 BD1 predictions were within 0.5 log units of the measured values demonstrating the utility of the Free-Wilson approach for the THQ template.

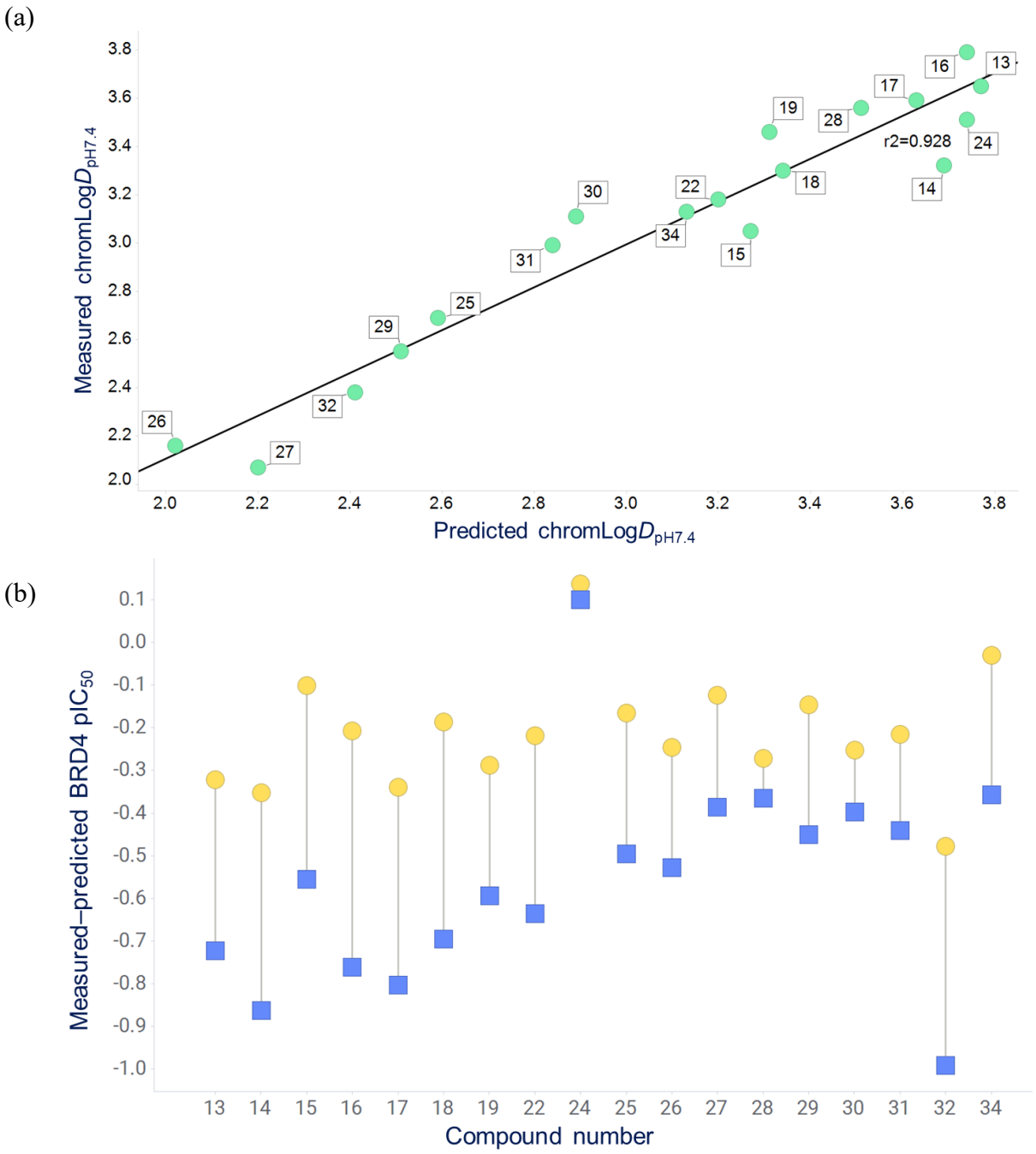

Figure 6. (a) Correlation of measured and predicted chromLog$D_{pH7.4}$ values for all compounds in Table 2 with the compound number shown in a box; (b) Difference in measured and Free-Wilson predicted potency calculated by measured pIC$_{50}$–predicted pIC$_{50}$ for BRD4 BD1 (yellow circles) and BRD4 BD2 (blue squares) for all compounds in Table 2.

Compounds with R^6 = H, **13**-**15** all demonstrated encouraging FaSSIF solubility (>100 μg/mL) and passive permeability (>30 nm/s), however the potency of all three compounds was insufficient to warrant further progression. When R^6 = F, with compounds **16**-**18**, the same story repeated itself, despite desirable solubility and permeability, the potency of the molecules precluded further progression. Clearly a substituent larger than H or F is required in the ZA channel to drive potency into acceptable ranges when targeting a chrom$Log D_{pH7.4}$ space of 2–4. Compounds **19** and **22** with R^6 = CN showed slightly improved potency, but still below the required BRD4 BD1 / BD2 pIC_{50} = 6.5 cut-off and despite the encouraging FaSSIF solubility and permeability of cyanopyridine **19**, it was not progressed any further. Primary carboxamide substituted **24**-**27** demonstrated a jump in BRD4 potency with all apart from methyl pyridine substituted **26** meeting the predefined cut-off for progression. Chlorobenzene **24**, pyridine **25** and pyrimidine **27** all met the permeability criteria (>30 nm/s), but **24** lacked the required FaSSIF solubility to be progressed further. Compounds **28**-**32** and **34** all contained an ethyl amide in the R^6 position with only **28**, **29** and **34** meeting the BRD4 BD1 / BD2 potency cut-off. FaSSIF solubility was sub-optimal for compounds **28** and **34**, with only **29** meeting both the solubility and permeability targets. From the original design hypothesis that targeting a chrom$Log D_{pH7.4}$ space of 2–4 would drive an increased probability of identifying molecules with FaSSIF >100 μg/mL and AMP >30 nm/s, 61% (11 / 18) of the target molecules met both of these target developability criteria.

Visualizing the relationship between potency, lipophilicity and lipophilic efficiency (LipE) is an important and powerful method to monitor the progression for all of these key molecular attributes of drug candidates.[36, 42] Accordingly, the compounds from Table 2 were visualized via scatter plots with BRD4 BD1 / BD2 pIC_{50} on the y-axis and chrom$Log D_{pH7.4}$ on the x-axis with diagonal lines representing different LipE values (Figure 7). From a BRD4 BD1 LipE perspective, five of the

compounds occupy space in the bottom right hand corner with an LipE <3 and a further seven clustered around the LipE = 3 line (Figure 7a). However, highlighting the utility of this type of visualization, the three compounds passing the predefined potency, solubility and permeability progression criteria are located towards the top left-hand corner with higher LipE values (**25**, **29**, and **27**). A similar pattern is also shown when visualizing the BRD4 BD2 LipE with the compounds that meet the pre-defined developability criteria for progression found with higher LipE values (Figure 7b). Of note is the stand-out BRD4 BD1 and BRD4 BD2 LipE for **27** compared to the complete set (LipE: 4.8 and 5.1) which gave the medicinal chemistry team optimism for future profiling.[36]

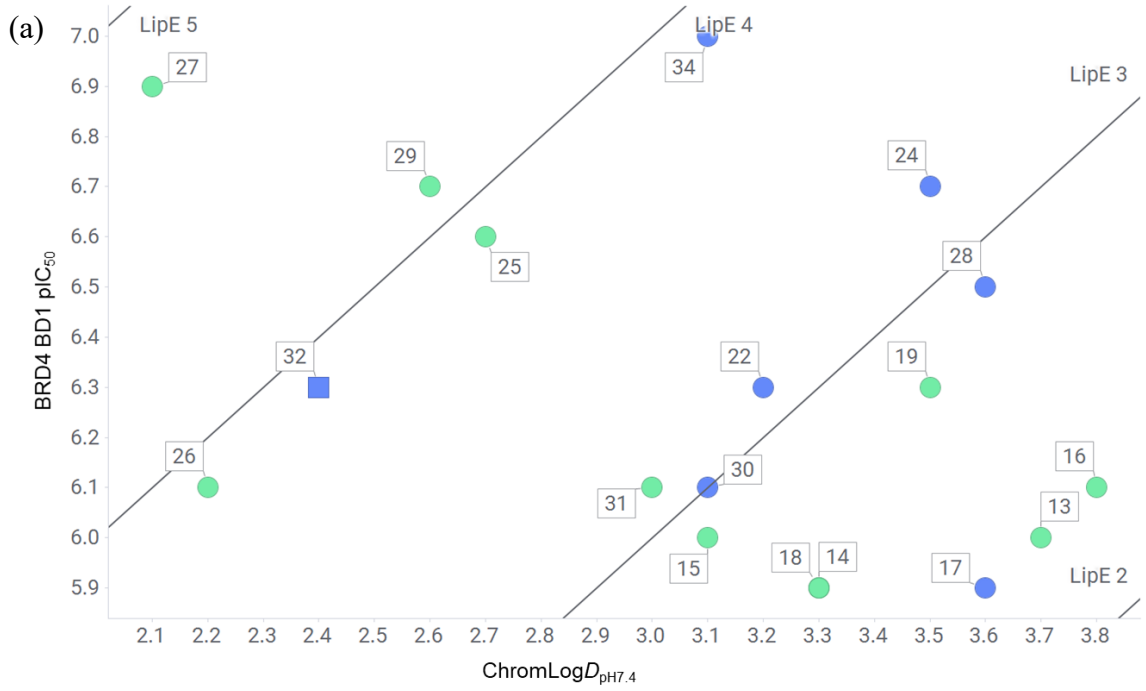

22

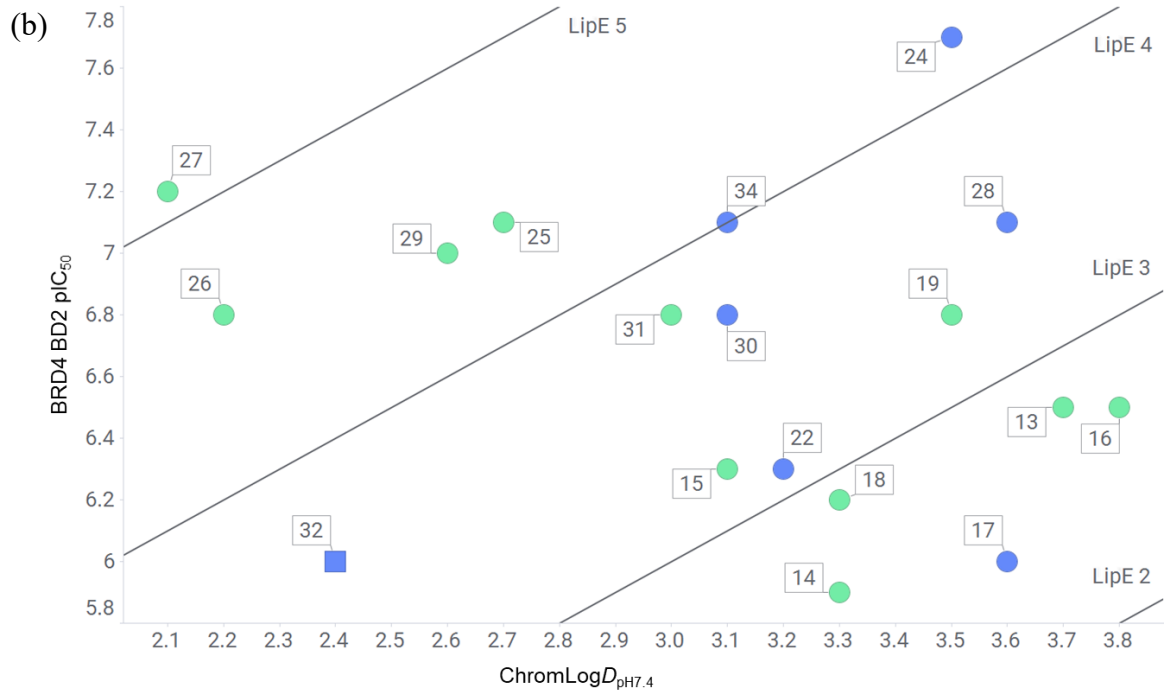

Figure 7. (a) Plot of BRD4 BD1 potency against chromLog$D_{pH7.4}$; (b) Plot of BRD4 BD2 potency against chromLog$D_{pH7.4}$. In both plots, the diagonal lines represent LipE values. Compounds with FaSSIF solubility >100 µg/mL are colored green and <100 µg/mL are blue. Compounds with AMP >30 nm/s are circles and <30 nm/s are squares.

Further biological and developability profiling. Only three THQ molecules were suitable for progression to the next phase of profiling, representing an 83% attrition from the 18 compounds initially synthesised. Accordingly, the compounds were profiled in pharmacologically relevant cellular assays, off-target liability assays and in vitro hepatocyte clearance assays (Table 3).

Table 3. Further profiling of compounds **25**, **27** and **29**.[a]

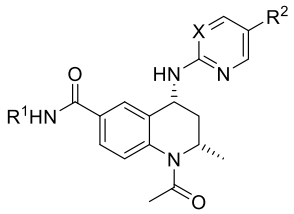

23

	R^1	X	R^2	hWB MCP-1 pIC_{50}	CYP3A4 pIC_{50}	CYP3A4 MDI	hERG pIC_{50}	Rat / Dog / Human hepatocyte CL_{int} (mL/min/g tissue)
25	H	CH	Cl	6.4	<4.4	No	<4.3	n.d.
27	H	N	Cl	6.7	<4.4	No	<4.3	<0.80 /<1.26 / <0.87
29	Et	CH	CN	6.6	<4.4	No	<4.3	4.30 / <1.26 / <0.87

[a] n.d. = not determined

With BET bromodomain inhibition driving a profound anti-inflammatory phenotype, cellular activity was examined. Inhibition of the proinflammatory cytokine monocyte chemoattractant protein-1 (MCP-1) in lipopolysaccharide (LPS) stimulated human whole blood (hWB) provides both evidence of cellular target engagement and a clinically relevant biomarker of BET inhibition.[43] The three remaining THQ compounds were screened in a LPS-stimulated hWB assay with all of them demonstrating inhibition of MCP-1 at concentrations <0.5 μM. Pleasingly, profiling against CYP3A4 demonstrated pIC_{50} <4.5 with no evidence of metabolism dependent inhibition (MDI) and all three compounds showed a low risk of hERG inhibition. At this stage compound **25** was down prioritised due to the lower levels of activity in the hWB assay compared to **27** and **29**. Progression into in vitro hepatocyte incubations revealed an interesting separation between the two remaining compounds: **27** and **29** both showed promising intrinsic clearance (CL_{int}) profiles in dog and human hepatocytes, however **29** was markedly less stable compared to **27** in rat hepatocytes. Although fraction unbound in hepatocytes was not generated at the time, with comparatively low levels of lipophilicity, it is likely that this difference in rat hepatocyte CL_{int} is real, rather than due to differential nonspecific hepatocyte binding.[44,45]

With desirable potency, developability data and a promising in vitro hepatic clearance profile, pyrimidine **27** was taken forward into a form screen which identified a single crystalline anhydrous phase pure form. This developable crystalline form with a 234°C melting point still showed desirable levels of solubility with >600 μg/mL solubility across a range of biorelevant media,

FaSSIF, fed state simulated intestinal fluid (FeSSIF) and simulated gastric fluid (SGF) (Supporting Information, Table S5).

Table 4. Pharmacokinetic profile of compound **27** following intravenous infusion and oral administration in male wistar han rat and beagle dog[a]

Species	Dose iv[b] / po[c] (mg/kg)	CL_b (mL/min/kg)	$CL_{b,u}$ (mL/min/kg)	CL_{renal} (mL/min/kg)	V_{ss} (L/kg)	$V_{ss,u}$ (L/kg)	$t½$ (h)	Fpo (%)	fu_b
rat	1.3 / 3	25	109	7	2.4	10.4	1.6	99[d]	0.23
dog	1.0 / 3	8.1	20	6.9	1.2	2.9	1.8	98	0.41

[a]Values are mean, n = 3 unless otherwise stated; [b]IV dose 1 h infusion in DMSO and (10%, w/v) Kleptose HPB in saline (2%:98% (v/v); [c]PO dose vehicle: 1% (w/v) methycellulose (400 cps) *(aq)*; [d]mean n = 2.

In both rat and dog, **27** had consistent in vivo pharmacokinetics with a moderate blood clearance, moderate volume of distribution and terminal half-life (Table 4). Renal clearance of parent drug was observed in both species, though the proportion of renal elimination to total clearance was higher in dog (85%) than in rat (28%). The mechanism of renal clearance was assumed to be net secretion as renal clearance was greater than the rate of filtration of unbound compound.[46] This mixture of elimination by hepatic and renal routes in both rat and dog makes the likelihood that **27** would be cleared solely by CYP3A4 in human low.[33] Following oral administration as a suspension in both species, compound **27** was found to be rapidly absorbed and completely bioavailable.

As the BET family represents only 8 members of the 61 bromodomains that comprise the human bromodomain phylogenetic tree, in parallel to the above pharmacokinetic studies, the bromodomain selectivity profile of compound **27** was determined.[47] BROMOscan profiling of **27** demonstrated a BET selective profile with expected activity against all eight BET family bromodomains (BET family pKd 7.4–8.3) and the closest off-target CREBBP / EP300 (pKd 5.6) (Supporting Information, Table S2).[48] Additionally, **27** had an excellent profile in the GSK enhanced cross-screening panel of 53 pharmacologically relevant off-target liability assays (Supporting Information, Table S3). As discussed above in the data analysis section, utilizing 4-

position anilinic substituents with a low risk of mutagenicity was a purposeful design choice. In the case of **27**, the 4-position aniline (5-chloro-2-aminopyrimidine) is a known Ames negative molecule and **27** itself was also not mutagenic when tested in the Ames assay.

Crystallography of **27** bound to BRD4 BD1 was used to confirm the expected binding mode and mechanism of action as an acetyl lysine mimetic (Figure 8). An overlay of **27** with I-BET726 (**12**) showed an almost identical overlap of the acetate acetyl lysine mimetic, 2*S* methyl group and THQ core making the same canonical hydrogen bonding interactions to Asn140 and via water to Tyr97 (Figure 8a and b). The 4-position substituent of **27** adopted a slightly different position and an altered torsion angle compared with I-BET726 (**12**), but still occupied the lipophilic WPF shelf region of the BRD4 BD1 bromodomain (Figure 8a and c). The pyrimidine makes a hydrogen bonding interaction with solvent molecules and the pendant chloro-group sits adjacent to Trp81. The 6-position carboxamide has a 22.6° dihedral angle relative to the THQ aryl ring consistent with that observed with other primary aryl carboxamides in the Mogul database.[49] The 6-position primary carboxamide occupies the ZA channel entrance and is engaged in hydrogen bonding with bulk water.

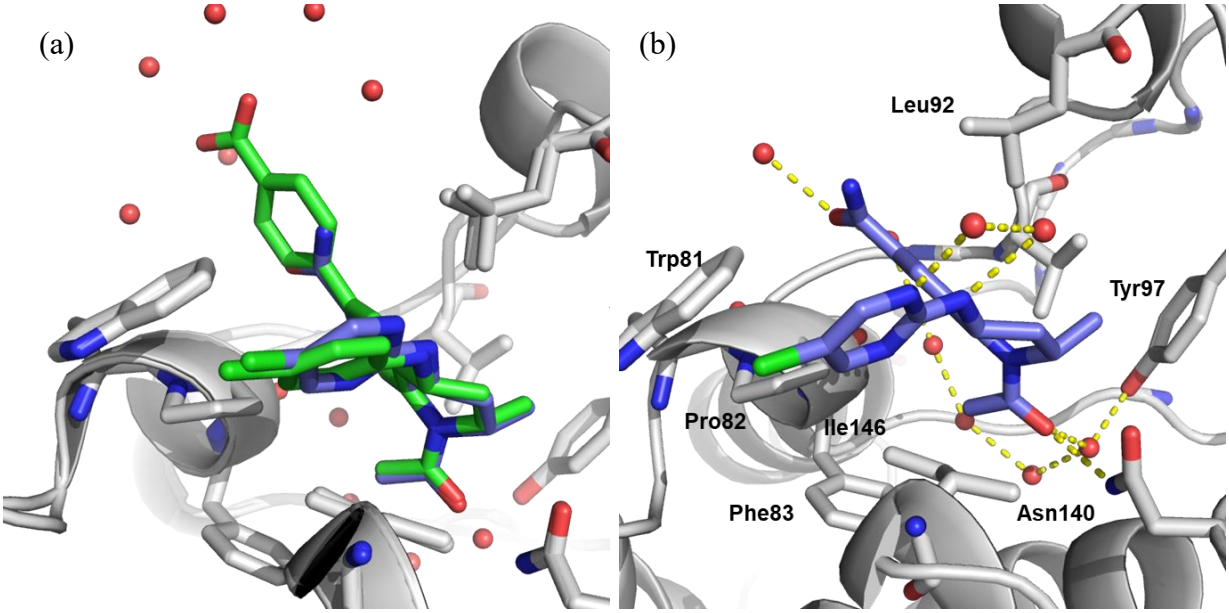

26

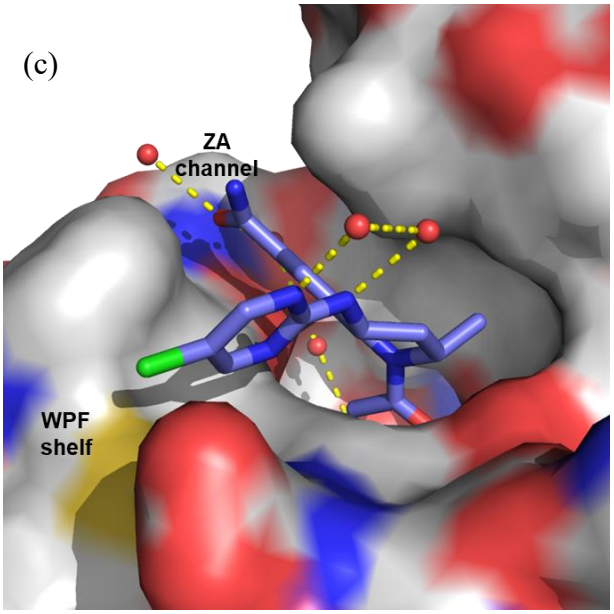

Figure 8. (a) Overlay of the crystal structure of I-BET726 (green) bound to BRD4 BD1 (grey) (pdb:4bjx) and **27** (blue) bound to BRD4 BD1 (grey) (pdb: 7qdl); (b) Crystal structure of **27** (blue) bound to BRD4 BD1 (grey) (pdb: 7qdl). Water molecules are shown as red spheres and hydrogen bonds are marked in yellow; (c) As (b), but with the protein surface shown.

Improved synthesis of 27. At this stage, the potency, developability and pharmacokinetic profile of **27** warranted further downstream in vivo studies and more material was required to support this. The first time compound **27** was made involved a 10-step sequence with an un-optimized 4.4% overall yield from commercial materials which involved nine isolated intermediates and four column chromatography purifications (Scheme 3). This original route was suitable for synthesis of the initial ~150 mg batch of material, however decagram amounts of **27** were required to support imminent in vivo efficacy and safety studies. While it was likely that the initial route could be optimized to improve yields, remove chromatographic purification and marginally reduce the number of steps, a drastic redesign was sought to access the compound in a fundamentally different manner with improved scalability and a vastly reduced step count.

However, this was not a trivial task as the complexity of the synthesis of **27** is directly related to the densely functionalized THQ core itself with the 2*S*, 4*R* absolute configuration essential for BET activity.[28] In the route described in Scheme 3, the relative and absolute 2*S*, 4*R*-stereochemistry of this core was accessed over 5 steps in 16.9% yield from a chiral amine derived from *L*-alanine. It had not escaped our attention that torcetrapib (**58**), a cholesterylester transfer protein (CETP) inhibitor, also contains a highly similar densely functionalized THQ core,[40,50] albeit with the opposite absolute stereochemistry to that required for **27**. As a result of the clinical development of torcetrapib, there have been multiple synthetic routes published, including an elegant chiral Brønsted acid catalyzed three-component Povarov reaction to rapidly access the THQ core.[51] This enantio- and diastereoselective reaction formed the cornerstone of a drastically improved synthetic route to **27** (Scheme 5).

Scheme 5. Four step scalable synthesis of **27** and structure of torcetrapib (**58**).[a]

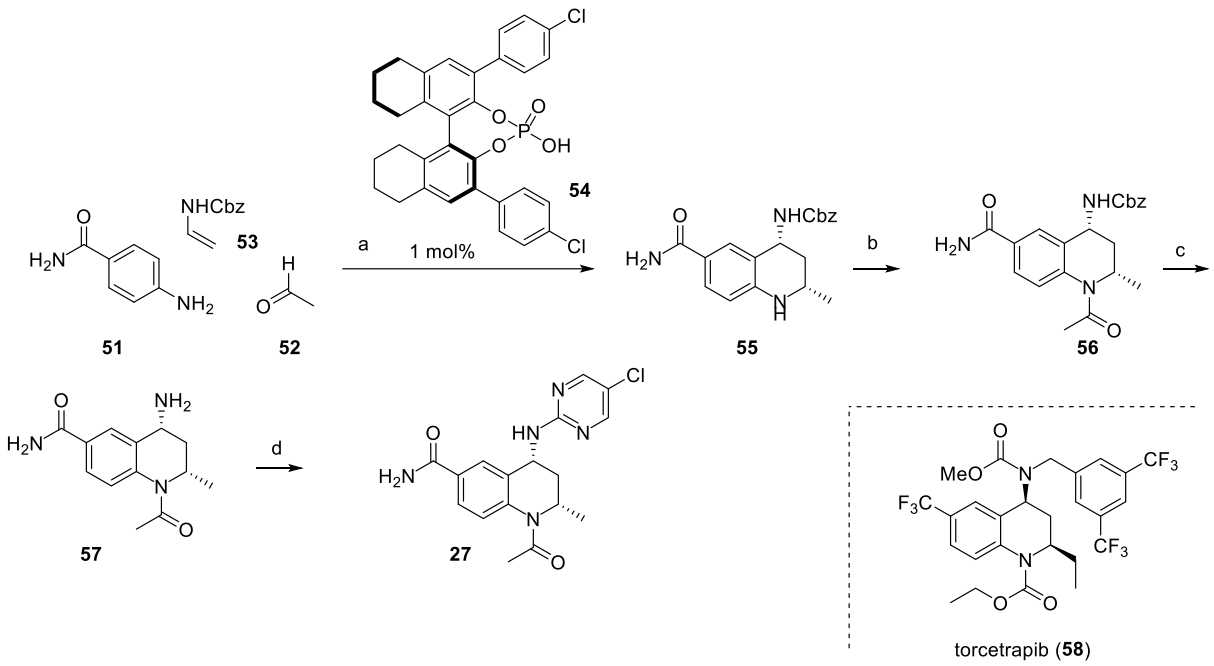

[a]Reagents and conditions: (a) CH_2Cl_2, 0 °C to rt, 66%; (b) AcCl, NMP, 0 °C to rt, 82%; (c) Pd/C, H_2, EtOH, 50 °C, 89%; (d) 2,5-dichloropyrimidine, DIPEA, DMSO, 120 °C, then seeded recrystallization, 65%.

There were no examples of acetaldehyde (**52**) or 4-aminobenzamide (**51**) being used as reaction components to deliver the THQ core in the original report from Liu and co-workers,[51] so we were delighted to see the reaction scope extend to provide functionalized core **55** in a single step in 66% yield. To deliver the required 2*S*, 4*R*-stereochemistry, the opposite enantiomer of the Brønsted acid catalyst **54** to that described by Liu and co-workers was utilized resulting in **55** as a single cis-diastereomer in >95% ee. With the key stereocenters set in a single step, acetylation, then hydrogenolysis and finally SNAr with 2,5-dichloropyrimidine proceeded smoothly to provide intermediate grade **27**. A seeded recrystallization delivered **27** as the desired anhydrous phase pure crystalline form with excellent purity, >99% ee and in 31% overall yield. This four-step reaction sequence proceeded without recourse to chromatography to rapidly provide 101 g of **27** in a single sequence. Minor tweaks to the solvent choice (EtOH to *i*-PrOH for the hydrogenolysis and DMSO to NMP for the SNAr) and telescoping the hydrogenolysis deprotection output into the SNAr step enabled subsequent delivery of 4.18 kg of **27** to support future non-clinical and clinical studies.

in vivo efficacy studies. With substantial amounts of **27** in hand, attention turned to demonstration of the in vivo efficacy of **27**. Numerous non-clinical studies of pan-BET inhibitors have demonstrated the profound anti-inflammatory effects of engaging the target in vivo.[52,53] The T cell dependent mouse immunization model is a mechanistic model representing immune activation to the T cell dependent antigen keyhole limpet haemocyanin 2, 4, 6-nitrophenol (KLH-TNP). Administration of a single dose of KLH-TNP provokes an antibody response which involves fundamental immune cell interactions between T and B cells and dendritic cells. Male CD1 mice (n=8 per group) were challenged with a single dose of KLH-TNP (via intraperitoneal route) 1 h post oral administration of **27** or the positive control (10 mg/kg pan-BET inhibitor I-

BET151).[54] A 30 mg/kg dose of **27** was selected for this study as this dose provided comparable potency adjusted exposure to other pan-BET inhibitors known to deliver efficacy in this model and was also considered to provide optimal probability of achieving efficacy following an intermittent dosing regimen.[53] Following oral administration of **27** at 30 mg/kg daily (QD), every other day (QOD) or every third day (QOED) over a 14 day period to KLH-TNP challenged mice, statistical analysis (one-way ANOVA with a post hoc Dunnett's test) indicated that significant reduction of IgG1 levels ($P < 0.001$) was observed following QD and QOD dosing (98% and 93% inhibition respectively) but not QOED dosing when compared to vehicle controls (Figure 9a). **27** was also shown to produce similar reduction of IgG1 as the positive control compound, pan-BET I-BET151, when dosed QD or QOD. PK analysis confirmed that following 30 mg/kg dose administration at QD, QOD and QOED, the C_{max} remained the same (8.5 µM) though a dose dependent reduction in $AUC_{0\text{-}72\ h}$ (103, 69 and 34 µM.h, respectively) and unbound C_{av} (1.43, 0.96 and 0.48 µM, respectively) over a 72 h dosing period was observed (Figure 9b). Mouse bodyweights were not significantly affected across the 14 days of compound administration indicating that **27** was well tolerated.

(a)

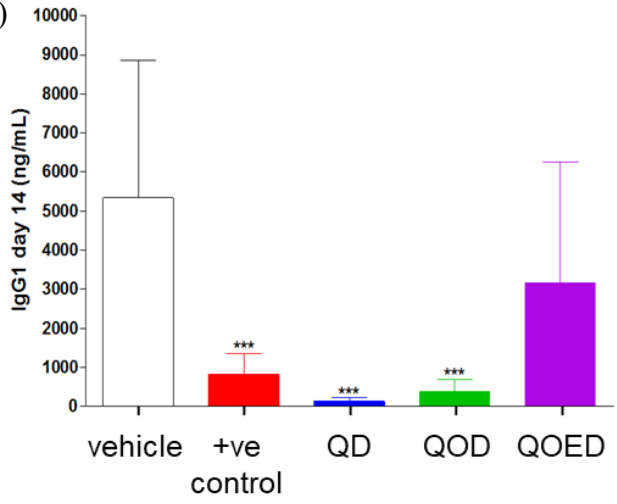

30

(b)

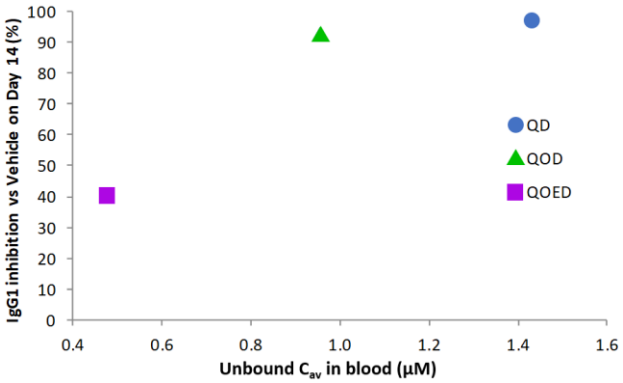

Figure 9. (a) Reduction in circulating IgG1 on Day 14 following daily dosing of positive control I-BET151 at 10 mg/kg and daily or intermittent oral dosing of **27** at 30 mg/kg in CD1 male mice (mean + SD) ***=P<0.001; (b) Mean unbound average concentration of **27** and IgG1 reduction on Day 14 in CD1 mice following daily and intermittent oral dosing of **27** at 30 mg/kg.

As mentioned previously, all the pan-BET inhibitors currently progressing through clinical trials are doing so in oncology studies. To investigate whether **27** can drive anti-neoplastic mechanisms in an in vivo setting following chronic oral dosing, a mouse xenograft tumor model was employed. The mouse strain used, NOD/SCID, is deficient for immune function and therefore allows human cancer cells to be administered without provoking a xenoantigenic immune response. Nuclear protein in testes (NUT) midline carcinoma (NMC) is a poorly differentiated carcinoma characterized by the occurrence of primary malignant epithelial tumors in the midline structures, a chromosomal translocation at t(15,19), and the expression of a fusion protein containing NUT and BRD3 or BRD4.[55] Consistent with the biology of this prototypic BET-driven malignancy, **27** effectively inhibited the proliferation of human NMC cell line 11060 in vitro with a mean $gpIC_{50}$: 6.2 (0.63 μM). To investigate the translatability of this finding in vivo,[56] NMC 11060 cells were administered to NOD/SCID male mice (n=7 per group), and tumors allowed to reach 160-300 mm^3 prior to randomization and commencement of once daily oral (PO) dosing of **27** at 3 mg/kg, 10 mg/kg or 30 mg/kg. Dosing was continued for 20 days with regular measurement of tumor

volumes. This led to a rapid and clear statistically significant reduction in tumor growth compared to vehicle controls at both 10 and 30 mg/kg (Figure 10a and b). No reduction was observed following administration at 3 mg/kg (data not shown). Furthermore, the 30 mg/kg dose reduced the mean tumor volume to below the day 1 starting volume, indicating that **27** can decrease tumor size. Measured drug concentrations at 0.5 h on day 20 in the mouse xenograft model are in line with those of simulated profiles derived from a standalone PK study at 3 mg/kg in CD1 mice indicating dose proportional exposure and that no accumulation occurs following repeat oral dosing (Supporting Information, Figure S3). Comparing tumor reduction to **27** concentration suggests an unbound C_{max} concentration of at least 2 µM and unbound $AUC_{0\text{-}24\ h}$ of at least 10 µM.h is associated with tumor volume reduction of more than 50% (Figure 10c). This corresponds with unbound exposure of **27** above the unbound NMC 11060 cell gIC_{50} for >3 up to 6 h each day (Supporting Information, Figure S3). However, a single mouse from the 10 mg/kg dose group did not show any reduction in tumor growth despite having similar unbound concentrations on days 1, 10 and 20 of **27** at 0.5 h post-dose compared to others within this dose group. All three doses were well tolerated by the mice, apart from one mouse in the 30 mg/kg group which lost 19.6% body weight resulting in euthanasia on day 20.

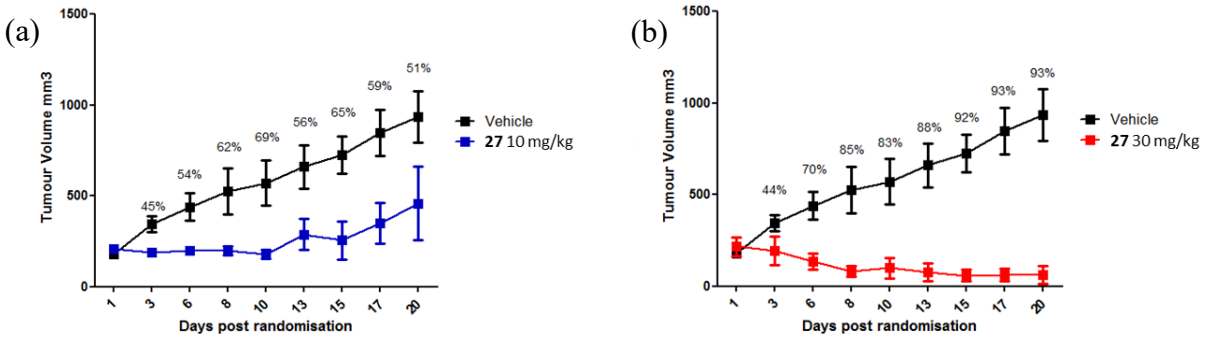

32

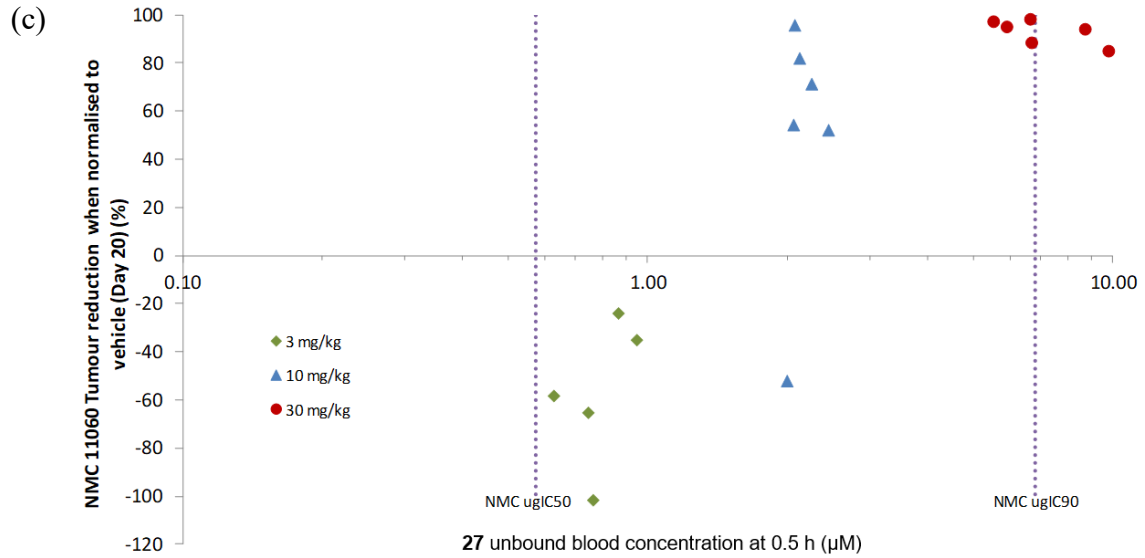

Figure 10. Mean +/- SD tumor volume in the mouse NMC Xenograft model over 20-day dosing period (n=7) at (a) 10 mg/kg and (b) 30 mg/kg. The % inhibition value quoted where statistical significance ($P<0.05$) was observed. The data are represented as means with standard deviation error bars; (c) Relationship between unbound blood concentrations of **27** and tumor reduction on Day 20 in individual NOD/SCID mice normalized to mean vehicle (n=5/6).

Taken together, the combination of efficacy, pharmacokinetics and developability data packages supported **27** (GSK3383567, I-BET567) as a desired candidate quality oral small molecule suitable for clinical progression.[57]

CONCLUSION

In conclusion, we report the medicinal chemistry strategy employed to exploit a large historical dataset for the identification of increased probability of success lipophilicity space for the design of oral pan-BET THQ molecules. Free-Wilson SAR analysis was leveraged to identify preferred groups for potency which underwent virtual enumeration and then targets with a predicted chromLog$D_{pH7.4}$ 2–4 selected for synthesis. 18 pan-BET THQ compounds were accessed, profiled, and triaged against pre-defined progression criteria with **27** (I-BET567) standing out due

to improved LipE which drove high solubility, permeability, low risk of off-target liabilities and suitable pharmacokinetics for in vivo studies. Following dramatic improvements to the synthetic route, a scalable enantioselective multi-component Povarov reaction was used to deliver the densely functionalized THQ core and drug substance to support downstream studies. Profound efficacy was demonstrated in vitro and in vivo via models of inflammation and oncology which, together with developability data, confirmed **27** as a desired quality oral candidate molecule for clinical progression.

EXPERIMENTAL SECTION

Physicochemical Properties. Artificial membrane permeability, chromatographicLog*D* at pH 7.4, FaSSIF solubility and CLND solubility were measured using published protocols.[13]

Chemistry methods. All solvents were purchased from Sigma Aldrich (anhydrous solvents) and commercially available reagents were used as received. All reactions were followed by TLC analysis (TLC plates GF254, Merck) or LCMS (liquid chromatography mass spectrometry) using a Waters ZQ instrument. NMR spectra were recorded at ambient temperature unless otherwise stated using standard pulse methods on any of the following spectrometers and signal frequencies: Bruker AV-400 (^{1}H = 400 MHz, ^{13}C = 100.6 MHz), Bruker AV-500 (^{1}H = 500 MHz, ^{13}C = 125.8 MHz), Bruker AVII+ 600 (^{1}H = 600 MHz, ^{13}C = 150.9 MHz). Chemical shifts are reported in ppm and are referenced to tetramethylsilane (TMS) or the following solvent peaks: $CDCl_3$ (^{1}H = 7.27 ppm, ^{13}C = 77.00 ppm), DMSO-d_6 (^{1}H = 2.50 ppm, ^{13}C = 39.51 ppm) and CD_3OD (^{1}H = 3.31 ppm, ^{13}C = 49.15 ppm). Coupling constants are quoted to the nearest 0.1 Hz and multiplicities are given by the following abbreviations and combinations thereof: s (singlet), d (doublet), t (triplet), q (quartet), m (multiplet), br (broad). Column chromatography was performed on pre-packed silica

gel columns using biotage SP4, Isolera One or Teledyne ISCO apparatus. High resolution mass spectra (HRMS) were recorded on a Micromass Q-Tof Ultima hybrid quadrupole time-of-flight mass spectrometer, with analytes separated on an Agilent 1100 Liquid Chromatograph equipped with a Phenomenex Luna C18(2) reversed phase column (100 mm × 2.1 mm, 3 µm packing diameter). LC conditions were 0.5 mL/min flow rate, 35 °C, injection volume 2-5 µL. Gradient elution with (A) H_2O containing 0.1% (v/v) formic acid and (B) acetonitrile containing 0.1% (v/v) formic acid. Gradient conditions were initially 5% B, increasing linearly to 100% B over 6 min, remaining at 100% B for 2.5 min then decreasing linearly to 5% B over 1 min followed by an equilibration period of 2.5 min prior to the next injection. LCMS analysis was carried out on a Waters Acquity UPLC instrument equipped with a BEH column (50 mm × 2.1 mm, 1.7 µm packing diameter) and Waters micromass ZQ MS using alternate-scan positive and negative electrospray. Analytes were detected as a summed UV wavelength of 210 – 350 nm. Two liquid phase methods were used:

Formic – 40 °C, 1 mL/min flow rate. Gradient elution with the mobile phases as (A) H_2O containing 0.1% volume/volume (v/v) formic acid and (B) acetonitrile containing 0.1% (v/v) formic acid. Gradient conditions were initially 1% B, increasing linearly to 97% B over 1.5 min, remaining at 97% B for 0.4 min then increasing to 100% B over 0.1 min.

High pH – 40 °C, 1 mL/min flow rate. Gradient elution with the mobile phases as (A) 10 mM aqueous ammonium bicarbonate solution, adjusted to pH 10 with 0.88 M aqueous ammonia and (B) acetonitrile. Gradient conditions were initially 1% B, increasing linearly to 97% B over 1.5 min, remaining at 97% B for 0.4 min then increasing to 100% B over 0.1 min.

Mass-directed automatic purification (MDAP) was carried out using a Waters ZQ MS using alternate-scan positive and negative electrospray and a summed UV wavelength of 210–350 nm. Two liquid phase methods were used:

Formic – Sunfire C18 column (100 mm × 19 mm, 5 μm packing diameter, 20 mL/min flow rate) or Sunfire C18 column (150 mm × 30 mm, 5 μm packing diameter, 40 mL/min flow rate). Gradient elution at ambient temperature with the mobile phases as (A) H_2O containing 0.1% volume/volume (v/v) formic acid and (B) acetonitrile containing 0.1% (v/v) formic acid.

High pH – Xbridge C18 column (100 mm × 19 mm, 5 μm packing diameter, 20 mL/min flow rate) or Xbridge C18 column (150 mm × 30 mm, 5 μm packing diameter, 40 mL/min flow rate). Gradient elution at ambient temperature with the mobile phases as (A) 10 mM aqueous ammonium bicarbonate solution, adjusted to pH 10 with 0.88 M aqueous ammonia and (B) acetonitrile.

Melting point analysis was carried out using Buchi M-565 melting point apparatus and are uncorrected. IR spectra were obtained on a Perkin Elmer Spectrum 1 FTIR apparatus, with major peaks reported. The purity of all compounds tested was determined by LCMS and ^{1}H NMR to be >95% apart from compound **13** which showed 92% purity.

Isopropyl ((2*S*,4*R*)-1-acetyl-2-methyl-1,2,3,4-tetrahydroquinolin-4-yl)carbamate (59). To a stirred solution of isopropyl ((2*S*,4*R*)-1-acetyl-6-bromo-2-methyl-1,2,3,4-tetrahydroquinolin-4-yl)carbamate (**35**)[28] (5.06 g, 13.70 mmol in THF (100 mL) cooled to –78 °C under N_2 was added dropwise sec-butyllithium (1.4 M in cyclohexane) (20.0 mL, 28.0 mmol) whilst maintaining the internal reaction temperature below –65 ºC. The mixture was stirred for 45 min and then ethyl chloroformate (1.5 mL, 15.62 mmol) was added dropwise whilst maintaining the internal reaction temperature below –65 °C, and stirring was continued at –78 °C for a further 15 min. The mixture was allowed to warm to –30 °C before being quenched by the careful addition of EtOH (5 mL).

After allowing to warm to rt, the mixture was partitioned between EtOAc (100 mL) and 2 M aqueous sodium carbonate solution. The phases were separated, and the aqueous phase was extracted with further EtOAc (2 × 50 mL). The combined organic phases were washed with H_2O (50 mL) and saturated brine solution (50 mL), dried ($MgSO_4$), filtered and the solvent evaporated *in vacuo* to give a clear gum. The gum was redissolved in CH_2Cl_2 (10mL) and was purified by Biotage SP4 flash chromatography (100 g silica SNAP cartridge) eluting with 0-100% EtOAc in cyclohexane. The required fractions were combined and evaporated *in vacuo* to give a residue. The residue was again dissolved in CH_2Cl_2 (10mL) and was purified by Biotage SP4 flash chromatography (split across 2 × 100g silica SNAP cartridge) eluting with 20-60% EtOAc in cyclohexane. The required fractions were combined and evaporated *in vacuo* to give a residue. The residue was dissolved in DMSO (21 mL) and was further purified by MDAP (high pH). The required fractions were combined and evaporated *in vacuo* to give **59** as a colorless crystalline solid (1.42 g, 36%). ^{1}H NMR (400 MHz, $CDCl_3$) δ 7.32–7.26 (m, 3H), 7.14 (d, J = 6.9 Hz, 1H), 5.01 (dt, J = 12.5, 6, 6 Hz, 1H), 4.93–4.87 (m, 1H), 4.78 (d, J = 9.3 Hz, 1H), 4.69–4.67 (m, 1H), 2.61 (ddd, J = 12.5, 8.3, 4.7 Hz, 1H), 2.13 (s, 3H), 1.33–1.14 (m, 10H); LCMS (formic) $(M+H)^+$ = 291.3, R_t = 0.91 min (98%).

1-((2*S*,4*R*)-4-Amino-2-methyl-3,4-dihydroquinolin-1(2H)-yl)ethenone (36). A stirred mixture of **59** (1.403 g, 4.83 mmol) and TBAF (1 M solution in THF) (15 mL, 15.00 mmol) was heated under N_2 at 65 °C for 21 h. Further TBAF (1 M solution in THF) (10 mL, 10.00 mmol) was added and the reaction mixture was allowed to heat under N_2 at 65 °C for a further 49 h. The reaction mixture had the solvent removed *in vacuo* to give a yellow residue which was redissolved in CH_2Cl_2 and applied to a 50 g SNAP silica column which was pre-wetted with cyclohexane and eluted with 0-100% EtOAc/ cyclohexane followed by 0-100% 3:1 EtOAC:EtOH in cyclohexane.

The required fractions were combined and had the solvent removed *in vacuo* to give an orange residue which was redissolved in MeOH and applied to a 70 g SCX cartridge which was pre-wetted with MeOH and washed with MeOH (2 CV) and 2 M ammonia in MeOH (6 CV). The 2 M ammonia in MeOH fractions were combined and had the solvent removed *in vacuo* to give an orange residue which was redissolved in MeOH and applied to another 70 g SCX cartridge which was pre-wetted with MeOH and washed with MeOH (2 CV) and 2 M ammonia in MeOH (6 CV). The 2 M ammonia in MeOH factions were combined and had the solvent removed *in vacuo* to give an orange residue which was redissolved in MeOH and had the solvent evaporated under a stream of N_2 to give **36** as a yellow solid (589 mg, 60 %). ^{1}H NMR (400 MHz, $CDCl_3$) δ 7.62–7.41 (m, 1H), 7.34–7.21 (m, 2H), 7.18–7.01 (m, 1H), 4.83 (br d, J = 6.4 Hz, 1H), 3.82 (br dd, J = 12.0, 3.7, 1H), 2.66–2.55 (m, 1H), 2.09 (s, 3H), 1.23–1.03 (m, 4H); LCMS (high pH) $(M+H)^+$ = poor ionisation, R_t = 0.65 min (100%).

6-(((2*S*,4*R*)-1-Acetyl-2-methyl-1,2,3,4-tetrahydroquinolin-4-yl)amino)nicotinonitrile (13). A mixture of i-Pent PEPPSI (37 mg, 0.05 mmol) and Cs_2CO_3 (601 mg, 1.84 mmol) in 1,4-dioxane (1.5 mL) was degassed by bubbling N_2 through the mixture for 10 min. To the mixture was added 6-bromonicotinonitrile (186 mg, 1.01 mmol) and a solution of **36** (188 mg, 0.92 mmol) in 1,4-dioxane (3.5 mL). The resulting mixture was heated in a sealed vial with stirring at 100 °C for 41 h. The crude reaction mixture was diluted with EtOAc (10 mL) and applied to a 10 g Celite cartridge which was eluted with EtOAc (3 × 10 mL). The required fractions were combined and had the solvent removed *in vacuo* to give a black residue which was redissolved in CH_2Cl_2 and applied to a 10 g SNAP silica column which was pre-wetted with cyclohexane and eluted with 0-100 % EtOAc/ cyclohexane. The required fractions were combined and had the solvent removed *in vacuo* to give a brown residue which was redissolved in CH_2Cl_2 and had the solvent evaporated

under a stream of N_2 to give **13** as a brown gum (70 mg, 25 %). ^{1}H NMR (400 MHz, $CDCl_3$) δ 8.42 (d, *J* = 2.9 Hz, 1H), 7.66 (dd, *J* = 8.8, 2.0 Hz, 1H), 7.43–7.29 (m, 1H), 7.27–7.16 (m, 3H), 6.50 (d, *J* = 8.8 Hz, 1H), 5.24–5.07 (m, 1H), 4.96–4.83 (m, 2H), 2.79–2.67 (m, 1H), 2.20 (s, 3H), 1.45–1.23 (m, 2H), 1.20 (d, *J* = 6.4 Hz, 3H); LCMS (formic) $(M+H)^+$ = 307.0, R_t = 0.89 min (92%).

5-(((2*S*,4*R*)-1-Acetyl-2-methyl-1,2,3,4-tetrahydroquinolin-4-yl)amino)pyrazine-2-carbonitrile (14). A mixture of i-Pent PEPPSI (41 mg, 0.052 mmol) and Cs_2CO_3 (645 mg, 1.98 mmol) in 1,4-dioxane (1.5 mL) was degassed by bubbling N_2 through the mixture. To the mixture was added 5-bromopyrazine-2-carbonitrile (165 mg, 0.90 mmol) and a solution of **36** (198 mg, 0.97 mmol) in 1,4-dioxane (3.5 mL). The resulting mixture was heated in a sealed vial with stirring at 100 °C for 17 h. The crude reaction mixture was diluted with EtOAc (10 mL) and applied to a 10 g Celite cartridge which was eluted with EtOAc (3 × 10 mL). The required fractions were combined and had the solvent removed *in vacuo* to give a black residue which was redissolved in CH_2Cl_2 and applied to a 10 g SNAP silica column which was pre-wetted with cyclohexane and eluted with 0-100 % EtOAc/ cyclohexane. The required fractions were combined and had the solvent removed *in vacuo* to give a brown residue which was redissolved in CH_2Cl_2 and had the solvent evaporated under a stream of N_2 to give **14** as a brown solid (172 mg, 58 %). ^{1}H NMR (400 MHz, d_6-DMSO) δ 8.60 (br d, *J* = 7.8 Hz, 1H), 8.49 (s, 1H), 8.17 (d, *J* = 1.5 Hz, 1H), 7.42–7.26 (m, 2H), 7.26–7.08 (m, 2H), 5.05–4.80 (m, 1H), 4.80–4.55 (m, 1H), 2.68–2.52 (m, 2H), 2.08 (s, 3H), 1.33 (td, *J* = 12.1, 9.0 Hz, 1H), 1.08 (d, *J* = 6.4 Hz, 3H); LCMS (high pH) (M-H) = 306.4, R_t = 0.89 min (100%).

1-((2*S*,4*R*)-2-Methyl-4-((5-methylpyrazin-2-yl)amino)-3,4-dihydroquinolin-1(2H)-yl)ethenone (15). A mixture of i-Pent PEPPSI (35 mg, 0.05 mmol) and Cs_2CO_3 (581 mg, 1.78

mmol) in 1,4-dioxane (1 mL) was degassed by bubbling N_2 through the mixture for 10 min. To the mixture was added 2-bromo-5-methylpyrazine (167 mg, 0.97 mmol) and a solution of **36** (182 mg, 0.89 mmol) in 1,4-dioxane (4 mL). The resulting mixture was heated in a sealed vial at 100 °C for 24 h. The reaction mixture was diluted with EtOAc (10 mL) and filtered using a 10 g Celite cartridge which was washed with further EtOAc (3 × 10 mL). The EtOAc fractions were combined and had the solvent removed *in vacuo* to give a purple residue which was applied to a 10 g SNAP silica cartridge which was pre-wetted with cyclohexane and eluted with 0-100 % EtOAc/cyclohexane. The required fractions were combined and had the solvent removed *in vacuo* to give a purple residue which was redissolved in CH_2Cl_2 and had the solvent evaporated under a stream of N_2 to give **15** as a brown foam (41 mg, 16 %). ^{1}H NMR (400 MHz, $CDCl_3$) δ 7.95–7.89 (m, 2H), 7.38–7.12 (m, 4H), 4.95–4.90 (m, 1H), 4.82 (ddd, J = 12.1, 8.2, 4.2 Hz, 1H), 4.55 (br d, J = 8.3 Hz, 1H), 2.69 (ddd, J = 12.3, 8.2, 4.4 Hz, 1H), 2.43 (s, 3H), 2.19 (s, 3H), 1.39–1.27 (m, 1H), 1.19 (d, J = 6.4 Hz, 3H); LCMS (high pH) (M-H) = 297.3, R_t = 0.79 min (97%).

(*S*)-*tert*-Butyl (3-((4-fluorophenyl)amino)butanoyl)carbamate (38). A mixture of 4-fluoroaniline (5.0 g, 45.0 mmol), (*E*)-*tert*-butyl but-2-enoylcarbamate (**37**) (10.0 g, 54.0 mmol) and [((R)-BINAP)Pd(MeCN)$_2$](OTf)$_2$ (1.25 g, 1.13 mmol) in toluene (25 mL) was stirred at 35 °C for 48 h. The reaction mixture was cooled to rt and the solvent was evaporated. The residue was chromatographed using 15% EtOAc/hexane, then re-chromatographed using 15% EtOAc/hexane to give **38** as a colourless solid (1.9 g, 14%). ^{1}H NMR (400 MHz, d_6-DMSO) δ 10.25 (s, 1H), 6.95–6.86 (m, 2H), 6.55 (s, 1H), 6.54–6.52 (m, 1H), 5.31 (d, J = 8.8 Hz, 1H), 3.82–3.68 (m, 1H), 2.66 (dd, J = 15.7, 5.4 Hz, 1H), 2.42 (dd, J = 15.6, 7.3 Hz, 1H), 1.43 (s, 9H), 1.11 (d, J = 6.4 Hz, 3H); LCMS (formic) $(M+H)^+$ = 297.2, R_t = 0.89 min (100%).

***tert*-Butyl ((2*S*,4*R*)-6-fluoro-2-methyl-1,2,3,4-tetrahydroquinolin-4-yl)carbamate (39).** A solution of **38** (3.10 g, 10.46 mmol) in EtOH (40 mL) was cooled to –15 °C. The solution was treated with sodium borohydride (594 mg, 15.69 mmol) followed by a solution of anhydrous magnesium chloride (1.05 g, 11.03 mmol) in H_2O (10 mL) added slowly, maintaining the temperature below –10 °C. The mixture was stirred at <0 °C for 1 h and then at rt for 1 h. The resulting suspension was poured onto a stirred mixture of citric acid (5.02 g, 26.2 mmol), 1 M aq. hydrochloric acid (50 mL) and CH_2Cl_2 (50 mL). The mixture was stirred for 30 min. The aqueous phase was separated, then basified by the addition of solid potassium carbonate and extracted with EtOAc (2 × 50 mL). The combined EtOAc portions were washed with H_2O and brine. The organic phase was dried and evaporated. The residue was chromatographed using 10-30% EtOAc/hexane to give **39** as a colorless solid (1.01 g, 34%). ^{1}H NMR (400 MHz, d_6-DMSO) δ 7.17 (d, J = 8.8 Hz, 1H), 6.74 (td, J = 8.7, 2.7 Hz, 1H), 6.64 (dd, J = 10.3, 2.4 Hz, 1H), 6.53 (dd, J = 9.0, 4.6 Hz, 1H), 6.44 (dd, J = 8.8, 4.9 Hz, 1H), 5.55 (s, 1H), 4.70 (br dd, J = 8.6, 6.1 Hz, 1H), 3.57–3.33 (m, 1H), 1.89 (br dd, J = 12.0, 5.6 Hz, 1H), 1.44 (s, 9H), 1.11 (d, J = 6.4 Hz, 3H); LCMS (formic) $(M+H)^+$ = 281.1, R_t = 1.00 min (99%).

***tert*-Butyl ((2*S*,4*R*)-1-acetyl-6-fluoro-2-methyl-1,2,3,4-tetrahydroquinolin-4-yl)carbamate (60).** Acetic anhydride (1.08 g, 1.0 mL, 10.6 mmol) was added to a stirred solution of **39** (1.0 g, 3.57 mmol) in CH_2Cl_2 (30 mL) and pyridine (10 mL). The reaction mixture was stirred at rt for 24 h. Acetic anhydride (1.08 g, 1.0 mL, 10.6 mmol) was added and stirring at rt continued for 24 h. A third portion of acetic anhydride (1.08 g, 1.0 mL, 10.6 mmol) was added and stirring at rt continued for 24 h. The solvent was evaporated, and the residue was azeotroped twice with toluene. The residue was chromatographed using 15-40 % EtOAc/hexane to give **60** as a colourless solid (1.14 g, 99%). ^{1}H NMR (400 MHz, $CDCl_3$) δ 7.19–6.96 (m, 3H), 4.90 (br d, J = 6.4 Hz, 1H), 4.68

(br d, *J* = 8.3 Hz, 1H), 4.59 (br d, *J* = 8.3 Hz, 1H), 2.59 (ddd, *J* = 12.6, 8.4, 4.4 Hz, 1H), 2.13–2.07 (m, 3H), 1.53 (s, 9H), 1.13 (d, *J* = 6.4 Hz, 3H); LCMS (formic) $(M+H)^+$ = 323.2, R_t = 0.98 min (88%).

1-((2*S*,4*R*)-4-Amino-6-fluoro-2-methyl-3,4-dihydroquinolin-1(2H)-yl)ethanone, hydrochloride salt (40). TFA (1 mL) was added to a stirred solution of **60** (1.0 g, 3.10 mmol) in CH_2Cl_2 (10 mL). The reaction mixture was stirred at rt for 24 h. TFA (1 mL) was added and the rection mixture stirred at rt for a further 2 h. The solvent was evaporated and the residue azeotroped with toluene twice. The residue was dissolved in MeOH (20 mL) and loaded onto an SCX column. The column was washed with MeOH (10 CV). The product was eluted with 2 M ammonia in MeOH (5 CV). The solvent was evaporated, and the residue dissolved in Et_2O (20 mL) and 1 M HCl in Et_2O (5 mL). The solid was filtered, washed with Et_2O and dried to give **40** as a colourless solid (758 mg, 94%). ^{1}H NMR (400 MHz, d_6-DMSO) δ 8.94 (br s, 3H), 7.46 (dd, *J* = 8.8, 4.9 Hz, 1H), 7.32–7.20 (m, 2H), 4.72–4.44 (m, 1H), 4.24–4.16 (m, 1H), 2.79–2.64 (m, 1H), 2.03 (s, 3H), 1.30 (td, *J* = 12.1, 9.0 Hz, 1H), 1.05 (d, *J* = 6.4 Hz, 3H); LCMS (high pH) $(M+H)^+$ = poor ionisation, R_t = 0.65 min (100%).

6-(((2*S*,4*R*)-1-Acetyl-6-fluoro-2-methyl-1,2,3,4-tetrahydroquinolin-4-yl)amino)nicotinonitrile (16). A mixture of i-Pent PEPPSI (15 mg, 0.02 mmol) and Cs_2CO_3 (249 mg, 0.77 mmol) in 1,4-dioxane (0.5 mL) was degassed by bubbling N_2 through the mixture. To the mixture was added 6-bromonicotinonitrile (77 mg, 0.42 mmol) and a solution of **40** (85 mg, 0.38 mmol) in 1,4-dioxane (0.5 mL). The resulting mixture was heated in a sealed vial with stirring at 100 °C for 20 h. The reaction mixture was diluted with EtOAc (5 mL) and applied to a 2.5 g Celite cartridge which was eluted with EtOAc (3 × 5 mL). The required fractions were combined, and the solvent removed *in vacuo* to give a black residue which was redissolved in CH_2Cl_2 and

applied to a 10 g SNAP silica column which was pre-wetted with cyclohexane and eluted with 0-100 % EtOAc/cyclohexane. The required fractions were combined and had the solvent removed *in vacuo* to give a brown residue which was redissolved in CH_2Cl_2 and had the solvent evaporated under a stream of N_2 to give a brown solid (90 mg). The solid was dissolved in EtOH (1 mL) and injected onto a 30 mm × 25 cm Chiralpak AS-H column using 35% EtOH (+0.2% isopropylamine) / heptane (+0.2% isopropylamine) as eluent at 30 mL/min flow and 215 nm wavelength. The appropriate fractions were combined and evaporated to give **16** as a clear glass (56 mg, 45%, >99% ee). ^{1}H NMR (400 MHz, $CDCl_3$) δ 8.49–8.34 (m, 1H), 7.67 (dd, *J* = 8.8, 2.0 Hz, 1H), 7.27–7.11 (m, 1H), 7.02 (td, *J* = 8.1, 2.9 Hz, 1H), 6.91 (ddd, *J* = 8.8, 2.9, 1.0 Hz, 1H), 6.52 (d, *J* = 8.8 Hz, 1H), 5.09 (br d, *J* = 7.3 Hz, 1H), 5.01–4.90 (m, 1H), 4.90–4.66 (m, 1H), 2.77–2.62 (m, 1H), 2.18 (s, 3H), 1.45–1.23 (m, 1H), 1.18 (d, *J* = 6.4 Hz, 3H); LCMS (formic) $(M+H)^+$ = 325.3, R_t = 0.93 min (99%); The enantiomeric excess was confirmed by chiral HPLC analysis, 25 cm Chiralpak AS-H column no.ASH0CE-RG029, 35% EtOH (+0.2% isopropylamine):heptane, flow rate: 1 mL/min, wavelength: 215 nm, temperature: rt. R_t = 15.0 min, undesired enantiomer = 6.2 min.

5-(((2*S*,4*R*)-1-Acetyl-6-fluoro-2-methyl-1,2,3,4-tetrahydroquinolin-4-yl)amino)pyrazine-2-carbonitrile (17). A mixture of **40** (50 mg, 0.19 mmol), 5-chloropyrazine2-carbonitrile (30 mg, 0.21 mmol), and DIPEA (0.17 mL, 0.97 mmol) in α,α,α-trifluorotoluene (2 mL) was heated at 150 °C for 6 h in a microwave. The solvent was evaporated and the residue was chromatographed using 0-4% MeOH/CH_2Cl_2 to give a brown oil. Trituration with Et_2O gave **17** as a brown solid (47 mg, 75%). ^{1}H NMR (400 MHz, d_6-DMSO) δ 8.59 (br d, *J* = 8.3 Hz, 1H), 8.50 (d, *J* = 1.5 Hz, 1H), 8.17 (d, *J* = 1.5 Hz, 1H), 7.42 (dd, *J* = 8.8, 4.9 Hz, 1H), 7.14 (td, *J* = 8.8, 2.9 Hz, 1H), 7.00 (br dd, *J* = 9.5, 2.2 Hz, 1H), 4.87 (ddd, *J* = 12.1, 7.7, 4.6 Hz, 1H), 4.71 (br d, *J* = 5.9 Hz, 1H), 2.66–2.53

(m, 1H), 2.08 (s, 3H), 1.33 (br d, J = 8.3 Hz, 1H), 1.07 (d, J = 6.4 Hz, 3H); LCMS (formic) $(M+H)^+$ = 326.2, R_t = 0.84 min (98%).

1-((2*S*,4*R*)-6-Fluoro-2-methyl-4-((5-methylpyrazin-2-yl)amino)-3,4-dihydroquinolin-1(2H)-yl)ethenone (18). A mixture of i-Pent PEPPSI (16 mg, 0.02 mmol) and Cs_2CO_3 (259 mg, 0.80 mmol) in 1,4-dioxane (0.5 mL) was degassed by bubbling N_2 through the mixture. To the mixture was added 2-bromo-5-methylpyrazine (76 mg, 0.44 mmol) and a solution of **40** (89 mg, 0.40 mmol) in 1,4-dioxane (0.5 mL). The resulting mixture was heated in a sealed vial with stirring at 100 °C for 20 h. The crude reaction mixture was diluted with EtOAc (5 mL) and applied to a 2.5 g Celite cartridge which was eluted with EtOAc (3 × 5 mL). The required fractions were combined and had the solvent removed *in vacuo* to give a black residue which was redissolved in CH_2Cl_2 and applied to a 10 g SNAP silica column which was pre-wetted with cyclohexane and eluted with 0-100 % EtOAc/cyclohexane. The required fractions were combined and had the solvent removed *in vacuo* to give a brown residue which was redissolved in MeOH and had the solvent evaporated under a stream of N_2 to give a pale brown foam (62 mg). The solid was dissolved in EtOH (1 mL) and injected onto a 30 mm × 25 cm Chiralpak AS-H column using 15% EtOH (+0.2% isopropylamine) / heptane (+0.2% isopropylamine) as eluent at 30 mL/min flow and 215 nm wavelength. The appropriate fractions were combined and evaporated to give **18** as a clear glass (28 mg, 22%, >99% ee). ^{1}H NMR (400 MHz, $CDCl_3$) δ 7.99–7.90 (m, 2H), 7.17–7.09 (m, 1H), 7.04–6.95 (m, 2H), 5.11–4.89 (m, 1H), 4.80 (ddd, J = 12.3, 7.9, 4.6 Hz, 1H), 4.50 (br d, J = 8.3 Hz, 1H), 2.81–2.62 (m, 1H), 2.44 (s, 3H), 2.17 (s, 3H), 1.36–1.25 (m, 1H), 1.18 (d, J = 6.4 Hz, 3H); LCMS (formic) $(M+H)^+$ = 315.3, R_t = 0.82 min (98%); The enantiomeric excess was confirmed by chiral HPLC analysis, 25 cm Chiralpak AS-H column no.ASH0CE-RG029, 10%

EtOH (+0.2% isopropylamine):heptane, flow rate: 1 mL/min, wavelength: 215 nm, temperature: rt. R_t = 28.5 min, undesired enantiomer = 13.5 min.

***tert*-Butyl ((2*S*,4*R*)-1-Acetyl-6-cyano-2-methyl-1,2,3,4-tetrahydroquinolin-4-yl)carbamate (61).** A mixture of *tert*-butyl ((2*S*,4*R*)-1-acetyl-6-bromo-2-methyl-1,2,3,4-tetrahydroquinolin-4-yl)carbamate (**44**)[41] (2.0 g, 5.22 mmol) and zinc cyanide (766 mg, 6.52 mmol) in dry, degassed DMF (20 mL) was treated with $Pd(PPh_3)_4$ (301 mg, 0.73 mmol). The reaction mixture was stirred at 115 ºC for 2 h. The reaction mixture was cooled to rt, filtered through celite and the solvent evaporated from the filtrate. The residue was partitioned between EtOAc (100 mL) and H_2O (50 mL). The organic phase was separated, washed with H_2O, brine, dried and evaporated. The residue was purified by column chromatography using a gradient of 25-50% EtOAc / cyclohexane to give **61** as a colorless solid (1.36 g, 79%). ^{1}H NMR (400 MHz, d_6-DMSO) δ 7.76 (dd, J = 8.2, 1.6 Hz, 1H), 7.55 (d, J = 8.1 Hz, 1H), 7.51–7.39 (m, 2H), 4.60 (d, J = 6.4 Hz, 1H), 4.42–4.31 (m, 1H), 2.47–2.41 (m, 1H), 2.09 (s, 3H), 1.46 (s, 9H), 1.31–1.15 (m, 1H), 1.05 (d, J = 6.4 Hz, 3H); LCMS (formic) $(M+H)^+$ = 330.2, R_t = 0.98 min (100%).

(2*S*,4*R*)-1-Acetyl-4-amino-2-methyl-1,2,3,4-tetrahydroquinoline-6-carbonitrile hydrochloride (45). 4 M hydrogen chloride in 1,4-dioxane (5 mL, 20 mmol) was added to a stirred solution of **61** (1.35 g, 4.1 mmol) in 1,4-dioxane (5 mL). The reaction mixture was stirred at rt for 24 h. Et_2O (50 mL) was added and the mixture stirred for 20 min. The solvent was decanted. The residue was triturated with Et_2O to give **45** as a colourless solid (0.98 g, 90%). ^{1}H NMR (400 MHz, d_6-DMSO) δ 9.08 (br. s., 3H), 7.91–7.83 (m, 2H), 7.64 (d, J = 8.8 Hz, 1H), 4.61 (d, J = 6.4 Hz, 1H), 4.31–4.29 (m, 1H), 2.75 (dt, J = 8.4, 4.1 Hz, 1H), 2.09 (s, 3H), 1.39 (dd, J = 12.0, 2.9 Hz, 1H), 1.11 (d, J = 6.4 Hz, 3H); LCMS (high pH) $(M)^+$ = 213.3 (loss of NH_2), R_t = 0.65 min (94%).

(2*S*,4*R*)-1-Acetyl-4-((5-cyanopyridin-2-yl)amino)-2-methyl-1,2,3,4-tetrahydroquinoline-6-carbonitrile (19). A mixture of **45** (100 mg, 0.38 mmol), 6-bromonicotinonitrile (207 mg, 1.13 mmol), and DIPEA (0.33 mL, 1.88 mmol) in NMP (2 mL) was heated in a microwave at 180 °C for 2 h. The crude reaction mixture was purified by high pH MDAP to give **19** as an off-white solid (87 mg, 70%). ^{1}H NMR (400 MHz, d_4-MeOH) δ 8.32 (d, J = 1.5 Hz, 1H), 7.78–7.64 (m, 2H), 7.53 (d, J = 8.3 Hz, 1H), 7.47 (d, J = 1.5 Hz, 1H), 6.78 (d, J = 8.8 Hz, 1H), 5.01 (br dd, J = 12.2, 3.4 Hz, 1H), 4.88–4.79 (m, 1H), 2.69 (ddd, J = 12.6, 8.4, 4.4 Hz, 1H), 2.23 (s, 3H), 1.44 (td, J = 12.5, 9.3 Hz, 1H), 1.20 (d, J = 6.4 Hz, 3H); LCMS (formic) $(M+H)^+$ = 332.0, R_t = 0.88 min (100%).

(2*S*,4*R*)-1-Acetyl-4-((5-cyanopyrazin-2-yl)amino)-2-methyl-1,2,3,4-tetrahydroquinoline-6-carbonitrile (22). A mixture of **45** (100 mg, 0.38 mmol), 5-chloropyrazine-2-carbonitrile (158 mg, 1.13 mmol), and DIPEA (0.33 mL, 1.88 mmol) in NMP (2 mL) was heated in a microwave at 180 C for 2 h. The crude reaction mixture was purified by high pH MDAP to give **22** as a brown solid (38 mg, 30 %). ^{1}H NMR (400 MHz, d_6-DMSO) δ 8.60 (br d, J = 7.8 Hz, 1H), 8.50 (d, J = 1.0 Hz, 1H), 8.17 (d, J = 1.5 Hz, 1H), 7.78 (dd, J = 8.1, 1.7 Hz, 1H), 7.67 (s, 1H), 7.60 (d, J = 8.3 Hz, 1H), 4.92 (ddd, J = 11.7, 7.3, 4.4 Hz, 1H), 4.77–4.56 (m, 1H), 2.62 (ddd, J = 12.7, 8.3, 4.4 Hz, 1H), 2.14 (s, 3H), 1.42 (td, J = 12.2, 8.8 Hz, 1H), 1.12 (d, J = 6.4 Hz, 3H); LCMS (formic) $(M+H)^+$ = 333.0, R_t = 0.85 min (100%).

(2*S*,4*R*)-1-Acetyl-4-((5-chloropyrimidin-2-yl)amino)-2-methyl-1,2,3,4-tetrahydroquinoline-6-carbonitrile (46). DIPEA (0.493 mL, 2.82 mmol) was added in a single portion to a stirred solution of **45** (250 mg, 0.941 mmol) and 2,5-dichloropyrimidine (280 mg, 1.882 mmol) in DMSO (2 mL) at rt. The vial was sealed and then heated in a Biotage Initiator microwave using initial high absorption setting to 160 °C for 30 min. Upon cooling to rt, the vial

was reheated in a Biotage Initiator microwave using initial high absorption setting to 160 ºC for 30 min. Upon cooling to rt, EtOAc (10 mL) and H_2O (10 mL) were added. The separated aqueous phase was extracted with EtOAc (2 × 10 mL). The combined organic phase was passed through a hydrophobic frit and evaporated under reduced pressure to give a brown oil. The oil was loaded in CH_2Cl_2 and purified by column chromatography (25 g silica) using a gradient of 0-50% EtOAc / cyclohexane. The appropriate fractions were combined and evaporated under vacuum to give **46** as a pale yellow oil (248 mg, 77%). ^{1}H NMR (400 MHz, $CDCl_3$) δ 8.29 (s, 2H), 7.61 (dd, *J* = 8.1, 1.2 Hz, 1H), 7.55–7.50 (m, 1H), 7.30 (s, 1H), 5.22 (d, *J* = 8.1 Hz, 1H), 4.99–4.81 (m, 2H), 2.71 (ddd, *J* = 12.7, 8.4, 4.6 Hz, 1H), 2.22 (s, 3H), 1.47–1.35 (m, 1H), 1.22 (d, *J* = 6.4 Hz, 3H); LCMS (formic) $(M+H)^+$ = 342.0, 344.0, R_t = 0.94 min (99%).

(2*S*,4*R*)-1-Acetyl-4-((5-chloropyrimidin-2-yl)amino)-2-methyl-1,2,3,4-tetrahydroquinoline-6-carboxamide (27, GSK3383567, I-BET567). Hydrogen peroxide (0.12 mL, 35% by weight in H_2O, 1.40 mmol) was added dropwise over 30 s to a stirred suspension of **46** (240 mg, 0.702 mmol) and potassium carbonate (388 mg, 2.81 mmol) in DMSO (5 mL) at rt under N_2. The resultant suspension was stirred at rt for 2 h. EtOAc (10 mL) and H_2O (10 mL) were added. The separated aqueous phase was extracted with EtOAc (2 × 10 mL), the combined organic phase was passed through a hydrophobic frit and evaporated under reduced pressure to give a pale yellow oil. The sample was loaded in CH_2Cl_2 and purified by column chromatography (25 g silica) using a gradient of 0-60% EtOAc / cyclohexane and then 0-10% EtOH / EtOAc. The appropriate fractions were combined and evaporated under vacuum to give **27** as a white solid (150 mg, 59%, >99% ee). m.p. 234 °C; ^{1}H NMR (600 MHz, d_6-DMSO) δ 8.39 (br s, 2H), 7.94 (br. s, 1H), 7.94 (d, *J* = 8.4 Hz, 1H), 7.78 (dd, *J* = 8.2, 1.8 Hz, 1H), 7.69 (s, 1H), 7.39 (d, *J* = 8.2 Hz, 1H), 7.28 (br. s, 1H), 4.81 (ddd, *J* = 12.5, 8.3, 4.3 Hz, 1H), 4.67 (ddq, *J* = 9.1, 8.5, 6.3 Hz, 1H),

2.54 (ddd, J = 12.7, 8.5, 4.4 Hz, 1H), 2.10 (s, 3H), 1.37 (td, J = 12.5, 9.1 Hz, 1H), 1.07 (d, J = 6.3 Hz, 3H); ^{13}C NMR (151 MHz, d_6-DMSO) δ 168.5, 167.4, 160.3, 156.6, 156.0, 138.9, 136.6, 130.9, 125.8, 125.5, 122.8, 117.8, 47.2, 47.1, 40.1, 22.7, 21.4; HRMS $(M+H)^+$ calculated for $C_{17}H_{19}ClN_5O_2$ 360.1222; found 360.1221; LCMS (formic) $(M+H)^+$ = 360.2, 362.0, R_t = 0.71 min (100%); The enantiomeric excess was confirmed by chiral HPLC analysis, 25 cm Chiralpak AD column no.ADOOCE-A1074, 40% EtOH:heptane, flow rate: 1 mL/min, wavelength: 215 nm, temperature: rt. R_t = 6.845 min, undesired enantiomer = 10.586 min, >99% ee.

(2*S*,4*R*)-Butyl 1-acetyl-4-amino-2-methyl-1,2,3,4-tetrahydroquinoline-6-carboxylate (48). $AlCl_3$ (3.82 g, 28.7 mmol) was suspended in CH_2Cl_2 (100 mL) under N_2 and cooled in an ice-bath and stirred. (2*S*,4*R*)-Butyl 1-acetyl-4-((isopropoxycarbonyl)amino)-2-methyl-1,2,3,4-tetrahydroquinoline-6-carboxylate (**47**)[41] (2.94 g, 7.54 mmol) was added and the mixture stirred for 30 min producing a clear solution. NEt_3 (12.61 mL, 90 mmol) in MeOH (13.33 mL) was slowly added producing a thick white precipitate. The reaction was stirred and allowed to warm to rt overnight. Further $AlCl_3$ (1.91 g) was added and stirring continued for a further 3 h. The reaction was re-cooled in an ice-bath and another portion of NEt_3 (6.3 mL) in MeOH (6.5 mL) was added. After stirring for a further 4 h, CH_2Cl_2 (100 mL) and sat. $NaHCO_3$ (100 mL) were added to the reaction mixture followed by Rochelle's salt (20 g) and stirring continued for 30 min. H_2O (100 mL) was added and stirring continued for a further 30 min. CH_2Cl_2 and H_2O (100 mL) were added and the layers separated. The aqueous phase was re-extracted with CH_2Cl_2 (2 x 200 mL) and the combined organic phase filtered through celite, eluted through a hydrophobic frit and concentrated *in vacuo* to give a clear oil. The oil was loaded in CH_2Cl_2 and purified by column chromatography using a gradient of 5-50% (3:1 EtOAc / EtOH) / cyclohexane. The appropriate fractions were concentrated *in vacuo* to give **48** as a yellow oil (2.08 g, 86%). ^{1}H NMR (400 MHz,

$CDCl_3$) δ 8.16 (s, 1H), 7.98 (dd, *J* = 8.2, 1.6 Hz, 1H), 7.17 (d, *J* = 8.3 Hz, 1H), 4.90–4.74 (m, 1H), 4.41–4.27 (m, 2H), 3.76 (dd, *J* = 12.1, 4.3 Hz, 1H), 2.56 (ddd, *J* = 12.7, 8.6, 4.4 Hz, 1H), 2.13 (s, 3H), 1.84–1.69 (m, 2H), 1.59 (br.s, 2H), 1.49 (dq, *J* = 15.0, 7.4 Hz, 2H), 1.21–1.08 (m, 4H), 0.99 (t, *J* = 7.5 Hz, 3H); LCMS (high pH) $(M+H)^+$ = 329.3, R_t = 0.98 min (100%).

(2*S*,4*R*)-Butyl 1-acetyl-4-((3-chlorophenyl)amino)-2-methyl-1,2,3,4-tetrahydroquinoline-6-carboxylate (49a). A mixture of **48** (500 mg, 1.64 mmol), Cs_2CO_3 (1.07 g, 3.29 mmol), QPhos (70 mg, 0.10 mmol), $Pd_2(dba)_3$ (48 mg, 0.05 mmol) and 1-bromo-3-chlorobenzene (0.232 mL, 1.97 mmol) in anhydrous 1,4-dioxane (5 mL) was degassed and then heated to 100 °C for 16 h under N_2. Upon cooling to rt, the EtOAc (30 mL) was added and the resultant mixture was filtered through celite. The filtrate was evaporated under reduced pressure to give a black oil which was purified by column chromatography eluting with 8%-38% EtOAc / cyclohexane. Appropriate fractions were combined and evaporated under reduced pressure to give **49a** as a brown oil (450 mg, 66%). ^{1}H NMR (400 MHz, d_4-MeOH) δ 8.00–7.87 (m, 2H), 7.40 (d, *J* = 8.1 Hz, 1H), 7.07 (t, *J* = 8.1 Hz, 1H), 6.68 (t, *J* = 2.1 Hz, 1H), 6.63–6.55 (m, 2H), 4.82–4.79 (m, 1H), 4.33–4.19 (m, 3H), 2.68 (t, *J* = 4.0 Hz, 1H), 2.22 (s, 3H), 1.72–1.58 (m, 2H), 1.41–1.29 (m, 3H), 1.17 (d, *J* = 6.4 Hz, 3H), 0.92 (t, *J* = 7.3 Hz, 3H); LCMS (formic) $(M+H)^+$ = 415.1, R_t = 1.38 min (95%).

(2*S*,4*R*)-1-Acetyl-4-((3-chlorophenyl)amino)-2-methyl-1,2,3,4-tetrahydroquinoline-6-carboxylic acid (50a). To a mixture of **49a** (450 mg, 1.09 mmol) in MeOH (5 mL) and THF (5 mL) was added LiOH (5.42 mL, 1 M aq. 5.42 mmol). The mixture was stirred under N_2 for 16 h and then the solvent was evaporated under reduced pressure. The residue was diluted with H_2O (50 mL), then made acidic (pH~5) by the dropwise addition 2 M aq. HCl. The aqueous phase was extracted with CH_2Cl_2 (3 × 50 mL), the combined organic phase passed through a hydrophobic frit and evaporated under reduced pressure to give **50a** as a brown solid (420 mg, 100%). ^{1}H NMR

(400 MHz, d_4-MeOH) δ 8.01–7.89 (m, 2H), 7.39 (d, J = 8.3 Hz, 1H), 7.07 (t, J = 8.1 Hz, 1H), 6.68 (t, J = 2.1 Hz, 1H), 6.65–6.53 (m, 2H), 4.81–4.77 (m, 1H), 4.25 (dd, J = 12.1, 4.0 Hz, 1H), 2.70–2.64 (s, 1H), 2.22 (s, 3H), 1.33 (d, J = 9.0 Hz, 1H), 1.17 (d, J=6.4 Hz, 3H); LCMS (formic) $(M+H)^+$ = 359.0, R_t = 1.03 min (98%).

(2*S*,4*R*)-1-Acetyl-4-((3-chlorophenyl)amino)-2-methyl-1,2,3,4-tetrahydroquinoline-6-carboxamide (24). A mixture of **50a** (430 mg, 1.20 mmol), EDC (276 mg, 1.44 mmol), N-ethylmorpholine (0.303 mL, 2.40 mmol), 1-hydroxy-1*H*-benzotriazole, ammonium salt (365 mg, 2.40 mmol) in DMF (6 mL) was stirred under N_2 at rt for 18 h. The mixture was then partitioned between EtOAc (50 mL) and sat. aq. sodium bicarbonate solution (50 mL). The separated aqueous phase was extracted with EtOAc (2 × 50 mL), the combined organics were passed through a hydrophobic frit and evaporated under reduced pressure. The residue was purified by column chromatography eluting with 8%-38% EtOAc/cyclohexane. The appropriate fractions were combined and evaporated under reduced pressure. The residue was then dissolved in 1:1 MeOH/DMSO (4 mL) and purified by MDAP (high pH). The appropriate fractions were combined and evaporated under reduced pressure to give **24** as a white solid (153 mg, 36%). ^{1}H NMR (400 MHz, d_4-MeOH) δ 7.86–7.77 (m, 2H), 7.39 (d, J = 8.1 Hz, 1H), 7.07 (t, J = 8.1 Hz, 1H), 6.69 (t, J = 2.0 Hz, 1H), 6.64–6.56 (m, 2H), 4.80–4.75 (m, 1H), 4.27 (dd, J = 12.0, 4.2 Hz, 1H), 2.71–2.64 (m, 1H), 2.22 (s, 3H), 1.36–1.28 (m, 1H), 1.16 (d, J = 6.4 Hz, 3H); LCMS (formic) $(M+H)^+$ = 358.0, R_t = 0.91 min (100%).

(2*S*,4*R*)-1-Acetyl-4-((5-chloropyridin-2-yl)amino)-2-methyl-1,2,3,4-tetrahydroquinoline-6-carboxylic acid (50b). A mixture of **48** (500 mg, 1.64 mmol), 2-bromo-5-chloropyridine (632 mg, 3.29 mmol), sodium *tert*-butoxide (316 mg, 3.29 mmol), $Pd_2(dba)_3$ (150 mg, 10 mol%), and DavePhos (129 mg, 20 mol%) in anhydrous degassed 1,4-dioxane (10 mL) was heated at 120 °C

under N_2 overnight. The cooled reaction mixture was diluted with EtOAc (20 mL) and filtered through celite. The solvent was evaporated from the filtrate and the residue purified by column chromatography eluting with 0-20% EtOH / EtOAc to give **50b** as a brown oil (64 mg, 11%). ^{1}H NMR (400 MHz, d_6-DMSO) δ 7.97 (d, J = 2.7 Hz, 1H), 7.83 (dd, J = 8.1, 1.7 Hz, 1H), 7.73 (s, 1H), 7.53 (dd, J = 9.0, 2.7 Hz, 1H), 7.42 (d, J = 8.3 Hz, 1H), 7.28 (d, J = 8.3 Hz, 1H), 6.72 (d, J = 8.8 Hz, 1H), 4.84–4.78 (m, 1H), 4.71– 4.65 (m, 1H), 2.60–2.57 (m, 1H), 2.12 (s, 3H), 1.33–1.20 (m, 1H), 1.09 (d, J = 6.1 Hz, 3H); LCMS (formic) $(M+H)^+$ = 360.0, 362.0 R_t = 0.81 min (84%).

(2*S*,4*R*)-1-Acetyl-4-((5-chloropyridin-2-yl)amino)-2-methyl-1,2,3,4-tetrahydroquinoline-6-carboxamide (25). A mixture of **50b** (30 mg, 0.08 mmol), N-ethylmorpholine (0.021 mL, 0.16 mmol), N-hydroxybenzotriazole ammonium salt (38 mg, 0.25 mmol) and EDC (20 mg, 0.10 mmol) in DMF (1 mL) was stirred at rt overnight. The reaction mixture was then purified by MDAP (high pH), the appropriate fractions were combined and evaporated under reduced pressure to give **25** as a white solid (19 mg, 64%). ^{1}H NMR (400 MHz, d_6-DMSO) δ 8.03–7.90 (m, 2H), 7.78 (d, J = 8.3 Hz, 1H), 7.71 (s, 1 H), 7.52 (dd, J = 8.9, 2.6 Hz, 1H), 7.40 (d, J = 8.1 Hz, 1H), 7.30 (br. s., 1H), 7.22 (d, J = 8.1 Hz, 1H), 6.71 (d, J = 8.8 Hz, 1H), 4.90–4.77 (m, 1H), 4.74–4.61 (m, 1H), 2.61–2.54 (m, 1H), 2.12 (s, 3H), 1.32–1.14 (m, 1H), 1.08 (d, J = 6.1 Hz, 3H); LCMS (formic) $(M+H)^+$ = 359.1, 361.1 R_t = 0.66 min (100%).

(2*S*,4*R*)-1-Acetyl-4-((5-chloropyridin-2-yl)amino)-N-ethyl-2-methyl-1,2,3,4-tetrahydroquinoline-6-carboxamide (28). A mixture of **50b** (150 mg, 0.42 mmol), DIPEA (108 mg, 0.146 mL, 0.83 mmol), HATU (190 mg, 0.50 mmol) and ethylamine hydrochloride (170 mg, 2.08 mmol) in DMF (2 mL) was stirred at rt for 24 h. The reaction mixture was treated with saturated $NaHCO_3$ (10 mL) and extracted with EtOAc (3 × 10 mL). The combined extracts were washed with H_2O and brine. The organic phase was dried and evaporated. The residue was

chromatographed using 0-15% EtOH/EtOAc to give **28** as a colourless solid (63 mg, 39%). ^{1}H NMR (400 MHz, d_6-DMSO) δ 8.43 (br s, 1H), 7.97 (br s, 1H), 7.80–7.61 (m, 2H), 7.52 (br dd, *J* = 8.8, 2.0 Hz, 1H), 7.41 (br d, *J* = 8.3 Hz, 1H), 7.23 (br d, *J* = 7.8 Hz, 1H), 6.72 (br d, *J* = 8.8 Hz, 1H), 4.84 (br s, 1H), 4.68 (br d, *J* = 6.4 Hz, 1H), 3.30–3.18 (m, 2H), 2.70–2.53 (m, 1H), 2.11 (s, 3H), 1.37–1.16 (m, 1H), 1.16–1.01 (m, 6H)l; LCMS (formic) $(M+H)^+$ = 387.0, 389.0, R_t = 0.81 min (100%).

(2*S*,4*R*)-Butyl 1-acetyl-2-methyl-4-((5-methylpyridin-2-yl)amino)-1,2,3,4-tetrahydroquinoline-6-carboxylate (49d). A mixture of *i*-pent PEPPSI (46 mg, 0.06 mmol) and Cs_2CO_3 (760 mg, 2.33 mmol) in 1,4-dioxane (1.5 mL) was degassed by bubbling N_2 through the mixture for 10 min. To the mixture was added 2-bromo-5-methylpyridine (221 mg, 1.28 mmol) and a solution of **48** (355 mg, 1.17 mmol) in 1,4-dioxane (3.5 mL). The resulting mixture was heated in a sealed vial with stirring at 100 °C for 41 h. The crude reaction mixture was diluted with EtOAc (10 mL) and applied to a 10 g celite cartridge which was eluted with EtOAc (3 × 10 mL). The filtrate was evaporated under reduced pressure and the resultant residue purified by column chromatography eluting with 0-100 % EtOAc/ cyclohexane. The appropriate fractions were combined and evaporated under reduced pressure to give **49d** as a red foam (141 mg, 31%). ^{1}H NMR (400 MHz, $CDCl_3$) δ 8.01–7.92 (m, 3H), 7.30 (dd, *J* = 8.4, 2.3 Hz, 1H), 7.20 (d, *J* = 8.1 Hz, 1H), 6.43 (d, *J* = 8.3 Hz, 1H), 4.88 (d, *J* = 6.4 Hz, 1H), 4.78 (ddd, *J* = 12.2, 8.4, 4.2 Hz, 1H), 4.45 (d, *J* = 8.6 Hz, 1H), 4.32–4.25 (m, 2H), 2.70 (ddd, *J* = 12.4, 8.4, 4.4 Hz, 1H), 2.21 (s, 3H), 2.20 (s, 3H), 1.73–1.68 (m, 2H), 1.46–1.37 (m, 2H), 1.35–1.23 (m, 1H), 1.19 (d, *J* = 6.4 Hz, 3H), 0.94 (t, *J* = 7.3 Hz, 3H); LCMS (formic) $(M+H)^+$ = 396.1, R_t = 0.73 min (94%).

(2*S*,4*R*)-1-Acetyl-2-methyl-4-((5-methylpyridin-2-yl)amino)-1,2,3,4-tetrahydroquinoline-6-carboxylic acid (50d). **49d** (141 mg, 0.36 mmol) was stirred in THF (2 mL), MeCN (2 mL) and

H_2O (2 mL) under N_2. LiOH (72 mg, 3.01 mmol) was added and the reaction stirred for at rt for 75.5 h. The mixture was evaporated to dryness under a stream of N_2 before 2 M aq. HCl (3 mL) was added and the mixture stirred for 5 min. The mixture was again evaporated to dryness under a stream of N_2, dissolved in DMSO (6 mL) and then purified by MDAP (high pH). The appropriate fractions were combined and evaporated under reduced pressure to give **50d** as a yellow solid (82 mg, 67%). ^{1}H NMR (400 MHz, d_6-DMSO) δ 7.86–7.73 (m, 3H), 7.38 (d, J = 8.3 Hz, 1H), 7.29 (dd, J = 8.6, 2.2 Hz, 1H), 6.77 (d, J = 8.3 Hz, 1H), 6.60 (d, J = 8.3 Hz, 1H), 4.80 (ddd, J = 12.2, 8.2, 4.3 Hz, 1H), 4.73–4.60 (m, 1H), 2.61–2.52 (m, 1H), 2.12 (s, 3H), 2.11 (s, 3H), 1.24 (td, J = 12.4, 9.2 Hz, 1H), 1.07 (d, J = 6.1 Hz, 3H); LCMS (formic) $(M+H)^+$ = 340.4, R_t = 0.44 min (100%).

(2*S*,4*R*)-1-Acetyl-2-methyl-4-((5-methylpyridin-2-yl)amino)-1,2,3,4-tetrahydroquinoline-6-carboxamide (26). A mixture of **50d** (40 mg, 0.12 mmol), NH_4Cl (32 mg, 0.60 mmol) and HATU (54 mg, 0.14 mmol) in DMF (1 mL) had DIPEA (0.104 mL, 0.60 mmol) added. The mixture was stirred at rt for 2.75 h. The reaction mixture was purified directly by MDAP (high pH). The appropriate fraction was evaporated under reduced pressure to give **26** as a pale-yellow solid (35 mg, 87%). ^{1}H NMR (400 MHz, d_6-DMSO) δ 7.93 (dd, J = 1.5, 0.7 Hz, 1H), 7.82–7.74 (m, 2H), 7.31 (dd, J = 8.4, 2.1 Hz, 1H), 7.23 (d, J = 8.8 Hz, 1H), 6.43 (d, J = 8.3 Hz, 1H), 6.17 (br. s., 1H), 5.82 (br. s., 1H), 4.87 (d, J = 6.4 Hz, 1H), 4.80–4.67 (m, 1H), 4.61 (d, J = 8.3 Hz, 1H), 2.70 (ddd, J = 12.5, 8.5, 4.4 Hz, 1H), 2.21 (s, 3H), 2.20 (s, 3H), 1.30 (td, J = 12.1, 9.0 Hz, 1H), 1.18 (d, J = 6.4 Hz, 3H); LCMS (formic) $(M+H)^+$ = 339.3, R_t = 0.37 min (100%).

(2*S*,4*R*)-1-Acetyl-N-ethyl-2-methyl-4-((5-methylpyridin-2-yl)amino)-1,2,3,4-tetrahydroquinoline-6-carboxamide (30). A mixture of **50d** (40 mg, 0.12 mmol), ethylamine (2 M in THF, 0.30 mL, 0.60 mmol) and HATU (58 mg, 0.15 mmol) in DMF (1.0 mL) had DIPEA (0.05 mL, 0.30 mmol) added. The mixture was stirred at rt for 2.75 h before further ethylamine (2

M in THF, 0.30 mL, 0.60 mmol) was added and stirring at rt continued for a further 1.25 h. The mixture was directly purified by MDAP (high pH) and the required fraction was evaporated under a stream of N_2 to give **30** as a pale-yellow solid (23 mg, 52%). ^{1}H NMR (400 MHz, $CDCl_3$) δ 8.01–7.90 (m, 1H), 7.77–7.69 (m, 2H), 7.32 (d, *J* = 8.1 Hz, 1H), 7.22 (d, *J* = 7.3 Hz, 1H), 6.43 (d, *J* = 8.3 Hz, 1H), 6.11 (br s, 1H), 4.96–4.83 (m, 1H), 4.77 (ddd, *J* = 12.2, 8.3, 4.4 Hz, 1H), 4.50 (br d, *J* = 8.3 Hz, 1H), 3.55–3.40 (m, 2H), 2.70 (ddd, *J* = 12.6, 8.4, 4.4 Hz, 1H), 2.22 (s, 3H), 2.19 (s, 3H), 1.33–1.16 (m, 7H); LCMS (formic) $(M+H)^+$ = 367.4, R_t = 0.45 min (100%).

(2*S*,4*R*)-Butyl 1-acetyl-4-((5-cyanopyridin-2-yl)amino)-2-methyl-1,2,3,4-tetrahydroquinoline-6-carboxylate (49c). DIPEA (0.384 mL, 2.20 mmol) was added in a single portion to a stirred solution of **48** (250 mg, 0.73 mmol) and 6-fluoronicotinonitrile (179 mg, 1.47 mmol) in DMSO (2 mL) at rt. The vial was sealed and then heated in a Biotage Initiator microwave using initial high absorption setting to 160 °C for 30 min. Upon cooling to rt, EtOAc (10 mL) and H_2O (10 mL) were added. The separated aqueous phase was extracted with EtOAc (2 × 10 mL). The combined organic phase was passed through a hydrophobic frit and evaporated under reduced pressure to give a brown oil. The sample was loaded in CH_2Cl_2 and purified by Biotage SP4 SNAP 25g silica using a gradient of 0-40% EtOAc / cyclohexane. The appropriate fractions were combined and evaporated under vacuum to give **49c** as a pale-yellow oil (285 mg, 96%). ^{1}H NMR (400 MHz, $CDCl_3$) δ 8.42 (d, *J* = 1.5 Hz, 1H), 8.01 (dd, *J* = 8.3, 2.0 Hz, 1H), 7.94–7.80 (m, 1H), 7.67 (dd, *J* = 8.6, 2.2 Hz, 1H), 7.26 (d, *J* = 7.6 Hz, 1H), 6.55 (d, *J* = 8.8 Hz, 1H), 5.10 (br d, *J* = 8.3 Hz, 1H), 5.03–4.85 (m, 2H), 4.35–4.25 (m, 2H), 2.73 (ddd, *J* = 12.6, 8.4, 4.4 Hz, 1H), 2.23 (s, 3H), 1.78–1.66 (m, 2H), 1.49–1.34 (m, 3H), 1.22 (d, *J* = 6.4 Hz, 3H), 0.97 (t, *J* = 7.3 Hz, 3H); LCMS (formic) $(M+H)^+$ = 407.1, R_t = 1.15 min (99%).

(2*S*,4*R*)-1-Acetyl-4-((5-cyanopyridin-2-yl)amino)-2-methyl-1,2,3,4-tetrahydroquinoline-6-carboxylic acid (50c). LiOH (2.10 mL, 1 M in H_2O, 2.10 mmol) was added in a single portion to a stirred solution of **49c** (285 mg, 0.70 mmol) in MeOH (2 mL) and THF (2 mL) at rt. The resultant solution was stirred at rt for 2 h and then 2 M aq. HCl (1 mL) was added. H_2O (20 mL) and EtOAc (20 mL) were added, the separated aqueous phase was extracted with EtOAc (2 × 10 mL). The combined organic phase was passed through a hydrophobic frit and evaporated under reduced pressure to give **50c** as a pale-yellow foam (223 mg, 91%). ^{1}H NMR (400 MHz, d_6-DMSO) δ 12.89 (br s, 1H), 8.42 (d, *J* = 2.4 Hz, 1H), 8.07 (d, *J* = 8.3 Hz, 1H), 7.94–7.73 (m, 2H), 7.68 (s, 1H), 7.48 (d, *J* = 8.3 Hz, 1H), 6.79 (br d, *J* = 8.8 Hz, 1H), 5.06–4.88 (m, 1H), 4.76–4.61 (m, 1H), 2.64–2.55 (m, 1H), 2.13 (s, 3H), 1.40–1.28 (m, 1H), 1.10 (d, *J* = 6.4 Hz, 3H); LCMS (formic) $(M+H)^+$ = 351.0, R_t = 0.78 min (99%).

(2*S*,4*R*)-1-Acetyl-4-((5-cyanopyridin-2-yl)amino)-N-ethyl-2-methyl-1,2,3,4-tetrahydroquinoline-6-carboxamide (29). HATU (266 mg, 0.70 mmol) was added in a single portion to a stirred solution of **50c** (223 mg, 0.64 mmol) and DIPEA (0.222 mL, 1.27 mmol) in DMF (5 mL) at rt under N_2. Following stirring at rt for 10 min, ethylamine (0.64 mL, 2 M in THF, 1.27 mmol) was added dropwise over 30 s. The resultant solution was stirred at rt for 16 h. EtOAc (10 mL) and H_2O (10 mL) were added and the separated aqueous phase was extracted with EtOAc (2 × 10 mL). The combined organic phase was passed through a hydrophobic frit and evaporated under reduced pressure to give a pale-yellow oil. The oil was dissolved in 1:1 MeOH:DMSO (3 mL) and purified by MDAP (high pH). The solvent was evaporated under vacuum to give **29** as a white solid (106 mg, 44%). ^{1}H NMR (400 MHz, d_6-DMSO) δ 8.52–8.36 (m, 2H), 8.11–7.97 (m, *J* = 8.3 Hz, 1H), 7.85–7.71 (m, 2H), 7.63 (s, 1H), 7.53–7.32 (m, *J* = 8.3 Hz, 1H), 6.78 (br d, *J* = 8.8 Hz, 1H), 5.00 (br d, *J* = 2.0 Hz, 1H), 4.75–4.61 (m, 1H), 3.29–3.20 (m, 2H), 2.62–2.52 (m,

1H), 2.12 (s, 3H), 1.31 (td, *J* = 12.0, 9.3 Hz, 1H), 1.15–1.03 (m, 6H); LCMS (formic) $(M+H)^+$ = 378.0, R_t = 0.77 min (99%).

(2*S*,4*R*)-Butyl 1-acetyl-4-((5-fluoropyridin-2-yl)amino)-2-methyl-1,2,3,4-tetrahydroquinoline-6-carboxylate (49e). A mixture of *i*-Pent PEPPSI (48 mg, 0.06 mmol) and Cs_2CO_3 (722 mg, 2.22 mmol) in 1,4-dioxane (1.5 mL) was degassed by bubbling N_2 through the mixture for 10 min. To the mixture was added 2-bromo-5-fluoropyridine (222 mg, 1.26 mmol) and a solution of **48** (344 mg, 1.13 mmol) in 1,4-dioxane (3.5 mL). The resulting mixture was heated in a sealed vial with stirring at 100 °C for 19 h. The reaction mixture was diluted with EtOAc (10 mL) and filtered through celite. The celite was washed with EtOAc (30 mL) and the filtrate was evaporated under reduced pressure to give a black residue. The residue was purified by column chromatography eluting with 0-100% EtOAc/cyclohexane. The appropriate fractions were combined and evaporated under reduced pressure to give **49e** as a red foam (163 mg, 36%). ^{1}H NMR (400 MHz, $CDCl_3$) δ 8.04–7.89 (m, 3H), 7.32–7.17 (m, 2H), 6.47 (dd, *J* = 9.0, 3.4 Hz, 1H) 4.89 (d, *J* = 6.4 Hz, 1H), 4.83–4.71 (m, 1H), 4.52 (d, *J* = 8.3 Hz, 1H) 4.29 (td, *J* = 6.6, 2.7 Hz, 2H) 2.70 (ddd, *J* = 12.4, 8.4, 4.4 Hz, 1H) 2.20 (s, 3H), 1.77–1.64 (m, 2H), 1.49–1.24 (m, 3H), 1.19 (d, *J* = 6.4 Hz, 3H) 0.95 (t, *J* = 7.3 Hz, 3H); LCMS (formic) $(M+H)^+$ = 400.1, R_t = 1.15 min (100%).

(2*S*,4*R*)-1-Acetyl-4-((5-fluoropyridin-2-yl)amino)-2-methyl-1,2,3,4-tetrahydroquinoline-6-carboxylic acid (50e). **49e** (163 mg, 0.41 mmol) was dissolved in THF (2 mL) and H_2O (2 mL) and treated with LiOH (49 mg, 2.04 mmol). The resulting mixture was stirred at rt under N_2 for 73 h. The reaction mixture was then loaded onto an amino propyl column (20 g) that had been prewashed with MeOH. The column was eluted with MeOH (4 CV), CH_2Cl_2 (4 CV) and 2 M aq. HCl (4 CV). The appropriate fractions were combined, and the solvent evaporated under reduced pressure to give **50e** as an orange solid (132 mg, 94%). ^{1}H NMR (400 MHz, d_6-DMSO) δ 7.90 (d,

J = 2.9 Hz, 1H), 7.80–7.71 (m, 2H), 7.41 (td, *J* = 8.8, 2.9 Hz, 1H), 7.15 (d, *J* = 8.6 Hz, 1H), 7.00 (d, *J* = 8.3 Hz, 1H), 6.68 (dd, *J* = 9.3, 3.7 Hz, 1H), 4.80–4.62 (m, 2H), 2.54–2.50 (m, 1H); 2.06 (s, 3H), 1.26–1.11 (m, 1H), 1.03 (d, *J* = 6.4 Hz, 3H); LCMS (formic) $(M+H)^+$ = 344.3, R_t = 0.69 min (100%).

(2*S*,4*R*)-1-Acetyl-N-ethyl-4-((5-fluoropyridin-2-yl)amino)-2-methyl-1,2,3,4-tetrahydroquinoline-6-carboxamide (31). To a solution of **50e** (83 mg, 0.24 mmol) in Anhydrous DMF (1 mL) was added DIPEA (0.211 mL, 1.21 mmol) and HATU (123 mg, 0.32 mmol) and allowed to stir at rt for 15 min after which ethanamine (2 M in THF, 0.600 mL, 1.20 mmol) was added and the reaction was allowed to stir for a further 4.75 hrs. The reaction mixture was diluted with DMF (1 mL) and purified directly by MDAP (formic). The required fractions were combined and had the solvent removed *in vacuo* to give a clear residue. The residue was redissolved in 1:1 DMSO:MeOH and re-purified by MDAP (high pH). The required fraction had the solvent removed *in vacuo* to give a residue which was redissolved in CH_2Cl_2 and had the solvent evaporated under a stream of N_2 to give **31** as a clear glass (6 mg, 7%). ^{1}H NMR (400 MHz, $CDCl_3$) δ 7.97 (d, *J* = 2.9 Hz, 1H), 7.76–7.64 (m, 2H), 7.26–7.20 (m, 2H), 6.47 (dd, *J* = 9.3, 3.4 Hz, 1H), 6.09 (br s, 1H), 4.87 (br d, *J* = 6.4 Hz, 1H), 4.77 (ddd, *J* = 12.2, 8.3, 4.4 Hz, 1H), 4.62 (d, *J* = 8.3 Hz, 1H), 3.53–3.42 (m, 2H), 2.69 (ddd, *J* = 12.3, 8.2, 4.4 Hz, 1H), 2.18 (s, 3H), 1.32–1.14 (m, 7H); LCMS (formic) $(M+H)^+$ = 344.3, R_t = 0.69 min (100%).

(2*S*,4*R*)-Butyl 1-acetyl-4-((5-cyanopyrazin-2-yl)amino)-2-methyl-1,2,3,4-tetrahydroquinoline-6-carboxylate (49f). A mixture of **48** (100 mg, 0.33 mmol), 5-chloropyrazine-2-carbonitrile (92 mg, 0.66 mmol), and DIPEA (127 mg, 172 mL, 0.99 mmol) in NMP (2 mL) was heated in a microwave at 180 °C for 2 h. The crude reaction mixture was purified by high pH MDAP to give **49f** as a brown solid (30 mg, 22%). ^{1}H NMR (400 MHz, d4-MeOH) δ

8.35 (d, J = 1.5 Hz, 1H), 8.17 (d, J = 1.5 Hz, 1H), 8.00 (dd, J = 8.3, 2.0 Hz, 1H), 7.90–7.71 (m, 1H), 7.47 (d, J = 8.3 Hz, 1H), 5.03 (br dd, J = 12.2, 3.9 Hz, 1H), 4.92–4.86 (m, 1H), 4.29 (t, J = 6.6 Hz, 2H), 2.72 (ddd, J = 12.6, 8.4, 4.4 Hz, 1H), 2.22 (s, 3H), 1.81–1.60 (m, 2H), 1.53–1.34 (m, 3H), 1.21 (d, J = 6.4 Hz, 3H), 1.03 – 0.91 (m, 3H); LCMS (formic) $(M+H)^+$ = 408.1, R_t = 1.15 min (100%).

(2*S*,4*R*)-1-Acetyl-4-((5-cyanopyrazin-2-yl)amino)-2-methyl-1,2,3,4-tetrahydroquinoline-6-carboxylic acid (50f). 1 M LiOH solution (0.5 mL, 0.50 mmol) was added to a stirred solution of **49f** (30 mg, 0.07 mmol) in MeOH (0.5 mL) and THF (0.5 mL). The reaction mixture was stirred at rt overnight. The organic solvents were evaporated, and the residue was diluted with H_2O (5 mL). The solution was neutralised (pH 5) by the dropwise addition of 2 M hydrochloric acid. The mixture was extracted with CH_2Cl_2 (3 × 5 mL). The combined extracts were dried and evaporated to give **50f** as a colorless glass (14 mg, 54%). ^{1}H NMR (400 MHz, d_4-MeOH) δ 8.36 (d, *J* = 1.5 Hz, 1H), 8.17 (d, *J* = 1.5 Hz, 1H), 8.02 (dd, *J* = 8.3, 2.0 Hz, 1H), 7.88–7.81 (m, 1H), 7.45 (d, *J* = 8.3 Hz, 1H), 5.05 (br dd, *J* = 12.2, 4.4 Hz, 1H), 4.96–4.88 (m, 1H), 2.71 (ddd, *J* = 12.6, 8.4, 4.4 Hz, 1H), 2.22 (s, 3H), 1.47 (td, *J* = 12.2, 8.8 Hz, 1H), 1.21 (d, *J* = 6.4 Hz, 3H); LCMS (formic) $(M+H)^+$ = 352.0, R_t = 0.76 min (93%).

(2*S*,4*R*)-1-Acetyl-4-((5-cyanopyrazin-2-yl)amino)-N-ethyl-2-methyl-1,2,3,4-tetrahydroquinoline-6-carboxamide (32). A mixture of **50f** (14 mg, 0.04 mmol), N-ethylmorpholine (9 mg, 10 mL, 0.08 mmol), N-hydroxybenzotriazole hydrate (8 mg, 0.052 mmol) and EDC (10 mg, 0.052 mmol) in DMF (1 mL) was treated with 2 M ethylamine in THF (60 µL, 0.12 mmol). The reaction mixture was stirred at rt overnight and then purified directly by high pH MDAP to give **32** as a colorless glass (2 mg, 13%). ^{1}H NMR (400 MHz, d_4-MeOH) δ 8.35 (d, *J* = 1.0 Hz, 1H), 8.16 (d, *J* = 1.5 Hz, 1H), 7.82 (dd, *J* = 8.3, 1.5 Hz, 1H), 7.71 (dd, *J* = 2.0, 1.0 Hz,

1H), 7.44 (d, *J* = 8.3 Hz, 1H), 5.06 (br dd, *J* = 12.0, 4.2 Hz, 1H), 4.94–4.87 (m, 1H), 3.39 (q, *J* = 7.0 Hz, 2H), 2.70 (ddd, *J* = 12.6, 8.4, 4.4 Hz, 1H), 2.21 (s, 3H), 1.46 (td, *J* = 12.3, 9.0 Hz, 2H), 1.25–1.16 (m, 5H); LCMS (formic) $(M+H)^+$ = 379.1, R_t = 0.76 min (100%).

(2*S*,4*R*)-Butyl 1-acetyl-4-((5-chloropyrimidin-2-yl)amino)-2-methyl-1,2,3,4-tetrahydroquinoline-6-carboxylate (49g). DIPEA (0.344 mL, 1.97 mmol) was added in a single portion to a stirred solution of **48** (200 mg, 0.66 mmol) and 2,5-dichloropyrimidine (196 mg, 1.31 mmol) in DMSO (2 mL) at rt. The vial was sealed and then heated in a Biotage Initiator microwave using initial high absorption setting to 160 °C for 40 min. Upon cooling to rt, EtOAc (10 mL) and H_2O (10 mL) were added. The separated aqueous phase was extracted with EtOAc (2 × 10 mL). The combined organic phase was passed through a hydrophobic frit and evaporated under reduced pressure to give a brown oil. The sample was loaded in CH_2Cl_2 and purified by column chromatography (25 g, silica) using a gradient of 0-40% EtOAc / cyclohexane. The appropriate fractions were combined and evaporated under vacuum to give **49g** as a pale yellow oil (265 mg, 97%). ^{1}H NMR (400 MHz, $CDCl_3$) δ 8.28 (s, 2H), 7.99 (dd, *J* = 8.3, 1.5 Hz, 1H), 7.93 (s, 1H), 7.23 (d, *J* = 8.3 Hz, 1H), 5.32 (d, *J* = 9.0 Hz, 1H), 5.03–4.87 (m, 2H), 4.31 (t, *J* = 6.6 Hz, 2H), 2.70 (ddd, *J* = 12.5, 8.4, 4.5 Hz, 1H), 2.20 (s, 3H), 1.77–1.67 (m, 2H), 1.48–1.40 (m, 2H), 1.38–1.31 (m, 1H), 1.20 (d, *J* = 6.4 Hz, 3H), 0.96 (t, *J* = 7.5 Hz, 3H); LCMS (formic) $(M+H)^+$ = 417.1, 419.1, R_t = 1.23 min (100%).

(2*S*,4*R*)-1-Acetyl-4-((5-chloropyrimidin-2-yl)amino)-2-methyl-1,2,3,4-tetrahydroquinoline-6-carboxylic acid (50g). LiOH (1.91 mL, 1 M in H_2O, 1.91 mmol) was added in a single portion to a stirred solution of **49g** (265 mg, 0.64 mmol) in MeOH (2 mL) and THF (2 mL) at rt. The resultant solution was stirred at rt for 2 h and then 2 M HCl (1 mL) was added. H_2O (20 mL) and EtOAc (20 mL) were added, the separated aqueous phase was extracted

with EtOAc (2 × 10 mL). The combined organic phase was passed through a hydrophobic frit and evaporated under reduced pressure to give **50g** as a yellow oil (212 mg, 92%). ^{1}H NMR (400 MHz, d_6-DMSO) δ 12.88 (br. s., 1H), 8.41 (br. s., 2H), 8.05 (d, J = 8.3 Hz, 1H), 7.85 (dd, J = 8.2, 1.8 Hz, 1H), 7.70 (s, 1H), 7.46 (d, J = 8.3 Hz, 1H), 4.88–4.77 (m, 1H), 4.73–4.62 (m, 1H), 2.12 (s, 3H), 1.45–1.23 (m, 2H), 1.08 (d, J=6.4 Hz, 3H); LCMS (formic) $(M+H)^+$ = 361.0, 363.0, R_t = 0.83 min (100%).

(2*S*,4*R*)-1-Acetyl-4-((5-chloropyrimidin-2-yl)amino)-*N*-ethyl-2-methyl-1,2,3,4-tetrahydroquinoline-6-carboxamide (34). HATU (246 mg, 0.65 mmol) was added in a single portion to a stirred solution of **50g** (212 mg, 0.59 mmol) and DIPEA (0.205 mL, 1.18 mmol) in DMF (5 mL) at rt under N_2. Following stirring at rt for 10 min, ethylamine (0.59 mL, 2 M in THF, 1.18 mmol) was added dropwise over 30 s. The resultant solution was stirred at rt for 16 h. EtOAc (10 mL) and H_2O (10 mL) were added. The separated aqueous phase was extracted with EtOAc (2 × 10 mL). The combined organic phase was passed through a hydrophobic frit and evaporated under reduced pressure to give a pale-yellow oil. The oil was loaded in CH_2Cl_2 and purified by column chromatography (25 g silica) using a gradient of 0-100% EtOAc / cyclohexane. The appropriate fractions were combined and evaporated under vacuum to give a yellow oil. The oil was dissolved in 1:1 MeOH:DMSO (3 mL) and purified by MDAP (high pH). The solvent was evaporated under vacuum to give **34** as a white solid (67 mg, 29%). ^{1}H NMR (400 MHz, d_6-DMSO) δ 8.50–8.30 (m, 3H), 7.96 (d, J = 8.6 Hz, 1H), 7.74 (dd, J = 8.1, 1.7 Hz, 1H), 7.64 (s, 1H), 7.40 (d, J = 8.3 Hz, 1H), 4.81 (ddd, J = 12.4, 8.5, 4.0 Hz, 1H), 4.70–4.60 (m, 1H), 3.28–3.20 (m, 2H), 2.58–2.52 (m, 1H), 2.10 (s, 3H), 1.35 (td, J = 12.5, 9.3 Hz, 1H), 1.12–1.02 (m, 6H); LCMS (formic) $(M+H)^+$ = 388.0, 390.1, R_t = 0.83 min (100%).

Scale-up synthesis of 27 (GSK3383567, I-BET567): Benzyl ((2*S*,4*R*)-6-carbamoyl-2-methyl-1,2,3,4-tetrahydroquinolin-4-yl)carbamate (55). A mixture of 4-aminobenzamide (**51**) (170 g, 1.25 mol, 1 wt, 1 eq.) and acetaldehyde (**52**) (110 g, 2.5 mol, 0.647 wt, 2.0 eq.) in CH_2Cl_2 (4250 mL, 25 volumes) was stirred at 20-30 °C for 1 h under N_2 protection. To the cooled solution prepared above, was added solution of (11b*S*)-2,6-bis(4-chlorophenyl)-4-hydroxy-8,9,10,11,12,13,14,15-octahydrodinaphtho[2,1-d:1',2'-f][1,3,2] dioxaphosphepine 4-oxide (**54**)[51] (7.21 g, 12.49 mmol, 0.042 wt, 0.01 eq.) in CH_2Cl_2 (1700 mL, 10 volumes) and a solution of benzyl vinylcarbamate (**53**) (1.43 wt, 243.4 g, 1.37 mol, 1.1 eq) in CH_2Cl_2 (1700 mL, 10 volumes) successively at 0-5 °C. The reaction was stirred at 20-30 °C for 16 h until judged complete by HPLC. The mixture was filtered and rinsed with CH_2Cl_2 (3400 mL, 20 volumes). The filter cake was slurried with MeOH (1700 mL, 10 volumes) at 20-30 °C for 4 h, filtered and then washed with MeOH (170 mL, 1 volume). This slurrying process was repeated and then the solid was dried under vacuum at 50-60 ºC to give **55** as an off-white solid (280 g, 66%, 98.6% purity as judged by HPLC). ^{1}H NMR (400 MHz, d_6-DMSO) δ ppm 7.59–7.32 (m, 9H), 6.79 (br.s, 1H), 6.44 (d, J = 8.3 Hz, 1H), 6.20 (s, 1H), 5.16–5.07 (m, 2H), 4.81–4.75 (m, 1H), 3.54–3.50 (m, 1H), 2.01–1.97 (m, 1H), 1.47 (q, J = 11.8 Hz, 1H), 1.16 (d, J = 6.1 Hz, 3H); LCMS (formic) $(M + H)^+$ = 340.1, R_t = 0.88 min. On a 2.48 g reaction scale in the medicinal chemistry laboratory, the product (**55**) had 97.1% ee, as determined by chiral HPLC analysis, 25 cm Chiralpak AD column no.ADOOCE-A1074, 30% EtOH:heptane, flow rate: 1 mL/min, wavelength: 215 nm, temperature: rt. R_t = 11.018 min, undesired enantiomer = 17.842 min.

Benzyl ((2*S*,4*R*)-1-acetyl-6-carbamoyl-2-methyl-1,2,3,4-tetrahydroquinolin-4-yl)carbamate (56). AcCl (115.6 g, 1.47 mol, 0.46 wt, 2 eq.) was added to a pre-cooled solution of **55** (250 g, 736.6 mmol, 1 wt, 1 eq.) in NMP (1000 mL, 4 volumes) under N_2 while maintaining

the temperature below 5 °C. After 2 h of stirring at 20-30 °C, the reaction was judged complete by HPLC. The reaction mixture was added to a mixture of 7% $NaHCO_3$ aqueous solution (1500 mL, 6 volumes) and EtOAc (1500 mL, 6 volumes) with stirring. The phases were separated, and the aqueous phase was extracted with EtOAc (1500 mL, 6 volumes) twice. The combined organic phases were washed with 7% $NaHCO_3$ aqueous solution (1000 mL, 4 volumes) and H_2O (1000 mL, 4 volumes). The solvent was concentrated to 500 mL (2 volumes) and heptane (1500 mL, 6 volumes) was added. The mixture was stirred at 15-25 °C for 30 min. The solid was collected by filtration, washed with heptane (500 mL, 2 volumes) and dried under vacuum to give **56** as an off-white solid (230 g, 82%, 98.9% purity as judged by HPLC, 95.2% ee). ^{1}H NMR (400 MHz, d_6-DMSO) δ ppm 7.96 (br.s, 1H), 7.84–7.77 (m, 3H), 7.44–7.33 (m, 7H), 5.17–5.10 (m, 2H), 4.67–4.61 (m, 1H), 4.45 (ddd, J = 12, 9, 4 Hz, 1H), 2.48–2.44 (m, 1H), 2.08 (s, 3H), 1.24 (td, J = 12, 9 Hz, 1H), 1.04 (d, J = 6 Hz, 3H); LCMS (formic) $(M + H)^+$ = 382.2, R_t = 0.78 min.

(2*S*,4*R*)-1-Acetyl-4-amino-2-methyl-1,2,3,4-tetrahydroquinoline-6-carboxamide (57). The reaction was carried out in two batches: A mixture of **56** (100 g, 262.18 mmol, 1 wt, 1 eq.) and Pd/C (10 g, 0.1 wt, 50% wet) in EtOH (1000 mL, 10 volumes) was stirred at 40-50 °C under 40-50psi of H_2 for 4 h until judged complete by HPLC. The two batches were combined, the mixture was filtered, and the filter cake rinsed with EtOH (200 mL, 1 volume). The filtrate was concentrated to 200-400 mL (1-2 volumes) and *t*-BuOMe (600 mL, 3 volumes) was added. The solution was concentration to 400-600 mL (2-3 volumes) and *t*-BuOMe (600 mL, 3 volumes) was added. The resulting mixture was stirred at 15-25 °C for 1 h. The solid was collected by filtration, washed with *t*-BuOMe (100 mL, 0.5 volume) and dried under vacuum at 55 °C for 16 h to give **57** as an off-white solid (116 g, 89%, 99.1% purity as judged by HPLC). ^{1}H NMR (400 MHz, CD_3OD) δ ppm 8.05 (s, 1H), 7.93 (dd, J = 8, 2 Hz, 1H), 7.45 (d, J = 8 Hz, 1H), 4.85 – 4.81 (m,

1H), 3.91 (dd, *J* = 12, 4 Hz, 1H), 3.42 (app. s, 3H), 2.70 (ddd, *J* = 13, 9, 4 Hz, 1H), 2.21 (s, 3H), 1.21 – 1.15 (m, 5H); LCMS (high pH) $(M - H)^+ = 246.4$, $R_t = 0.47$ min.

(2*S*,4*R*)-1-Acetyl-4-((5-chloropyrimidin-2-yl)amino)-2-methyl-1,2,3,4-tetrahydroquinoline-6-carboxamide (27). A mixture of **57** (107 g, 432.69 mmol, 1 wt, 1 eq.), DIPEA (167.76 g, 1.30 mol, 1.57 wt, 3.0 eq.) and 2,5-dichloropyrimidine (70.91 g, 475.85 mmol, 0.66 wt, 1.1 eq.) in DMSO (640 mL, 6 volumes) was stirred under N_2 at 120-130 °C for 16 h until judged complete by HPLC. The reaction mixture was added to H_2O (1070 mL, 10 volumes) and extracted with EtOAc (1070 mL, 10 volumes) three times. The combined organic layers were washed with H_2O (1070 mL, 10 volumes) twice and concentrated to 214 mL (2 volumes) under vacuum. The resulting mixture was filtered, and the filter cake was dissolved in a mixture of MeCN and H_2O (1070 mL, 10 volumes) at 70-80 °C. The solution was filtered, and the filtrate was concentrated. The residue was dissolved in MeOH (1070 mL, 10 volumes) at 60 °C. The mixture was filtered, and the filtrate was stirred at 50-55 °C. Purified H_2O (535 mL, 5 volumes) was added at 50-55 °C. Crystalline **27** (0.1 g) was added and the mixture was stirred at 50-55 °C for 2 h. Additional purified H_2O (535 mL, 5 volumes) was added and the mixture was cooled slowly to 10 °C and stirred for 2 h. The mixture was filtered, washed with H_2O (214 mL, 2 volumes) and the filter cake was dried under vacuum at 55 °C for 60 h to give crystalline **27** as a slightly colored solid (101 g, 65%, >99% ee, 99.9% purity as judged by HPLC). Analytical data the same as above.

in vitro assays. All TR-FRET, hWB cytokine, developability, hepatic clearance and in vitro pharmacokinetic assays have been described previously.[13]

Cellular proliferation assay. The NMC line 11060 was obtained under licence from Prof. Chris French, Brigham and Women's Hospital, Boston, MA. NMC 11060 cells were maintained in RPMI 1640 medium (Invitrogen) supplemented with 10% HI-FBS (Heat-Inactivated Fetal Bovine

Serum, Hyclone) and 2 mM L-glutamine (Invitrogen) at 37°C and an atmosphere of 5% CO_2. Cells were diluted to 1.11×10^5 cells/mL and 90 µL/well plated into black sided, clear bottomed 96 well tissue culture plates (Corning), using growth media supplemented with penicillin / streptomycin (Invitrogen). Cells were incubated overnight at 37 °C and in one plate, ATP levels were measured using the CellTiter Glo assay (Promega) according to the manufacturer's instructions, to give a baseline reading (t=0). 3-fold serial dilutions of **27** ranging from 6 mM to 0.3 µM were prepared in 100% DMSO. The DMSO dilution series was diluted 20-fold in growth media before 10 µl of the resulting dilutions were added to the appropriate wells of the remaining cell plates. The final compound concentrations in the wells ranged from 30 µM to 1.5 nM in 0.5% DMSO. Cells were incubated with compounds for 72 hours before assaying for ATP content using CellTiter Glo (t=72). CellTiter Glo data from each t=72 time point was normalized to the relevant t=0 time point data and expressed as %t=0. This data was analyzed using GraphPad Prism V5.04 software with sigmoidal curve fitting (log(inhibitor) vs. response – variable slope (four parameters)), constraining the minimum value of the curve to values ≥100% to obtain $gpIC_{50}$ values.

in vivo studies statement. All animal studies were ethically reviewed and carried out in accordance with Animals (Scientific Procedures) Act 1986 and the GSK Policy on the Care, Welfare, and Treatment of Animals.

in vivo efficacy study: trinitrophenol-keyhole limpet hemocyanin (TNP-KLH) induced Immunoglobulin-1 (IgG1) production mouse study. Male CD1 mice (Charles River Laboratories, 8 per group) received a single oral administration of compound (in 1% (w/v) methylcellulose, *aq* 400) either once every day (QD), once every 48 h (QOD) or once every 72 h (QOED) over a 14 day dosing period. On day 1 of the study, each mouse received a single bolus intraperitoneal (ip) administration of TNP-KLH (100 ug/kg, T-5060-25, Lot # 021562-06) 1 hour

after oral administration of compound. Serial blood samples were collected at 1 h post oral compound administration via tail veil on days 1, 4, 7, 9 and 11 or via cardiac puncture (terminal sample) on day 14 and the serum harvested from the blood samples was frozen at -80 ºC. On the day of analysis, the serum was thawed to room temperature and levels of IgG1 were measured using a TNP ELISA (developed in-house) and read on a SpectraMax 190 spectrophotometer (Molecular Devices, CA). The mean IgG1 values were generated and the mean percent IgG1 reduction on day 14 following treatment with compound was calculated compared to the corresponding vehicle treated group. Levels of significance were calculated by analysis of variance (ANOVA) followed by Dunnett's multiple comparison *t*-test using Graphpad Prism version 5.04 (Graphpad Software, San Diego, CA).

in vivo efficacy study: NMC 11060 xenograft mouse model. The NMC line 11060 was obtained under license from Prof. Chris French, Brigham and Women's Hospital, Boston, MA. 1×10^7 NMC 11060 cells, in 200 μL of 75% matrigel, were injected subcutaneously into each NOD/SCID mouse. Randomized oral administration of vehicle formulation, 1% methycellulose (MC), or **27** was initiated from the day tumor volume reached between 160-301 mm^3. Tumor volume was then measured every third day until either 21 days post inoculation or tumor volume had surpassed approximately 1000 mm^3.

ASSOCIATED CONTENT

Supporting Information. The following files are available free of charge. All screening statistics, detailed pharmacokinetic data for **27**, solubility of **27** in biorelevant media, representative LCMS traces of target compounds, ^1H and ^{13}C NMR spectra for **27**, data analysis plots of predicted and measured chromLog$D_{pH7.4}$, full BROMO*scan* and selectivity data and X-ray data collection and refinement statistics (PDF).

Molecular formula strings (CSV)

Accession Codes. Coordinates have been deposited with the Protein Data Bank under accession code 7qdl (BRD4 BD1/**27** complex). Authors will release atomic coordinates and experimental data upon article publication.

AUTHOR INFORMATION

Corresponding Author

*E-mail: philip.g.humphreys@gsk.com. Phone: +44 (0)7384 799695.

Present Addresses

S.J.A.: Discovery Sciences, AstraZeneca, Cambridge Science Park, Milton Road, Cambridge CB4 0WG, U.K.

M. G. BicycleTx Ltd, 900 Building, Babraham Research Campus, Cambridge, CB22 3AT, U.K.

T.G.H.: Discovery Sciences, AstraZeneca, Cambridge Science Park, Milton Road, Cambridge CB4 0WG, U.K.

M.L.: Respiratory, Inflammation and Autoimmune (RIA) BioPharmaceuticals R&D, AstraZeneca, SE-431 83, Mölndal, Sweden.

C.L. Clinical Pharmacology and Safety Sciences, AstraZeneca, Melbourn Science Park, Cambridge Road, Melbourn, Hertfordshire, SG8 6HB, U.K.

J.M.: Galapagos NV, Generaal De Wittelaan L11 A3, 2800 Mechelen, Belgium.

S.T.: Drug Discovery Services Europe, Pharmaron, Hertford Road, Hoddesdon, EN11 9BU, UK.

N.H.T: The University of Manchester, Oxford Road, Manchester, M13 9PL, U.K.

Author Contributions

The manuscript was written through contributions of all authors. All authors have given approval to the final version of the manuscript.

Notes

The authors declare the following competing financial interest(s): All authors except G.G., F.S., D.T., L.Z and N.C.O.T, are current or former employees of GlaxoSmithKline.

ACKNOWLEDGMENT

N.H.T. is grateful to GlaxoSmithKline R&D, Stevenage and the University of Strathclyde for Ph.D. studentship and we thank the EPSRC for funding via Prosperity Partnership EP/S035990/1. We also thank Sean Lynn and Richard Upton for assistance with NMR; Steve Jackson and Eric Hortense for chiral HPLC, Tony Cook for high resolution mass spectrometry support and the GSK Physchem Team for physicochemical data generation.

ABBREVIATIONS

AMP, artificial membrane permeability; BD1, bromodomain 1 (N-terminal bromodomain); BD2, bromodomain 2 (C-terminal bromodomain); BRD2, bromodomain containing protein 2; BRD3, bromodomain containing protein 3; BRD4, bromodomain containing protein 4; BRDT, bromodomain containing protein, testis-specific; CAD, charged aerosol detection; CL_b, blood clearance; $CL_{b,u}$, unbound blood clearance; CL_{int}, intrinsic clearance; CL_{renal}, renal clearance; CLND, chemiluminescent nitrogen detection; CREBBP, CREB binding protein; EP300, E1A-associated protein p300; FaSSIF, fasted state simulated intestinal fluid; Fu_b, fraction unbound in blood; LCMS, liquid chromatography mass spectrometry; KLH-TNP, keyhole limpet haemocyanin 2, 4, 6-nitrophenol; LE, ligand efficiency; LipE, lipophilic efficiency; MCP-1, monocyte chemoattractant protein-1; MDAP, mass-directed auto preparation; MDI, metabolism dependent inhibition; NMC, nuclear protein in testis midline carcinoma; PEPPSI, pyridine-

enhanced precatalyst preparation stabilization and initiation; $pIC_{50,}$ $-\log_{10}(IC_{50})$; THQ, 1,2,3,4-tetrahydroquinoline; TR-FRET, time-resolved Förster resonance energy transfer; V_{ss}, volume of distribution at steady state; $V_{ss,u}$, unbound volume of distribution at steady state; WPF, tryptophan-proline-phenylalanine.

REFERENCES

(1) Smith, S. G.; Zhou, M.-M. The Bromodomain: A New Target in Emerging Epigenetic Medicine. *ACS Chem. Biol.* **2016**, *11*, 598–608.

(2) Filippakopoulos, P.; Knapp, S. Targeting Bromodomains: Epigenetic Readers of Lysine Acetylation. *Nat. Rev. Drug Discov.* **2014**, *13*, 337–356.

(3) Zaware, N.; Zhou, M.-M. Bromodomain Biology and Drug Discovery. *Nat. Struct. Mol. Biol.* **2019**, *26*, 870–879.

(4) Zhang, F.; Ma, S. Disrupting Acetyl-Lysine Interactions: Recent Advance in the Development of BET Inhibitors. *Curr. Drug Targets* **2018**, *19*, 1148–1165.

(5) Muller, S.; Filippakopoulos, P.; Knapp, S. Bromodomains as Therapeutic Targets. *Expert Rev. Mol. Med.* **2011**, *13*, e29.

(6) Jain, A. K.; Barton, M. C. Bromodomain Histone Readers and Cancer. *J. Mol. Biol.* **2017**, *429*, 2003–2010.

(7) Padmanabhan, B.; Mathur, S.; Manjula, R.; Tripathi, S. Bromodomain and Extra-Terminal (BET) Family Proteins: New Therapeutic Targets in Major Diseases. *J. Biosci.* **2016**, *41*, 295–311.

(8) Gilan, O.; Rioja, I.; Knezevic, K.; Bell, M. J.; Yeung, M. M.; Harker, N. R.; Lam, E. Y. N.; Chung, C.-W.; Bamborough, P.; Petretich, M.; Urh, M.; Atkinson, S. J.; Bassil, A. K.; Roberts, E. J.; Vassiliadis, D.; Burr, M. L.; Preston, A. G. S.; Wellaway, C.; Werner, T.; Gray, J. R.; Michon, A.-M.; Gobbetti, T.; Kumar, V.; Soden, P. E.; Haynes, A.; Vappiani, J.; Tough, D. F.; Taylor, S.; Dawson, S.-J.; Bantscheff, M.; Lindon, M.; Drewes, G.; Demont, E. H.; Daniels, D. L.; Grandi, P.; Prinjha, R. K.; Dawson, M. A., Selective Targeting of BD1 and BD2 of the BET Proteins in Cancer and Immuno-Inflammation. *Science* **2020**, *368*, 387–394.

(9) Wellaway, C.R.; Bamborough, P.; Bernard, S. G.; Chung, C.-W.; Craggs, P. D.; Cutler, L.; Demont, E. H.; Evans, J. P.; Gordon, L.; Karamshi, B.; Lewis, A. J.; Lindon, M. J.; Mitchell, D. J.; Rioja, I.; Soden, P. E.; Taylor, S.; Watson, R. J.; Willis, R.; Woolven, J. M.; Wyspiańska, B. S.; Kerr, W. J.; Prinjha, R. K. Structure-Based Design of a Bromodomain and Extraterminal Domain (BET) Inhibitor Selective for the N-Terminal Bromodomains that Retains an Anti-inflammatory and Antiproliferative Phenotype. *J. Med. Chem.* **2020**, *63*, 9020–9044.

(10) Watson, R. J.; Bamborough, P.; Barnett, H.; Chung, C.-W.; Davis, R.; Gordon, L.; Grandi, P.; Petretich, M.; Phillipou, A.; Prinjha, R. K.; Rioja, I.; Soden, P.; Werner, T.; Demont, E. H. GSK789: A Selective Inhibitor of the First Bromodomains (BD1) of the Bromo and Extra Terminal Domain (BET) Proteins. *J. Med. Chem.* **2020**, *63*, 9045–9069.

(11) Faivre, E. J.; McDaniel. K. F.; Albert, D. H.; Mantena, S. R.; Plotnik, J. P.; Wilcox, D.; Zhang, L.; Bui, M. H.; Sheppard, G. S.; Wang, L.; Sehgal, V.; Lin, X.; Huang, X.; Uziel, T.; Hessler, P.; Lam, L. T.; Bellin, R. J.; Mehta, G.; Fidanze, S.; Pratt, J. K.; Liu, D.; Hasvold, L. A.; Sun, C.; Panchal, S. C.; Nicolette, J. J.; Fossey, S. L.; Park, C. H.; Longenecker, K.; Bigelow, L.;

Torrent, M.; Rosenberg, S. H.; Kati, W. M.; Shen, Y. Selective Inhibition of the BD2 Bromodomain of BET Proteins in Prostate Cancer. *Nature* **2020**, *578*, 306–310.

(12) Sheppard, G. S.; Wang, L.; Fidanze, S. D.; Hasvold, L. A.; Liu, D.; Pratt, J. K.; Park, C. H.; Longenecker, K.; Qiu, W.; Torrent, M.; Kovar, P. J.; Bui, M.; Faivre, E.; Huang, X.; Lin, X.; Wilcox, D.; Zhang, L.; Shen, Y.; Albert, D. H.; Magoc, T. J.; Rajaraman, G.; Kati, W. M.; McDaniel, K. F. Discovery of N-Ethyl-4-[2-(4-fluoro-2,6-dimethyl-phenoxy)-5-(1-hydroxy-1-methyl-ethyl)phenyl]-6-methyl-7-oxo-1H-pyrrolo[2,3-c]pyridine-2-carboxamide (ABBV-744), a BET Bromodomain Inhibitor with Selectivity for the Second Bromodomain. *J. Med. Chem.* **2020**, *63*, 5585–5623.

(13) Seal, J. T.; Atkinson, S. J.; Aylott, H.; Bamborough, P.; Chung, C.-W.; Copley, R. C. B.; Gordon, L.; Grandi, P.; Gray, J. R.; Harrison, L. A.; Hayhow, T. G.; Lindon, M.; Messenger, C.; Michon, A.-M.; Mitchell, D.; Preston, A.; Prinjha, R. K.; Rioja, I.; Taylor, S.; Wall, I. D.; Watson, R. J.; Woolven, J. M.; Demont, E. H. The Optimization of a Novel, Weak Bromo and Extra Terminal Domain (BET) Bromodomain Fragment Ligand to a Potent and Selective Second Bromodomain (BD2) Inhibitor. *J. Med. Chem.* **2020**, *63*, 9093–9126.

(14) Shorstova, T.; Foulkes, W. D.; Witcher, M. Achieving Clinical Success with BET Inhibitors as Anti-Cancer Agents. *Brit. J. Cancer.* **2021**, *124*, 1478–1490.

(15) Mirguet, O.; Gosmini, R.; Toum, J.; Clement, C. A.; Barnathan, M.; Brusq, J. M.; Mordaunt, J. E.; Grimes, R. M.; Crowe, M.; Pineau, O.; Ajakane, M.; Daugan, A.; Jeffrey, P.; Cutler, L.; Haynes, A. C.; Smithers, N. N.; Chung, C.-W.; Bamborough, P.; Uings, I. J.; Lewis, A.;

Witherington, J.; Parr, N.; Prinjha, R. K.; Nicodeme, E., Discovery of Epigenetic Regulator I-BET762: Lead Optimization to Afford a Clinical Candidate Inhibitor of the BET Bromodomains. *J. Med. Chem.* **2013**, *56*, 7501–7515.

(16) Herait, P. E.; Berthon, C.; Thieblemont, C.; Raffoux, E.; Magarotto, V.; Stathis, A.; Thomas, X.; Leleu, X.; Gomez-Roca, C.; Odore, E.; Roumier, C.; Bourdel, F.; Quesnel, B.; Zucca, E.; Michallet, M.; Recher, C.; Cvitkovic, E.; Rezai, K.; Preudhomme, C.; Facon, T.; Palumbo, A.; Dombret, H., Abstract CT231: BET-Bromodomain Inhibitor OTX015 Shows Clinically Meaningful Activity at Nontoxic Doses: Interim Results of an Ongoing Phase I trial in Hematologic Malignancies. *Cancer Research* **2014**, *74*, CT231.

(17) Albrecht, B. K.; Gehling, V. S.; Hewitt, M. C.; Vaswani, R. G.; Cote, A.; Leblanc, Y.; Nasveschuk, C. G.; Bellon, S.; Bergeron, L.; Campbell, R.; Cantone, N.; Cooper, M. R.; Cummings, R. T.; Jayaram, H.; Joshi, S.; Mertz, J. A.; Neiss, A.; Normant, E.; O'Meara, M.; Pardo, E.; Poy, F.; Sandy, P.; Supko, J.; Sims, R. J.; Harmange, J.-C.; Taylor, A. M.; Audia, J. E. Identification of a Benzoisoxazoloazepine Inhibitor (CPI-0610) of the Bromodomain and Extra-Terminal (BET) Family as a Candidate for Human Clinical Trials. *J. Med. Chem.* **2016**, *59*, 1330−1339.

(18) Postel-Vinay, S.; Herbschle, K.; Massard, C.; Woodcock, V.; Soria, J.-C.; Walter, A. O.; Ewerton, F.; Poelman, M.; Benson, N.; Ocker, M.; Wilkinson, G.; Middleton, M. First-in-Human Phase I Study of the Bromodomain and Extraterminal Motif Inhibitor BAY 1238097: Emerging

Pharmacokinetic/Pharmacodynamic Relationship and Early Termination Due to Unexpected Toxicity. *Eur. J. Cancer* **2019**, *109*, 103–110.

(19) McDaniel, K. F.; Wang, L.; Soltwedel, T.; Fidanze, S. D.; Hasvold, L. A.; Liu, D.; Mantei, R. A.; Pratt, J. K.; Sheppard, G. S.; Bui, M. H.; Faivre, E. J.; Huang, X.; Li, L.; Lin, X.; Wang, R.; Warder, S. E.; Wilcox, D.; Albert, D. H.; Magoc, T. J.; Rajaraman, G.; Park, C. H.; Hutchins, C. W.; Shen, J. J.; Edalji, R. P.; Sun, C. C.; Martin, R.; Gao, W.; Wong, S.; Fang, G.; Elmore, S. W.; Shen, Y.; Kati, W. M. Discovery of N-(4-(2,4-Difluorophenoxy)-3-(6-methyl-7-oxo-6,7-dihydro-1H-pyrrolo[2,3-c]pyridin-4-yl)phenyl)ethanesulfonamide (ABBV-075/Mivebresib), a Potent and Orally Available Bromodomain and Extraterminal Domain (BET) Family Bromodomain Inhibitor. *J. Med. Chem.* **2017**, *60*, 8369–8384.

(20) Stubbs, M. C.; Maduskuie, T.; Burn, T.; Diamond-Fosbenner, S.; Falahatpisheh, N.; Volgina, A.; Zolotarjova, N.; Wen, X.; Feldman, P.; Rupar, M.; Collins, R.; Marando, C.; Ruggeri, B.; Covington, M.; Liu, X. M.; Wynn, R.; Yeleswaram, S.; Yao, W.; Huber, R.; Hollis, G.; Scherle, P.; Combs, A. P.; Liu, P. C. Abstract 5071: Preclinical Characterization of the Potent and Selective BET Inhibitor INCB057643 in Models of hematologic malignancies. *Cancer Res.* **2017**, *77*, 5071.

(21) Liu, P. C. C.; Liu, X. M.; Stubbs, M. C.; Maduskuie, T.; Sparks, R.; Zolotarjova, N.; Li, J.; Wen, X.; Favata, M.; Feldman, P.; Volgina, A.; DiMatteo, D.; Collins, R.; Falahatpisheh, N.; Polam, P.; Li, Y.; Covington, M.; Diamond-Fosbenner, S.; Wynn, R.; Burn, T.; Vaddi, K.; Yeleswaram, S.; Combs, A. P.; Yao, W.; Huber, R.; Scherle, P.; Hollis, G. Abstract 3523: Discovery of a Novel BET inhibitor INCB054329. Cancer Res. 2015, 75, 3523. Combs, A. P. Invention of INCB054329 and INCB057643, Two Potent and Selective BET Inhibitors in Clinical

Trials for Oncology. ACS Spring 2018 255th National Meeting, March 18−22, 2018, New Orleans, LA, Abstract MEDI 306.

(22) Ozer, H. G.; El-Gamal, D.; Powell, B.; Hing, Z. A.; Blachly, J. S.; Harrington, B.; Mitchell, S.; Grieselhuber, N. R.; Williams, K.; Lai, T.-H.; Alinari, L.; Baiocchi, R. A.; Brinton, L.; Baskin, E.; Cannon, M.; Beaver, L.; Goettl, V. M.; Lucas, D. M.; Woyach, J. A.; Sampath, D.; Lehman, A. M.; Yu, L.; Zhang, J.; Ma, Y.; Zhang, Y.; Spevak, W.; Shi, S.; Severson, P.; Shellooe, R.; Carias, H.; Tsang, G.; Dong, K.; Ewing, T.; Marimuthu, A.; Tantoy, C.; Walters, J.; Sanftner, L.; Rezaei, H.; Nespi, M.; Matusow, B.; Habets, G.; Ibrahim, P.; Zhang, C.; Mathé, E. A.; Bollag, G.; Byrd, J. C.; Lapalombella, R. BRD4 Profiling Identifies Critical Chronic Lymphocytic Leukemia Oncogenic Circuits and Reveals Sensitivity to PLX51107, a Novel Structurally Distinct BET Inhibitor. *Cancer Discovery* **2018**, *8*, 458–477.

(23) Jones, K. L.; Beaumont, D. M.; Bernard, S. G.; Bit, R. A.; Campbell, S. P.; Chung, C.-W.; Cutler, L.; Demont, E. H.; Dennis, K.; Gordon, L.; Gray, J. R.; Haase, M. V.; Lewis, A. J.; McCleary, S.; Mitchell, D. J.; Moore, S. M.; Parr, N.; Robb, O. J.; Smithers, N.; Soden, P. E.; Suckling, C. J.; Taylor, S.; Walker, A. L.; Watson, R. J.; Prinjha, R. K. Discovery of a Novel Bromodomain and Extra Terminal Domain (BET) Protein Inhibitor, I-BET282E, Suitable for Clinical Progression. *J. Med. Chem.* **2021**, *64*, 12200–12227.

(24) Gavai, A. V.; Norris, D.; Delucca, G.; Tortolani, D.; Tokarski, J. S.; Dodd, D.; O'Maley, D.; Zhao, Y.; Quesnelle, C.; Gill, P.; Vaccaro, W.; Huynh, T.; Ahuja, VV.; Han, W.-C.; Mussari, C.; Harikrishnan, L.; Kamau, M.; Poss, M.; Sheriff, S.; Yan, C.; Marsilio, F.; Menard, K.; Wen,

M.-L.; Rampulla, R.; Wu, D.-R.; Li, J.; Zhang, H.; Li, P.; Su, D.; Yip, H.; Traeger, S. C.; Zhang, Y.; Mathur, A.; Zhang, H.; Huang, C.; Yang, Z.; Ranasinghe, A.; Everlof, G.; Raghaven, N.; Tye, C. K.; Wee, S.; Hunt, J. T.; Vite, G.; Westhouse, R.; Lee, F. Y. Discovery and Preclinical Pharmacology of an Oral Bromodomain and Extra-Terminal (BET) Inhibitor Using Scaffold-Hopping and Structure-Guided Drug Design. *J. Med. Chem.* **2021**, asap.

(25) Bradbury, R. H.; Callis, R.; Carr, G. R.; Chen, H.; Clark, E.; Feron, L.; Glossop, S.; Graham, M. A.; Hattersley, M.; Jones, C.; Lamont, S. G.; Ouvry, G.; Patel, A.; Patel, J.; Rabow, A. A.; Roberts, C. A.; Stokes, S.; Stratton, N.; Walker, G. E.; Wardm L.; Whalley, D.; Whittaker, D.; Wrigley, G.; Waring, M. J. Optimization of a Series of Bivalent Triazolopyridazine Based Bromodomain and Extraterminal Inhibitors: The Discovery of (3R)-4-[2-[4-[1-(3-Methoxy-[1,2,4]triazolo[4,3-b]pyridazin-6-yl)-4-piperidyl]phenoxy]ethyl]-1,3-dimethyl-piperazin-2-one (AZD5153). *J. Med. Chem.* **2016**, *59*, 7801–7817.

(26) Waring, M. J.; Chen, H.; Rabow, A. A.; Walker, G.; Bobby, R.; Boiko, S.; Bradbury, R. H.; Callis, R.; Clark, E.; Dale, I.; Daniels, D. L.; Dulak, A.; Flavell, L.; Holdgate, G.; Jowitt, T. A.; Kikhney, A.; McAlister, M.; Méndez, J.; Ogg, D.; Patel, J.; Petteruti, P.; Robb, G. R.; Robers, M. B.; Saif, S.; Stratton, N.; Svergun, D. I.; Wang, W.; Whittaker, D.; Wilson, D. M.; Yao, Y. Potent and Selective Bivalent Inhibitors of BET Bromodomains. *Nature Chem. Biol.* **2016**, *12*, 1097–1104.

(27) Chung, C.-W.; Dean, A. W.; Woolven, J. M.; Bamborough, P. Fragment-Based Discovery of Bromodomain Inhibitors Part 1: Inhibitor Binding Modes and Implications for Lead Discovery. *J. Med. Chem.* **2012**, *55*, 576–586.

(28). Gosmini, R.; Nguyen, V. L.; Toum, J.; Simon, C.; Brusq, J.-M. G.; Krysa, G.; Mirguet, O.; Riou-Eymard, A. M.; Boursier, E. V.; Trottet, L.; Bamborough, P.; Clark, H.; Chung, C.-W.; Cutler, L.; Demont, E. H.; Kaur, R.; Lewis, A. J.; Schilling, M. B.; Soden, P. E.; Taylor, S.; Walker, A. L.; Walker, M. D.; Prinjha, R. K.; Nicodème, E. The Discovery of I-BET726 (GSK1324726A), a Potent Tetrahydroquinoline ApoA1 Up-Regulator and Selective BET Bromodomain Inhibitor. *J. Med. Chem.* **2014**, *57*, 8111–8131.

(29) Hewings, D. S.; Fedorov, O.; Filippakopoulos, P.; Martin, S.; Picaud, S.; Tumber, A.; Wells, C.; Olcina, M. M.; Freeman, K.; Gill, A.; Ritchie, A. J.; Sheppard, D. W.; Russell, A. J.; Hammond, E. M.; Knapp, S.; Brennan, P. E.; Conway, S. J. Optimization of 3,5-Dimethylisoxazole Derivatives as Potent Bromodomain Ligands. *J. Med. Chem.* **2013**, *56*, 3217–3227.

(30) Bair, K. W.; Herbertz, T.; Kauffman, G. S.; Kayser-Bricker, K. J.; Luke, G. P.; Martin, M. W.; Millan, D. S.; Schiller, S. E. R.; Talbot, A. C. Tetrahydroquinoline Compositions as BET Bromodomain Inhibitors. US20160256448A1, 2016.

(31) Stock, D. A.; Molinoff, P. B. The Value of Backup Compounds to Drug Development Programs. *Ther. Innov. Regul. Sci.* **2002**, *36*, 95–113.

(32) Bayliss, M. K.; Butler, J.; Feldman, P. L.; Green, D. V. S.; Leeson, P. D.; Palovich, M. R.; Taylor, A. J. Quality Guidelines for Oral Drug Candidates: Dose, Solubility and Lipophilicity. *Drug Disc. Today* **2016**, *21*, 1719–1727.

(33) Riddell, K.; Patel, A.; Collins, G.; Zhou, Y.; Schramek, D.; Kremer, B. E.; Ferron-Brady, G. An Adaptive Physiologically Based Pharmacokinetic-Driven Design to Investigate the Effect of Itraconazole and Rifampicin on the Pharmacokinetics of Molibresib (GSK525762) in Healthy Female Volunteers. *J. Clin. Pharmacol.* **2021**, *61*, 125–137.

(34) Mosedale, M.; Watkins, P. B. Understanding Idiosyncratic Toxicity: Lessons Learned from Drug-Induced Liver Injury. *J. Med. Chem.* **2020**, *63*, 6436–6461.

(35) Gleeson, M. P. Generation of a Set of Simple, Interpretable ADMET Rule of Thumb. *J. Med. Chem.* **2008**, *51*, 817–834.

(36) Johnson, T. W.; Gallego, R. A.; Edwards, M. P. Lipophilic Efficiency as an Important Metric in Drug Design. *J. Med. Chem.* **2018**, *61*, 6401–6420.

(37) Free, S. M.; Wilson, J. W. A Mathematical Contribution to Structure-Activity Studies. *J. Med. Chem.* **1964**, *7*, 395–399.

(38) Ames, B. N. Identifying Environmental Chemicals Causing Mutations and Cancer. *Science* **1979**, *204*, 587−593.

(39) Preston, A.; Atkinson, S. J.; Seal, J.; Mitchell, D. J.; Watson, R. J.; Gray, J. R. J.; Woolven, J.; Wall, I.; Chung, C.-W.; Bamborough, Paul; Rianjongdee, F.; Taylor, S.; Michon, A.-M.;

Grandi, P.; Rioja, I.; Gordon, L.; Jones, E. J.; Craggs, P. D.; Prinjha, R. K.; Lindon, M.; Demont, E. H., Design and Synthesis of a Highly Selective and In Vivo Capable Inhibitor of the Second Bromodomain (BD2) of the Bromodomain and Extra Terminal Domain (BET) Family of Proteins. *J. Med. Chem.* **2020**, *63*, 9070–9092.

(40) Damon, D. B.; Dugger, R. W.; Hubbs, S. E.; Scott, J. M.; Scott, R. W. Asymmetric Synthesis of the Cholesteryl Ester Transfer Protein Inhibitor Torcetrapib. *Org. Process Res. Dev.* **2006**, *10*, 472–480.

(41) Demont, E. H.; Garton, N. S.; Gosmini, R. L. M.; Hayhow, T. G. C.; Seal, J.; Wilson, D. M.; Woodorw, M. D. Tetrahydroquinoline Derivatives and Their Pharmaceutical Use. WO 2011054841A1, 2011.

(42) Freeman-Cook, K. D.; Hoffman, R. L.; Johnson, T. W. Lipophilic Efficiency: The Most Important Efficiency Metric in Medicinal Chemistry. *Future Med. Chem.* **2013**, *5*, 113–116.

(43) Piha-Paul, S. A.; Hann, C. L.; French, C. A.; Cousin, S.; Braña, I.; Cassier, P. A.; Moreno, V.; de Bono, J. S.; Duckworth Harward, S.; Ferron-Brady, G.; Barbash, O.; Wyce, A.; Wu, Y.; Horner, T.; Annan, M.; Parr, N. J.; Prinjha, R. K.; Carpenter, C. L.; Hilton, J.; Hong, D. S.; Haas, N. B.; Markowski, M. C.; Dhar, A.; O'Dwyer, P. J.; Shapiro, G. I. Phase 1 Study of Molibresib (GSK525762), a Bromodomain and Extra-Terminal Domain Protein Inhibitor, in NUT Carcinoma and Other Solid Tumors. *JNCI Cancer Spectrum* **2020**, *4*, pkz093.

(44) Chang, G.; Steyn, S. J.; Umland, J. P.; Scott, D. O. Strategic Use of Plasma and Microsome Binding to Exploit in Vitro Clearance in Early Drug Discovery. *ACS Med. Chem. Lett.* **2010**, *13*, 50–53.

(45) Barr, J. T.; Lade, J. M.; Tran, T. B.; Dahal, U. P. Fraction Unbound for Liver Microsome and Hepatocyte Incubations for All Major Species Can Be Approximated Using a Single-Species Surrogate. *Drug Metab. Dispos.* **2019**, *47*, 419–423.

(46) Davies, B.; Morris, T. Physiological Parameters in Laboratory Animals and Humans. *Pharm. Res.* **1993**, *10*, 1093–1095.

(47) Clegg, M. A.; Tomkinson, N. C. O.; Prinjha, R. K.; Humphreys, P. G. Advancements in the Development of Non-BET Bromodomain Chemical Probes. *ChemMedChem* **2019**, *14*, 362–385.

(48) BROMOscan recombinant protein binding assays were carried out at DiscoverX, http://www.discoverx.com.

(49) Bruno, I. J.; Cole, J. C.; Kessler, M.; Luo, J.; Motherwell, W. D. S.; Purkis, L. H.; Smith, B. R.; Taylor, R.; Cooper, R. I.; Harris, S. E.; Orpen, A. G. Retrieval of Crystallographically-Derived Molecular Geometry Information. *J. Chem. Inf. Comput. Sci.* **2004**, *44*, 2133–2144.

(50) Damon, D. B.; Dugger, R. W.; Magnus-Aryitey, G.; Ruggeri, R. B.; Wester, R. T.; Tu, M.; Abramov, Y. Synthesis of the CETP Inhibitor Torcetrapib: The Resolution Route and Origin of Stereoselectivity in the Iminium Ion Cyclization. *Org. Proc. Res. Dev.* **2006**, *10*, 464–471.

(51) Liu, H.; Dagousset, G.; Masson, G.; Ratailleau, P.; Zhu, J. Chiral Bronsted Acid-Catalyzed Enantioselective Three-Component Povarov Reaction. *J. Am. Chem. Soc.* **2009**, *131*, 4598–4599.

(52) Nicodeme, E.; Jeffrey, K. L.; Schaefer, U.; Beinke, S.; Dewell, S.; Chung, C.-W.; Chandwani, R.; Marazzi, I.; Wilson, P.; Coste, H.; White, J.; Kirilovsky, J.; Rice, C. M.; Lora, J. M.; Prinjha, R. K.; Lee, K.; Tarakhovsky, A. Suppression of Inflammation by a Synthetic Histone Mimic. *Nature* **2010**, *468*, 1119−1123.

(53) Wellaway, C.R.; Amans, D.; Bamborough, P.; Barnett, H.; Bit, R. A.; Brown, J. A.; Carlson, N. R.; Chung, C.-W.; Cooper, A. W. J.; Craggs, P. D.; Davis, R. P.; Dean, T. W.; Evans, J. P.; Gordon, L.; Harada, I. L.; Hirst, D. J.; Humphreys, P. G.; Jones, K. L.; Lewis, A. J.; Lindon, M. J.; Lugo, D.; Mahmood, M.; McCleary, S.; Mederiros, P.; Mitchell, D. J.; O'Sullivan, M.; Le Gall, A.; Patel, V. K.; Patten, C.; Poole, D. L.; Shah, R. R.; Smith, J. E.; Stafford, K. A. J.; Thomas, P. J.; Vimal, M.; Wall, I. D.; Watson, R. J.; Wellaway, N.; Yao, G.; Prinjha, R. K. Discovery of a Bromodomain and Extraterminal Inhibitor with a Low Predicted Human Dose Through Synergistic Use of Encoded Library Technology and Fragment Screening. *J. Med. Chem.* **2020**, *63*, 714–746.

(54) Mirguet, O.; Lamotte, Y.; Donche, F.; Toum, J.; Gellibert, F.; Bouillot, A.; Gosmini, R.; Nguyen, V. L.; Delannee, D.; Seal, J.; Blandel, F.; Boullay, A. B.; Boursier, E.; Martin, S.; Brusq, J. M.; Krysa, G.; Riou, A.; Tellier, R.; Costaz, A.; Huet, P.; Dudit, Y.; Trottet, L.; Kirilovsky, J.; Nicodeme, E. From ApoA1 Upregulation to BET Family Bromodomain Inhibition: Discovery of I-BET151. *Bioorg Med. Chem. Lett.* **2012**, *22*, 2963–2967.

(55) Bauer, D. E.; Mitchell, C. M.; Strait, K. M.; Lathan, C. S.; Stelow, E. B.; Lüer, S. C.; Muhammed, S.; Evans, A. G.; Sholl, L. M.; Rosai, J.; Giraldi, E.; Oakley, R. P.; Rodriguez-Galindo, C.; London, W. B.; Sallan, S. E.; Bradner, J. E.; French, C. A. Clinicopathologic Features and Long-Term Outcomes of NUT Midline Carcinoma. *Clin. Cancer. Res.* **2012**, *18*, 5773–5779.

(56) Filippakopoulos, P.; Qi, J.; Picaud, S.; Shen, Y.; Smith, W. B.; Fedorov, O.; Morse, E. M.; Keates, T.; Hickman, T. T.; Felletar, I.; Philpott, M.; Munro, S.; McKeown, M. R.; Wang, Y.; Christie, A. L.; West, N.; Cameron, M. J.; Schwartz, B.; Heightman, T. D.; La Thangue, N.; French, C. A.; Wiest, O.; Kung, A. L.; Knapp, S.; Bradner, J. E. Selective Inhibition of BET Bromodomains. *Nature* **2010,** *468*, 1067–1073.

(57) Atkinson, S. J.; Hirst, D. J.; Humphreys, P. G.; Lindon, M. J.; Preston, A. G.; Seal, J. T.; Wellaway, C. R. Tetrahydroquinoline Derivatives as Bromodomain Inhibitors. WO2016038120A1, 2016.

Table of contents graphic